Universitat Autònoma de Barcelona

High-Performance Embedded Systems for Digital Laser Marking and Printing

Francesc Bravo Montero

Universitat Autònoma de Barcelona

High-Performance Embedded Systems for Digital Laser Marking and Printing

Ph.D. dissertation
Electronic and Telecommunication Engineering

Author:
Francesc Bravo Montero

Supervisors:
David Castells Rufas
Jordi Carrabina Bordoll

Universitat Autònoma de Barcelona (UAB)
Department of Microelectronics and Electronic Systems (MiSE)

2021, Barcelona, Spain

Universitat Autònoma de Barcelona

The undersigned Dr. **David Castells Rufas** and Prof. Dr. **Jordi Carrabina Bordoll**, from the Department of Microelectronics and Electronic Systems, of the Universitat Autònoma de Barcelona,

CERTIFY

That the dissertation entitled "High-Performance Embedded Systems for Digital Laser Marking and Printing" has been written by **Francesc Bravo Montero** under their supervision, in partial fulfillment of the requirements for the degree of Doctor of Philosophy.

And hereby to acknowledge the above, sign the present

Signature **David Castells Rufas** Signature **Jordi Carrabina Bordoll**

Barcelona, Spain, 8th October 2021.

Abstract

High-Performance Embedded Systems for Digital Laser Marking and Printing

Laser marking is a common part of many manufacturing processes in the industry, with great importance in the fast-moving consumer goods (FMCG) industry since respects the environment without losing productivity. The speed of production lines is a key determinant of the output capacity of many industries, but their scalability could be hindered by some fundamental limits of current laser marking technologies. Currently, most laser marking equipment is based on a single laser beam with the corresponding sequential processing that culminates in a performance bottleneck which limits printing production line speed to a de facto barrier of 8 m/s.

In this thesis, I review state-of-the-art technologies, their limiting factors, and analyze how future systems can overcome them. I propose, implement and validate several platforms that overcome these barriers by using a matrix of laser beams from semiconductor laser arrays or fiber-coupled laser diode arrays, for its industrial use in high-speed printing and high-resolution printing (f-LDA) and very-high-speed coding (HP f-LDA) type of applications. In all cases, they are controlled in real-time by using an embedded high-performance computing reconfigurable architecture based on FPGAs.

As an alternative to generating and processing multiple laser beams in parallel, I also propose to project images formed by laser beamlets onto surfaces. These images are generated using SLM or DLP technologies. To do this effectively, images must be rendered correctly to match the required resolution, grayscale, and print width; and the control system needs to calculate this information along with the desired position of the printed image and the speed of the product to be printed or marked, which can be acquired from industrial encoders and sensors.

Additionally, I present a novel multi-beam method to print paper and cardboard without ink. The method is based on the carbonization of paper by a combination of lasers working on different wavelengths. A proof-of-concept system is created based on combining existing commercial systems to demonstrate the viability of the method. The results show that no debris is generated, and the quality of the mark is superior in terms of contrast and resolution to previously known methods.

The industrialized solutions presented in this thesis can print images from 50 to more than 300 dpi resolution on printing substrates widths ranging from 570 µm up to 100 mm, at production line speeds of up to 16 m/s. The analysis performed suggests that even higher speeds could be achieved by investing in additional laser beams, leading to a full range of new applications in Industry 4.0.

Keywords: Digital Printing, Diode Lasers, Digital Light Processing (DLP), Field Programmable Gate Arrays (FPGA), Industrial Control, Industry 4.0, Inkless Printing, Laser Diode Arrays (LDA), Laser Applications, Laser Marking, Optical fibers, Real-Time Systems, Reconfigurable Architectures, Semiconductor Laser Arrays, Spatial Light Modulator (SLM).

Resum

Sistemes Encastats d'Alt Rendiment per a Marcatge i Impressió Digital Làser

El marcatge per làser és una part habitual de molts processos de fabricació en la indústria, amb gran importància en el sector dels béns de consum ràpid (FMCG), ja que respecta el medi ambient sense perdre productivitat. La velocitat de les línies de producció és un factor determinant en la capacitat de producció de moltes indústries, però la seva escalabilitat es podria veure obstaculitzada per alguns límits fonamentals de les actuals tecnologies de marcatge làser. En l'actualitat, la majoria dels equips de marcatge làser es basen en un únic feix làser amb el corresponent processament seqüencial, que culmina en un coll d'ampolla de rendiment que limita la velocitat de la línia de producció d'impressió a una barrera de facto de 8 m/s.

En aquesta tesi, reviso les tecnologies més avançades, els seus factors limitants i analitzo com poden superar-les futurs sistemes. Proposo, implemento i valido diverses plataformes que superen aquestes barreres mitjançant l'ús d'una matriu de feixos làser originats per matrius lineals de làsers semiconductors o matrius lineals de díodes làser acoblats a fibra, per al seu ús industrial en aplicacions d'impressió d'alta velocitat i alta resolució (f-LDA) i de codificació de molt alta velocitat (HP f-LDA). En tots els casos, es controlen en temps real mitjançant l'ús d'una arquitectura de computació reconfigurable d'alt rendiment integrada basada en FPGAs.

Com a alternativa a la generació i processament de múltiples feixos làser en paral·lel, també proposo projectar imatges formades per *beamlets* làser sobre superfícies. Aquestes imatges es generen mitjançant tecnologies SLM o DLP. Per fer-ho de forma eficaç, les imatges han de renderizar-se correctament perquè coincideixin amb la resolució, l'escala de grisos i l'amplada d'impressió requerides; i el sistema de control ha de calcular aquesta informació juntament amb la posició desitjada de la imatge impresa i la velocitat del producte que s'ha d'imprimir o marcar, la qual pot adquirir-se a partir d'encoders i sensors industrials.

A més, presento un nou mètode multi-feix per imprimir en paper i cartró sense tinta. El mètode es basa en la carbonització del paper mitjançant una combinació de làsers que treballen en diferents longituds d'ona. Es crea un sistema de prova de concepte, basat en la combinació de sistemes comercials existents, per demostrar la viabilitat del mètode. Els resultats mostren que no es generen residus i que la qualitat de la marca és superior en termes de contrast i resolució als mètodes coneguts anteriorment.

Les solucions industrialitzades presentades en aquesta tesi, poden imprimir imatges des de 50 a més de 300 ppp de resolució en substrats d'impressió amb amplades que van des de 570 μm fins a 100 mm, a velocitats de línia de producció de fins a 16 m/s. L'anàlisi realitzat, suggereix que podrien aconseguir-se velocitats encara més ràpides invertint en feixos làser addicionals, el que donaria lloc a tota una gamma de noves aplicacions en la Indústria 4.0.

Resumen

Sistemas Embebidos de Alto Rendimiento para Marcaje e Impresion Digital Laser

El marcado por láser es una parte habitual de muchos procesos de fabricación en la industria, con gran importancia en el sector de los bienes de consumo rápido (en inglés *fast-moving consumer goods*, FMCG), ya que respeta el medio ambiente sin perder productividad. La velocidad de las líneas de producción es un factor determinante en la capacidad de producción de muchas industrias, pero su escalabilidad podría verse obstaculizada por algunos límites fundamentales de las actuales tecnologías de marcado láser. En la actualidad, la mayoría de los equipos de marcado láser se basan en un único rayo láser con el correspondiente procesamiento secuencial que culmina en un cuello de botella de rendimiento que limita la velocidad de la línea de producción de impresión a una barrera de facto de 8 m/s.

En esta tesis, reviso las tecnologías más avanzadas, sus factores limitantes y analizo cómo pueden superarlos los futuros sistemas. Propongo, implemento y valido varias plataformas que superan estas barreras mediante el uso de una matriz de rayos láser de matrices de láseres semiconductores o matrices de diodos láser acoplados a fibra para su uso industrial en aplicaciones de impresión de alta velocidad y alta resolución (f-LDA) y de codificación de muy alta velocidad (HP f-LDA). En todos los casos, se controlan en tiempo real mediante el uso de una arquitectura de computación reconfigurable de alto rendimiento integrada basada en FPGAs.

Como alternativa a la generación y procesamiento de múltiples haces láser en paralelo, también propongo proyectar imágenes formadas por *beamlets* láser sobre superficies. Estas imágenes se generan mediante tecnologías SLM o DLP. Para hacerlo de forma eficaz, las imágenes deben renderizarse correctamente para que coincidan con la resolución, la escala de grises y la anchura de impresión requeridas; y el sistema de control debe calcular esta información junto con la posición deseada de la imagen impresa y la velocidad del producto que debe imprimirse o marcarse, que puede adquirirse a partir de codificadores y sensores industriales.

Además, presento un novedoso método multi-haz para imprimir en papel y cartón sin tinta. El método se basa en la carbonización del papel mediante una combinación de láseres que trabajan en diferentes longitudes de onda. Se crea un sistema de prueba de concepto, basado en la combinación de sistemas comerciales existentes, para demostrar la viabilidad del método. Los resultados muestran que no se generan residuos y que la calidad de la marca es superior en términos de contraste y resolución a los métodos conocidos anteriormente.

Las soluciones industrializadas presentadas en esta tesis, pueden imprimir imágenes desde 50 a más de 300 ppp de resolución en sustratos de impresión con anchos que van desde 570 µm hasta 100 mm, a velocidades de línea de producto de hasta 16 m/s. El análisis realizado sugiere que podrían alcanzarse velocidades aún mayores invirtiendo en rayos láser adicionales, lo que daría lugar a toda una gama de nuevas aplicaciones en la Industria 4.0.

Acknowledgments

“Para mí la familia ha sido lo máximo. Uno no tiene que ufanarse de sus logros porque esas son cosas humanas que pasan y se olvidan. Uno extraña una cosa muy importante y son los compañeros”

Lucio Chiquito, Doctor engineer.

These were his words at the ceremony held by the University. He submitted his doctoral thesis at 104 years old. Lucio, de mayor quiero ser como tú.

I hereby sincerely acknowledge my supervisors, Prof. Dr. Jordi Carrabina and Dr. David Castells who always give me encouragement, help, and advice during the ups and downs of my research.

I also appreciate the help from my colleagues in Macsa, my colleagues in the doctorate program, and my colleagues in the Escola d'Enginyeria, very especially to Byron Quezada.

I am very grateful to everyone from the companies that have participated in projects related to this thesis, who helped in my research, in particular, to the engineers from PARC, Xerox, and DataLase.

I would like to thank the members of the Academic Commissions of the Doctorate Program in Electrical and Telecommunication Engineering, reviewers of papers, and patent examiners, for his kind guidance and smart questions.

I would like to thank my parents, Francisco and Carmen, my wife Isabel, and my children Sergi and Pep. They have been supporting me unconditionally throughout my studies. Without them, this thesis would never have been submitted (literally).

This research has been partly funded by the Catalan Government Industrial Ph.D. program under grants 2015-DI-022

To the memory of my mother.

Publications list

2022:

[1] **F. Bravo-Montero**, D. Castells-Rufas, and J. Carrabina, "High-Speed Laser Marking with Diode Arrays," *Opt. Laser Technol.*, vol. 146, no. Feb 2022, p. 107551, 2022.

2021:

[2] D. Castells-Rufas, **F. Bravo-Montero**, and J. Carrabina, "Speed Limits for Single-Beam Laser Marking," in *IECON 2021 The 47th Annual Conference of the IEEE Industrial Electronics Society*, 2021, pp. 1974--1979.

[3] S. A. Vogler, **F. Bravo-Montero**, C. Gannau, and J. Almirall, "Method and system for marking paper, cardboard and/or fabric," WO2021/023898, 2021. *(patent)*

[4] S. A. Vogler, **F. Bravo-Montero**, C. Gannau, and J. Almirall, "Procedure and system for marking paper, cardboard, and textile," EP3771572, 2021. *(patent)*

2020:

[5] **F. Bravo-Montero**, D. Castells-Rufas, S. A. Vogler, and J. Carrabina, "Laser Inkless Eco-Printing on Paper and Cardboard," in *2020 IEEE International Conference on Industrial Technology (ICIT)*, 2020, vol. 2020-Feb, pp. 59–64.

2019:

[6] S. A. Vogler, V. Boira-Plans, **F. Bravo-Montero**, and J. Camps-Claramunt, "Control procedure for a laser marking matrix system," JP6518719, 2019. *(patent)*

[7] S. A. Vogler, V. Boira-Plans, **F. Bravo-Montero**, and J. Camps-Claramunt, "Control procedure for a laser marking matrix system," US10265967, 2019. *(patent)*

2018:

[8] D. Castells-Rufas, **F. Bravo-Montero**, B. Quezada-Benalcazar, J. Carrabina, and M. Codina, "Automatic real-time tilt correction of DMD-based displays for augmented reality applications," in *Emerging Digital Micromirror Device Based Systems and Applications X*, 2018, vol. 10546, p. 22.

2017:

[9] **F. Bravo-Montero**, S. A. Vogler, and J. Camps Claramunt, "On-demand LASER marking device manufacturing method and LASER marking device obtained by said method," JP2017042820, 2017. *(patent)*

[10] **F. Bravo Montero**, S. A. Vogler, and J. Camps Claramunt, "On-demand LASER marking device manufacturing method and LASER marking device obtained by said method," US10220470, 2017. *(patent)*

[11] **F. Bravo-Montero**, S. A. Vogler, and J. Camps Claramunt, "On-demand LASER marking device manufacturing method and LASER marking device obtained by said method," EP3136521, 2017. *(patent)*

[12] S. A. Vogler, V. Boira-Plans, **F. Bravo-Montero**, and J. Camps-Claramunt, "Procedure for controlling a laser marking matrix system," EP3251783, 2017. *(patent)*

[13] **F. Bravo-Montero**, S. Vogler, and J. Camps Claramunt, "Procedimiento de fabricación de equipos para marcaje de productos por LASER bajo demanda, y equipo para marcaje de productos por láser obtenido con dicho procedimiento," ES2603751, 2017. *(patent)*

[14] S. A. Vogler, V. Boira-Plans, **F. Bravo-Montero**, and J. Camps-Claramunt, "Procedimiento de control de un sistema matricial de marcaje LASER," ES2644261, 2017. *(patent)*

2016:

[15] S. A. Vogler, J. Camps Claramunt, and **F. Bravo-Montero**, "Device for the LASER marking of products," US20160236300, 2016. *(patent)*

[16] S. A. Vogler, J. Camps Claramunt, and **F. Bravo-Montero**, "Device for LASER marking of products," EP3043428, 2016. *(patent)*

2015:

[17] **F. Bravo Montero,** S. A. Vogler, and J. Camps Claramunt, "Equipo para marcaje de productos por LASER," ES2576962, 2015. *(patent)*

Patents previous to the admission at the doctorate program:

[18] J. Camps Claramunt, **F. Bravo Montero**, S. A. Vogler, and V. Boira Plans, "Chamber for laser apparatus with extruded base frame," US8388194, 2013.

[19] S. A. Vogler and **F. Bravo-Montero**, "Dispositivo y procedimiento para marcar mediante LASER un objeto en movimiento," ES2401499, 2013.

[20] S. A. Vogler and **F. Bravo-Montero**, "Device and process for marking a moving object by LASER," US8466944, 2013.

[21] S. A. Vogler and **F. Bravo-Montero**, “Device and process for marking a moving object by LASER,” EP2380693, 2011.

[22] J. Camps Claramunt, **F. Bravo-Montero**, S. A. Vogler, and V. Boira Plans, “LASER apparatus,” EP2214271, 2010.

[23] J. Camps Claramunt, **F. Bravo Montero**, S. A. Vogler, and V. Boira Plans, “Aparato LASER,” ES2324275, 2009.

Table of Contents

List of figures

List of tables

List of acronyms and symbols

List of Acronyms

ADC	Analog to Digital Converter
ANP	Analytic Network Process
AOD	Acousto-optic Deflector
AOM	Acousto-Optic Modulator
APD	Ablative Photodecomposition
API	Application Programming Interface
ASIC	Application Specific Integrated Circuit
AXI	Advanced eXtensible Interface
BW	Bandwidth
CAD	Computer-Aided Design
CISC	Complex Instruction Set Computer
CPU	Central Processing Unit
CT	Computing Throughput
CW	Continuous Wave
DC	Direct Current
DFE	Digital Front End
DLP	Digital Light Processing
DMD	Digital Micro-mirror Device
DPM	Direct Part Marketing
DPSS	Diode-Pumped Solid-State
DRAM	Dynamic Random-Access Memory
DSP	Digital Signal Processor
E^2PROM	Electrically Erasable Programmable Read-Only Memory **(**EEPROM)
EDA	Electronic Design Automation
EHPC	Embedded High-Performance Computing
EMC	Electromagnetic Compatibility
EOM	Electro-Optic Modulator
EOS	Electro-optical Systems
EUV	Extreme Ultraviolet
FIFO	First in, First out
f-LDA	Fiber-coupled Laser Diode Array
FMCG	Fast-Moving Consumer Gods
FPGA	Field Programmable Gate Array
GL	Gray level
GOPS	Giga Operations Per Second
GPC	General Purpose Computing
GPIO	General Purpose Input/Outputs
GS	Galvo Scanners
HDL	Hardware Description Language
HMI	Human Machine Interface
HP f-LDA	High Power Fiber-coupled Laser Diode Array
HPC	High Performance Computing
HPLD	High Power Laser Diodes

HPRC	High-Performance Reconfigurable Computing
HPS	Hard Processor System
I/O	Input/Output
I2C	Inter-Integrated Circuit
IC	Integrated Circuit
ICD	In-Circuit Debugger
IDP	Inline Digital Printing
IOE	I/O Elements
IoT	Internet of Things
IP	Intellectual Property
IPC	Instructions Per Cycle
IR	Infrared
ISA	Instruction Set Architecture
LASER	Light Amplification by Stimulated Emission of Radiation
LD	Laser Diode
LDA	Laser Diode Array
LE	Logic Elements
LIFT	Laser-Induced Forward Transfer
LIPSS	Laser-Induced Periodic Surface Structures
LSI	Large Scale Integration
LUT	Look Up Table
MASER	Microwave Amplification by Stimulated Emission of Radiation
MCU	Microcontroller Unit
MMA	Micro Mirror Array
MOEMS	Micro-Optic-Electro-Mechanical System
MOPA	Mater Oscillator Power Amplifier
MOS	Metal-Oxide Semiconductor
MOSFET	Metal-Oxide-Semiconductor Field-Effect Transistor
MPSoC	Multiprocessor System-on-Chip
NA	Numerical Aperture
NIR	Near Infrared
NoC	Network on Chip
NRE	Non-Recurring Engineering
NVRAM	Non-Volatile Random-Access Memory
OD	Optical Density
OEE	Overall Equipment Effectiveness
OPC	Operations per Cycle
OPSL	Optically Pumped Semiconductor Lasers
OS	Operative System
PARC	Palo Alto Research Center
PCB	Printed Circuit Board
PLD	Programmable Logic Device
PM	Polygonal Mirrors
PWM	Pulse-width Modulation
QoS	Quality of Service
R&D	Research and Development
RF	Radio Frequency
RIP	Raster Image Processor

RISC	Reduced Instruction Set Computer
RTL	Register-Transfer Level
RTOS	Real-Time Operative System
SaaS	Software as a Service
SCI	Serial Communication Interfaces
SDRAM	Synchronous Dynamic Random-Access Memory
SEM	Scanning Electron Microscopy
SLM	Spatial Light Modulator
SoA	State of the Art
SoC	System on Chip
SPI	Serial Peripheral Interface
TCB	Trusted Computing Base
TDLAS	Tumble Diode Laser Absorption Spectroscopy
TEM	Transverse Electromagnetic Mode
TET	Total Execution Time
USP	Ultra-short Pulses
UV	Ultraviolet
VCSEL	Vertical Cavity Surface Emitting Lasers
WCET	Worst Case Execution Time
XML	Extensible Markup Language

List of symbols

Symbol	Unit	Description
f	mm	Focal length
F	J/cm^2	Fluence: Laser energy density
I	W/cm^2	Irradiance: Laser power density
n	n/a	Refraction index
d_f	mm	Beam diameter at focal plane
Δt_p	ns	Pulse duration / width
Δt	µs	Pulse period
E_{ph}	J	Energy of each photon
h	J Hz^{-1}	Planck constant
c	m/s	Speed of light
λ	nm	Wavelength
v	Hz	Frequency
L	m	Cavity length
N	n/a	Integer
M^2	n/a	Beam quality
δ_p	mm	Optical penetration skin depth
α	mm^{-1}	Absorption coefficient
LD	mm	Diffusion length
Φ	W	Radiant flux / Power

$\boldsymbol{\pi}$	n/a	Pi number
$\boldsymbol{d_{spot}}$	µm	Spot diameter
$\boldsymbol{F_{th}}$	J/cm^2	Fluence threshold: Laser energy density
$\boldsymbol{Q_e}$	J	Radiant energy
$\boldsymbol{\Phi peak}$	W	Peak power
$\boldsymbol{\Phi_{avg}}$	W	Average power of the system
$\boldsymbol{f_p}$	kHz	Pulse repetition rate
$\boldsymbol{V_{sc}}$	m/s	Scribing speed
$\boldsymbol{t}$	s	Scribing time
$\boldsymbol{x_{pitch}}$	µm	Dot pitch
$\boldsymbol{AR_p}$	n/a	Aspect ratio of the area irradiated by the pulse
$\boldsymbol{I_{preheat}}$	W/cm^2	Irradiance provided by the preheat
$\boldsymbol{d_{preheat}}$	cm	Diameter of the circular area affected by the preheat
$\boldsymbol{l_{path}}$	mm	Length of the scan path
$\boldsymbol{A_w}$	mm	Width of the marking area
$\mathbf{V}_{\boldsymbol{line}}$	m/min	Line speed
$\boldsymbol{\theta_{max}}$	rad	Maximum deflection angle
$\boldsymbol{\omega_{max}}$	rad/s	Maximum angle speed
$\Delta\boldsymbol{\theta min}$	rad	Resolution of the angle values
$\boldsymbol{A}$	mm	Aperture
$\boldsymbol{I}$	kg m^2	Moment of inertia
$\boldsymbol{T}$	%	Transparency / Efficiency
$\Delta\boldsymbol{X_{min}}$	mm	Linear resolution
$\boldsymbol{V_{sc\,def}}$	m/s	V_{sc} according to deflection system
$\boldsymbol{A_h}$	dots	Marking area height
$\boldsymbol{w_0}$	mm	Beam size / Spot radius
$\boldsymbol{V_x}$	m/s	Speed in the *x* direction
$\boldsymbol{l_w}$	µm	Line width of a marked line
$\boldsymbol{L_c}$	n/a	Number of laser diode columns
$\boldsymbol{BE}$	kJ/mol	Bond enthalpy
$\boldsymbol{\lambda_{th}}$	nm	Required wavelength to break the molecular bond
$\boldsymbol{L_{max}}$	ms	Maximum process latency
$\boldsymbol{\varepsilon_{max}}$	µm	Maximum acceptable position error
$\boldsymbol{I_{max}}$	kW/cm^2	Maximum irradiance
$\boldsymbol{I_h/I_w}$	Pixel	Number of pixels
$\boldsymbol{P_h/P_w}$	mm	High and width of the image to print
$\boldsymbol{m}$	O	Operations per pixel
$\boldsymbol{M}$	O	Operations per image
$\boldsymbol{BW}$	Mbps	Bandwidth
$\boldsymbol{CT}$	GOPS	Computing throughput

1. Introduction

This thesis is related to an Industrial Ph.D. promoted by Macsa that is considering this project inside its strategic R&D. We research, design, and develop marking methods and control systems that will allow the development of new laser marking and printing systems for industrial environments. The aim is to cover the current gap that exists in marking and printing in high-performance production lines.

1.1. Background and Motivation

Laser printing, in a broad sense of the concept, is a digital printing process. Produces high-quality text and graphics by passing a laser beam over a surface (usually paper) to define an image. Laser marking is the process of labeling parts and materials with a laser beam. In this sense, different processes are distinguished, such as etching, removal, dyeing, annealing, and foaming.

A product code is an identifier, assigned to each finished/manufactured product that is ready, to be marketed or for sale. Package labeling is any written, electronic, or graphic communication on the package or on a separate but associated label.

Industrial marking and printing systems are typically integrated into high-speed production lines to generate visible marks on produced goods. The technologies used to imprint them include mechanical engraving, ink deposition, laser marking, and others. Given this variety of methods, the most appropriate ones are selected depending on the type of surface material to treat and the cost required to install and operate the equipment.

Companies that need to mark their products face many challenges in terms of productivity and high-quality product coding since traditional marking systems do not always provide the optimal result they are looking for.

The objectives of intelligent packaging processes are to guarantee the traceability of each product unit as well as to facilitate engagement and communication between the manufacturer and the end customer. Current marking and printing technologies do not reach the high printing speed required by actual industrial high-performance production lines.

This thesis addresses the problem of implementing efficient systems for marking and printing addressing the required coupling of the two key enabling technologies: photonics and electronics through, more specifically, proposing embedded systems architectures controlling the laser marking systems. I propose FPGA-based embedded systems controlling high-performance digital laser printing and marking systems to reach an optimal trade-off between the high speed and high quality as required by industrial high-performance production lines for intelligent packaging.

The literature related to high-performance laser marking and printing belongs to many different fields of research. To cite some examples: laser printing [1], laser marking [2][3][4], laser systems [5], industrial machine architectures, photonics and optoelectronic devices [6][7], digital printing, printing control, image forming [8][9], image processing [10], digital light processing [11][12][13], real-time processing, marking on-the-fly [14], data pumping, embedded systems, field programable gate arrays, systems on a chip, chip multi-soft-core processors [15], parallel embedded computing, high-performance computing, embedded systems software architecture, scalable parallel architectures [16], etc.

Laser marking is a method for labeling the surface of products with 2D codes, barcodes, logos, human-readable characters, etc.; to indicate manufacturing dates, expiry dates, serial numbers, part numbers, etc.

Laser marking is based on the optical appearance changes caused on a surface by a laser beam [17] using different techniques such as vector scanning, raster scanning, projection, or masks. The energy of the laser beam can induce physicochemical processes such as pyrolysis, melting, annealing, vaporization, and photochemical decomposition. As a result, lasers are being used for etching, engraving, ablating, welding, cutting, carbonizing organic materials, transforming pigments, expanding a polymer, generating surface structures, and other processes of industrial interest [3][4].

Plastics, cardboard, paper, acrylic, are often marked with CO2 lasers (wavelengths around 10 μm). For metallic surfaces, used wavelengths are in the region of 1 um, which can be obtained with Nd:YAG lasers, laser diodes, or fiber lasers. Other shorter wavelengths, such as 532 nm, can be advantageous in certain applications. Typical laser powers used for marking are on the order of 10 to 100 W.

Laser systems for marking applications must meet some demands. A certain optical irradiance and fluence thresholds must be achieved on the surface to be printed for a satisfactory marking process. This requires a suitable combination of laser power, laser energy, beam diameter, and pulse duration. High resolution means small spots, but also a reasonable working distance is required; this means that a high-quality beam is a must. For fast processing, the laser source must provide a high enough pulse repetition rate, which together with a threshold pulse energy means a certain average power.

Other requirements for laser marking systems are accurate positioning of the beam, high reproducibility, high speed, flexibility, high efficiency, and low operating cost. The laser setup must be compact enough for saving a footprint on the production floor and not requiring complex cooling. The total cost of ownership (installation, lifetime, and maintenance) should be moderate. Since industrial environments can be harsh, a robust laser design is essential for reliable operation.

Due to its adaptability and print quality, laser marking has been able to meet the challenges of innovative materials and new product designs. Laser marking technology has great flexibility in automation. Direct writing of digital patterns can be set by

computer-controlled synchronization of laser beams and the advance of the surface to be printed.

Laser markers have outstanding advantages compared to other marking technologies. They can mark with high quality even in materials that complicate the readability and contrast of the marks. A correctly designed laser system will be able to modify the optical appearance of a surface without compromising the sealing while ensuring that the information is highlighted and can be red correctly. In addition, with appropriate laser management software, the design to be marked can be adapted to any packaging, improving the perceived product quality. The laser produces a permanent mark on a wide range of materials, even if it gets wet or wrinkled, which is crucial for traceability information.

For many surfaces, laser marking is used as the most cost-effective option. Moreover, it often has a lower environmental impact than competing technologies [18]. One of the benefits of laser technology is that they use little or no added material to produce marks. This eliminates the use of consumables thus, helping to reduce the economic cost. Other alternatives, like ink printing, require large material deposition and need a drying phase, which reduces the processing speed and increases the dimension and cost of lines. The environmental impact of laser marking is low although in some cases relevant. A different number of wasting materials are produced depending on the technique. For instance, one of the common laser-based techniques used on inorganic surfaces is ablation. It volatilizes surface material thus creating small particles that must be removed with vacuum cleaning systems.

Materials of vegetable origin such as wood, paper, cardboard, or textile fabrics are typically marked with ablation or carbonization. They present some additional difficulties compared with other surfaces based on synthetic materials. Being natural products, they are intrinsically irregular. This is important when analyzing the effect of laser beams on them. For wood and cork surfaces, the surface irregularity does not have any big impact as they are typically thicker than the effect of the laser beam on them. This allows some tolerance factor on the beam parameters that produce marking differences that are often unnoticed to the human eye.

Paper, cardboard, and organic textiles are much thinner. They represent a more challenging scenario that does not allow such big tolerances in the laser beam characteristics. Small differences can cause a visible change, and surface irregularities can cause a major difference in the final marking results. However, marking these surfaces has great industrial interest as packaging is usually based on paper or cardboard. If laser ablation is used on these surfaces, there is the risk of perforating the material. If carbonization is used, a lot of debris can be produced, and it is hard to avoid polluting the production line without incurring added costs. There is also a risk of setting fire when not used in an inert ambient. The inert ambient also increases the economic cost.

There have been some attempts to print without ink using carbonization of the organic surface (such as [19]), but the products created in the process require some extra

industrial processes either to remove them or to stick them on the same printed surface. Again, those processes increase the overall system economic cost. Other strategies try to reduce the power to avoid the volatilization of residues, but the printing contrast does not suffice to meet industrial requirements.

The laser can mark in difficult production environments (humidity, temperature, dust), unlike other marking systems. Laser marking can increment the production line productivity compared to other methods while requiring minimum maintenance and significantly reducing the need for operator intervention so that coding does not slow or stop production.

The advantages of laser marking hardly can be achieved without an appropriate marking method and control system. As an essential part of a production process, laser marking systems must often be integrated into high-speed production lines. Therefore, they must be carefully designed to avoid becoming a system bottleneck.

Furthermore, production lines usually require printing product-dependent variable (and often unique) information with resolutions, speed, and print width values that are not covered by the state of the art of marking technologies. As an example, as far as we know, there is no industrial laser marking system in the literature that can be integrated into a production line and can print unique variable codes, with high precision and reproducibility, at line speeds higher than 8 m/s, with reasonably low operational costs.

1.2. Aim and Objectives

In this thesis, I propose marking methods and control systems that will allow the development of new laser marking and printing systems that, to the best of our knowledge, do not exist nowadays, and that will cover the current gap in the industry.

These laser systems will allow digital packaging, facilitating traceability, ensuring that food is processed and packaged correctly, the retailer receives the right products, in the right quantities, at the right time, ensuring more effective management of manufacturing, and packaging is recycled efficiently.

This thesis discusses how to solve the problem of developing high-performance digital printing and marking solutions capable to be integrated into high-speed production lines. Specifically, I detail how industrial laser marking systems can be designed for printing on the fly variable codes, to be integrated into a production line running at speeds up to 16 m/s. I also explain how to design a scalable modular system implemented in an embedded platform that will control the individual laser beams; and how to design and implement the parallel processing system using FPGA technologies.

The final goal of this work is to create a novel high speed, high quality, and high performance in-line digital laser marking and printing solutions to print variable data (2D

codes, bar codes, expiry dates, logos, etc.), synchronizing laser beams and product motion in real-time conditions, with low latency and low jitter.

These laser systems can extend the current marking and printing ranges to resolutions between 50dpi and 300dpi, images of widths ranging from 6 mm to 100 mm, at product speed up to 16 m/s (above the speed of any production line in the industry), creating up to 100 unique 2D codes per second. These can work with high marking precision producing high-definition marks without quality loss. These laser systems could print with precisions in the order of microns, for which 2D codes (QR, DataMatrix, etc.) would meet Grade A high-definition criteria [20].

Our goal is to use these printing systems for unique serialized coding so that better insights about the consumer (such as profile, location, and time of purchase) can be obtained; as well as the control over every produced article that provides traceability information to the producer, distributor, consumer or administration thus contributing to the new Industry 4.0 scenario.

This thesis also discusses how to create laser marking systems that can print with minimal debris and the quality of the printing is superior in terms of contrast and resolution with previously known methods.

Current technologies based on the sequential work of a single laser beam can never attain speeds of high-performance production lines. Parallel processing of multiple laser beams can overcome the current speed limitations of printing variable data in real time.

Although sufficiently fast scanning systems already exist (using galvanometers, polygonal scanners, etc.) [21][22][23][24][25][26], marking processes that use a single laser beam cannot reach the fluence threshold of the surface to be printed in the time required by the high-performance production lines. I will show that it will be possible to implement a laser marking method and a control system that allow printing variable codes at speeds exceeding 16 m/s, using parallel laser beams controlled by a high-performance embedded system.

This thesis details the specifications, theoretical foundations, the design and implementation of embedded platforms for the image processing together with FPGA modules, using cutting-edge technologies, and the management of a high number (up to hundreds) of laser beams operating in parallel. This complete system allows achieving high-performance digital laser marking and printing systems, capable to be integrated into high-speed and high-quality production lines.

This thesis also discusses that using a laser source with the appropriate wavelength preheating the printing area, it is possible to create laser marking systems that print with high contrast, producing minimal waste while increasing the speed.

I plan to experimentally demonstrate the previous hypotheses by researching, designing, and developing new laser systems for industrial environments. I have contributed to building prototypes and reached to test them experimentally.

This thesis explains the research I have done on the projects of the R&D line of marking and printing with multiple laser beams, of which I have been the technical representative of Macsa. To date, and since I started my industrial doctorate, there have been almost 6 years of collaboration with a dozen companies, research centers, and universities, with the participation of about fifty engineers. It is in this context that I speak in the first person when I have made outstanding contributions to this thesis, and in the plural when I speak about developments or joint research with other engineers or researchers, especially at the UAB.

The research work is developed on the main components of a laser marking system: interaction of laser beams and the marking surface (thermo-chronic additive [27], cardboard, paper [28], paint, etc.), laser sources (wavelengths, power levels, optics configuration, and temporal dynamics), marking methods (multiple laser beams instead of a deflection system) as well as the computation and communication system. The work is especially focused on the development of high-performance embedded systems for digital laser marking and printing.

I have verified the hypothesis since, under the same conditions in which current systems fail to meet the requirements of high-performance production lines, the systems I propose can meet these requirements. I am currently testing these solutions on real production lines. And I am verifying that it is possible to print the required information at the required speed. The prototypes developed from our proposal are being accepted by customers that validate the final prototypes.

1.3. Overview of this thesis

This thesis is organized in the following way:

Chapter 2 provides an overview of relevant background information on the concepts related to industrial laser marking and digital printing and introduces its performance drivers. It describes the dependencies introduced by the surface to be marked (material properties, textures, shapes, etc.) in the system performance; it also analyzes the different features of laser sources (wavelength, pulse duration, radiant flux, etc.) and their performance implications for printing and marking applications (physicochemical processes triggered by different fluences, irradiances, etc. in different material surfaces); and describes the laser beam deflection methods. This chapter focuses on paper and cardboard substrate materials to be printed as especially relevant materials for printing and marking applications and reviews previous attempts to print without ink.

Chapter 3 describes the experimental equipment and methods for building multibeam laser marking systems. It presents how multibeam methods increase the performance of the laser systems. This chapter shows my proposals for printing methods with multibeam systems: (1) printing using a thermochromic coating (IR color activation); (2) marking by ablating the surface material; (3) printing for different wavelength multibeam laser systems (pyrolysis and carbonization). The chapter also analyzes the computing requirements for the laser controller system.

Chapter 4 presents a method for marking objects made of paper, cardboard, and/or fabric with low residue generation. It details how the proposed multibeam laser systems overcome the printing speed, resolution, and width limitations of current single-beam laser systems, analyzing how the marking results on paper and cardboard depend on the wavelength and showing the experimentation results.

Chapter 5 gives an overview of the embodiments of the proposed systems by presenting the implementation details of the controller; discussing a Laser Diode Array multi-beam system, a fiber-optic coupled LDA system, and an f-LDA system using high power laser sources. This chapter describes how we implemented several methods for multibeam laser marking using industrial means and analyzes how the constraints previously shown in chapter 3 could affect the performance of future systems.

Chapter 6 shows the economic trade-off that appears when we add laser sources to increase resolution and print width and discusses my proposal based on the use of micromirrors arrays (MMA) and spatial light modulators (SLM).

Finally, chapter 7 presents the main conclusions of my research and discusses the remaining open challenges, mapping out potential future industrial applications and providing suggestions for future work.

2. Industrial laser marking and printing

A LASER is a device that emits light through a process of optical modification based on the stimulated emission of electromagnetic radiation. The laser would not have been possible without an understanding that light is a form of electromagnetic radiation.

2.1. Background

Max Planck [29] deduced the relationship between energy and the frequency of radiation. The theoretical foundation of the laser was established by Albert Einstein in 1917 [30], who predicted that excited atoms could convert stored energy into light by a process called stimulated emission. Charles Townes [31] demonstrates the first MASER (microwave amplification by stimulated emission of radiation), the first device based on Einstein's predictions. Gordon Gould [32][7] discovered that photon emission could be stimulated by other photons when atoms are in an excited state. Gould wrote down his ideas for building a laser in his notebook in 1957. It is considered the first use of the acronym LASER, light amplification by stimulated emission of radiation.

Laser systems take profit from this phenomenon to create coherent, monochromatic, and collimated light beams. Gould applied for laser-related patents in 1959. But Townes and Schawlow were granted a US patent for the optical maser in 1960. With their application denied, Gould launched what would become a 30-year patent dispute related to laser invention [33]. The first functioning laser was operated by Theodore H. Maiman at Hughes Research Laboratories, California in 1960 [34]. Since that, laser techniques have been widely used in many scientific, engineering, and industrial fields.

From a historical perspective, laser technology has evolved in several directions. Hecht [5] has a good account of the progress done in several directions after its discovery. After the initial research works, the development of CO_2 gas lasers was an important step, since it increased significantly the maximum possible radiant flux. Nd:YAG lasers allowed to work with shorter (more energetic) wavelengths and smaller dot sizes. Optical pumping with Q-Switches allowed increasing peak power on many laser systems. Then, excimer lasers allowed working on the ultraviolet region, opening new opportunities by using very high energetic photons. New advances were made on reducing the pulse width to the femtosecond range. Then, the use of fibers gained popularity. Diode lasers have been integrated into large-scale integrated circuits and are used in silicon photonics, especially for communications. But lasers continue to be of great interest to many industrial applications. Some of the more recent lines of research are addressing shorter pulses in the attosecond range tunable wavelengths and many other material-specific challenges.

Lasers and embedded systems are enabling technologies that complement each other and follow a parallel evolution. The MOS LSI technology applied to computing was the basis for the first embedded systems in the early 1960s. The first single-chip microprocessor was the Intel 4004, released in 1971. In the early 1980s, the memory and input-output systems were integrated into the processor forming a microcontroller. Nowadays, embedded systems are found in all areas of the economy: industry, consumer, automotive, electrical appliances, medicine, telecommunications, etc.

From a commercial perspective, lasers have become essential to many industries, growing their impact exponentially since their invention. Early 1963 Barron's magazine estimates annual sales for the commercial laser market at $1 million. In the early 2020s estimates annual sales are around $17 billion [35]. Laser continues to perform well in many sectors of the market: optical components and systems, defense photonics, solar energy, flat panel displays, lighting, information technology, optical communications, medical technology and life sciences, measurement and automated vision, production technology, etc. The use of lasers is essential in critical sectors of the economy. Laser-powered lithography today is basic for the semiconductors industry, for instance. Global semiconductor revenue will grow to $545 billion in 2021 and over $600 billion in 2022 [36].

Maiman's assistant joked that the laser was "a solution looking for a problem". Under appropriate conditions, a laser beam can modify the optical appearance of a surface that it hits. The high energy of the beam can induce physicochemical processes such as pyrolysis, melting, annealing, vaporization, or photochemical decomposition. As a result, lasers are being used for etching, engraving, ablating, welding, cutting, transforming pigments, and other processes of industrial interest as described in detail by Eichler et al. [37]. See below for several examples of industrial applications showing that to date the development of laser applications in the industry is not finished yet.

We do not believe that there is a single laser technology that can be used for most applications. Best-in-class quality for each laser material process requires optimal parameters, which consequently define the specifications of the applied laser source. The industry offers a wide range of laser sources for high-tech industries: wavelengths ranging from extreme ultraviolet (EUV) to far-infrared (FIR), a full bandwidth of laser pulse duration from continuous wave (CW) up to ultra-short pulses (USP), modulated up to an MHz range and high-power lasers (up to petawatt). We can find an unimaginable number of laser applications in the industry [14] [38]:

- Sheet metal and non-metal cutting
- Cleaning surfaces by laser without causing damage.
- Remote laser welding
- Micromachining by ultra-fast lasers: fuel injection nozzle drilling, display glass cutting, sapphire cutting, ceramics ablation, cardiovascular stent cutting, thin-film ablation, etc.

- Manufacture of flat panel displays with laser (patterning of functional layers, laser transfer technique, silicon laser annealing, laser technique to repair broken conductors, laser technique for clean cutting of glass, etc.)
- Laser fabrication such as via-hole drilling, surface texturing, and FPCB cutting.
- Laser cladding involves creating a new surface on a base material to improve surface properties.
- Solar cell laser processing.
- Laser digital converting: turning web-type materials into performed packaging (cutting, scoring, slitting, perforating, etc.)
- Production of images, cutouts, and fake 3D effects on jeans.
- Precision instrumentation, for example, laser interferometers for machine tool diagnostics.
- Life science instrumentation such as tunable diode laser absorption spectroscopy (TDLAS).
- Medical and aesthetic applications such as brain or eye surgery and laser hair removal.
- And a long list of applications.

The laser is a key enabling technology for microelectronics. Innovations in the use of 13.5nm light set the stage for volume introduction of 7, 5, and 3 nm nodes [39]. The architecture of a high-power CO_2 laser is of great importance in successfully scaling the EUV power emitted by the laser-produced plasma. A 30 kW Master Oscillator Power Amplifier (MOPA) CO_2 laser system serves as a drive laser for the generation of high harmonics in tin (Sn) droplets at 13.5 nm wavelength (EUV) for microlithography systems. This approach currently represents the most promising way to produce the next generation of microchips [40]. Promising progress in EUV lithography with a high numerical aperture (NA) will help advance Moore's Law in the next decade with the 2 nm node [41].

Another of the most widespread applications in the industry is laser marking. The evolution of laser marking systems is the story of two developments: on the one hand, highly specialized equipment and, on the other, low-cost, low-maintenance general-purpose equipment. Historically, the electronics and semiconductor industries have been two of the most important industries for laser marking. Other important markets include the consumer packaging, medical, automotive, and aerospace industries. One of the early successes was the use of CO_2 TEA lasers to mark date and batch information on beer bottles. Another prominent application is marking ceramic capacitors. One of the major applications of excimer lasers is mark tefzel and Teflon cables for the aerospace industry. Other laser marking applications include marking on contact lenses, marking 2D codes used on flat panels and other high-value glass substrates, and laser marking systems for printed circuit boards (PCB).

Highly specialized marking equipment generally requires special software and user interface. Very often, they also use automation and robotics. There are systems with better precision and repeatability of beam positioning with better control and stability of

laser energy. An example of laser marking evolution is the development of wafer serialization [42]. The first laser marking system for wafers was based on a lamp-pumped Nd:YAG laser. Wafer processing technology has changed dramatically, as well as the requirements for applying the marks used to record batch numbers, process parameters, etc. In the early days of large lithography, 5 to 20 μm deep marks were sufficient. The main concerns were the legibility and durability of the markings. As device sizes were reduced to submicron levels and the number of process steps increased, the industry placed more stringent requirements on the depth of marks, spatter, and debris. Therefore, other types of marks were developed using diode-pumped solid-state lasers. Later, when the debris become the most important concern of the process, a specialized super-stable solid-state laser was developed, to generate marks without producing debris.

In addition to the equipment, new materials and additives for laser marking have been studied and developed. While lasers can mark almost all types of industrial materials, the quality of the marks is not always good enough for all applications. One of the technologies used to improve marking is to add special additives to the material. This is particularly effective for plastics.

In summary, laser marking systems have been improving, both in specialized equipment and in versatile markers for general use. New types of lasers, such as ultra-fast lasers, will continue to change the landscape of laser marking applications

2.1.1. Fundamentals of lasers

LASER is an acronym for light amplification by stimulated emission of radiation. Devices operating on this principle at higher frequencies than microwaves (infrared, visible, ultraviolet, X, and gamma rays) are termed lasers. MASERs are devices that operate with this principle in the microwave or lower radio frequencies.

In a conventional light source, excited atoms produce spontaneous emission (without interrelationships between individual photons). The process of stimulated emission begins with an excited atom which produces a photon by spontaneous emission that reaches another excited atom; the interaction stimulates that atom to emit a second photon with identical properties to the first one (wavelength, direction, phase, and polarization) [43]. This process is multiplicative. This ability to "amplify" light in the presence of a sufficient number of excited atoms leads to an "optical gain" which is the basis of laser operation (Figure 1).

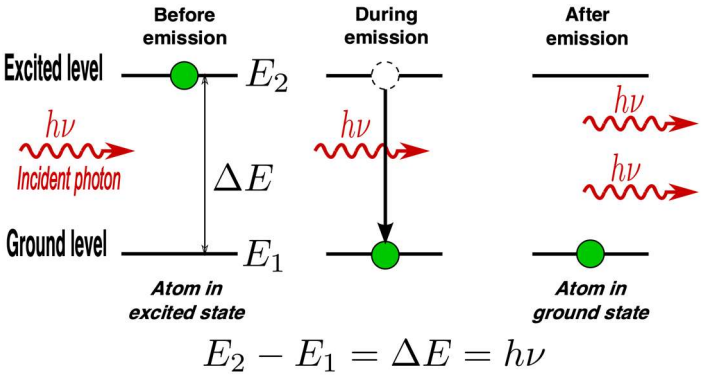

Figure 1: Stimulated Emission [44]

A laser comprises: (i) an active medium, also called gain medium or lasing medium; (ii) a mechanism for energizing; and (iii) and optical feedback [45]. In the process of generating laser, the medium (which may be solid, liquid, gas, or plasma) is excited by a pump source to the amplification status wherein the light of a specific wavelength increases in power. Pump sources can be flash lamps, lasers, electrons, chemical reactions, ion beams, or x-ray sources [46]. The two most common pump sources are optical and electrical. For optical pumping, the most common is another laser. Electrical pumping can be performed by DC (as laser diodes), an electric discharge (noble gas lasers and excimer lasers), or radio frequency discharge (some CO_2 lasers).

For most lasers, it is necessary to increase the gain with multiple passes through the laser medium. This is implemented along an optical axis defined by a set of mirrors that produce feedback, which allows the stimulated emission to predominantly amplify an optical frequency (Figure 2).

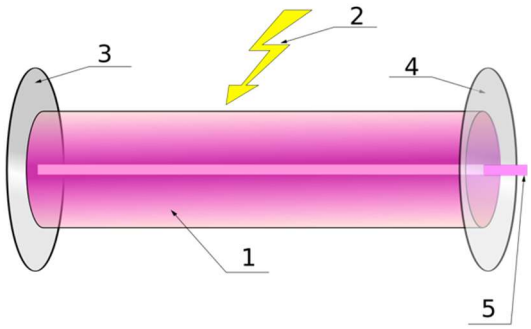

Figure 2: Components of a typical laser: 1. Gain medium, 2. Laser pumping energy, 3. High reflector, 4. Output coupler, 5. Laser beam [47]

The gain medium of a laser is a material of controlled purity, size, concentration, and shape. Its particles can interact with light by absorbing or emitting photons. When the number of particles in an excited state exceeds the number of particles in some lower-energy state, population inversion is achieved. In this state, the stimulated emission rate is higher than the light absorption rate in the medium, and therefore the light is amplified.

The laser medium is positioned along the optical axis of the resonator which, with a very high optical gain, also becomes the direction of propagation of the laser beam. The

simplest cavity is defined by two facing mirrors: a total reflector and a partial reflector. The light bounces gaining strength with each pass through the gain medium. As the laser light is amplified, part of the light escapes the oscillator through the partial reflector. When balanced (for CW), these "optical losses" are compensated with optical gain within the cavity. If the gain (amplification) in the medium is greater than the resonator losses, then the power of the recirculating light can increase exponentially. But each stimulated emission event returns an atom from its excited state to the ground state, reducing the gain of the medium. When the net gain (gain minus loss) is reduced to unity the gain medium is saturated. In a continuous wave laser (CW) an equilibrium value of the laser power occurs within the cavity; this balance determines the operating point of the laser. If the pumping power is too small, the gain will never be enough to overcome the cavity losses and no laser light will occur. The minimum pump power required to initiate laser action is called the lasing threshold. The laser output is the part of the beam transmitted by the output coupler. In an ideal laser, all photons in the output beam are identical, resulting in perfect directionality and monochromaticity. This determines the unique coherence and brightness of a laser source.

The energy of each photon is given by Eq.*(1)*, where h is the Planck constant, c the speed of light, λ the photon wavelength, and v photon frequency.

$$E_{ph} = \frac{hc}{\lambda} = hv \qquad (1)$$

An ideal laser would emit all photons with the same energy, and therefore the same wavelength, and would be perfectly monochromatic. Real lasers are not perfectly monochromatic due to various mechanisms that widen the frequency (and energy) bandwidth of the emitted photons.

The exact wavelengths or lines are determined by the characteristics of the laser medium. For example, CO_2 lasers emit in the range between 9.3 and 10.6 microns, depending on the composition of the gas, while crystals lasers based on neodymium (as YAG or vanadate) produce wavelengths in the range between 1047 and 1064 nm. Each laser wavelength is associated with a line width, which depends on various factors such as the gain bandwidth of the laser medium and the design of the optical resonator, which may include elements to deliberately narrow the line width, such as filters or etalons. However, even a single laser line covers a range of wavelengths. For example, laser diodes produce light in a wavelength range of several nanometers corresponding to their gain bandwidth.

In addition to sharing the same wavelength, the photons that make up a laser beam are all in phase (coherent), resulting in an electric and magnetic field that propagates with a uniform wavefront. Spatial coherence allows a laser to focus on a narrow point and allows a laser beam to remain narrow over long distances (collimated). Well-designed lasers produce a beam of light that will expand (diverge) only by the minimum amount prescribed by the diffraction laws. For example, diffraction dictates that the minimum spot that a laser beam can produce is approximately equal to its wavelength.

Resonance is a factor in the amplification of the laser intensity. Depending on the wavelength of the stimulated emission and the length of the cavity, the waves reflected from the mirrors will either constructively interfere and be strongly amplified or destructively interfere and cancel the laser activity. Since the waves within the cavity are all coherent and in phase, they will remain in phase when reflected off the mirrors if the length of the cavity is equal to an integer number of wavelengths. Therefore, after making a complete oscillation in the cavity, the light waves have traveled a path length equal to twice the length of the cavity. Eq. (2) defines the resonance condition that must be met for strong amplification to occur in the laser cavity, where N is an integer, λ is the wavelength, and L is the cavity length

$$N\lambda = 2L \qquad (2)$$

Figure 3 illustrates a typical example in which various resonance values of N, called longitudinal modes of the laser are matched to the gain bandwidth.

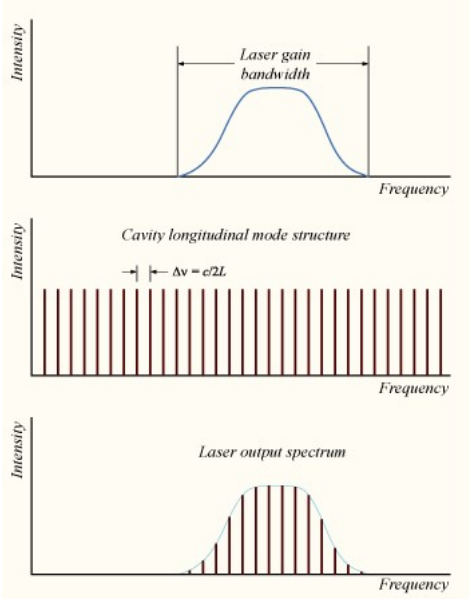

Figure 3: Gain bandwidth and cavity resonance modes [48].

The design of the resonator also affects the transverse modes, responsible for the intensity distribution in the plane perpendicular to the direction of the beam. The ideal laser beam has a radially symmetrical cross-section: the intensity is greatest in the center and fades at the edges, following a Gaussian profile. This corresponds to the fundamental, transverse electromagnetic output mode TEM00. Lasers can also produce many other TEM modes, some of which are shown in Figure 4. In the multi-transverse mode operation, many modes are present at the same time, which often results in a profile that appears to be gaussian but has degraded properties (greater divergence and lower radiance). Often, the quality of a laser beam is specified by the parameter M^2. For example, a YAG laser that operates exclusively in TEM00 mode has $M^2 = 1$, while multimode laser diodes have M^2 in the hundreds.

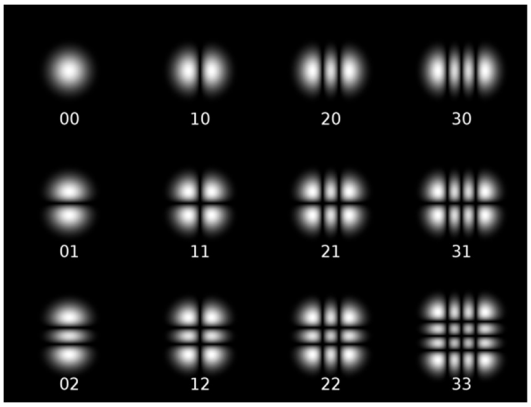

Figure 4: Lasers can emit any number of transverse modes, of which the TEM00 usually is most desirable [49].

The brightness of a laser is increased if its beam quality (M^2) is improved for a fixed output power level. The radiance (brightness) is defined as the amount of light coming from the source per unit of area and unit of solid angle. This can be expressed in terms of the beam quality factor, M^2, as (Eq. (3) [50], which shows the paramount relevance of the transverse modes and the wavelength.

$$R = \frac{\Phi}{a\,\Omega} = \frac{\Phi}{(M^2)^2\,\lambda^2} \qquad (3)$$

By its mode of operation, we can classify a laser as continuous or pulsed, depending on whether the power output is essentially continuous in time or if it takes the form of light pulses on some time scale. A laser whose output is normally continuous can be intentionally turned on and off at a certain speed to create pulses of light, then it is classified as a modulated continuous wave (CW) laser.

Most CW laser applications require the power to be as stable as possible. To ensure this stability also in the presence of varying environmental conditions such as the temperature and aging of the laser itself, control loops are implemented using embedded systems. For continuous wave operation, it is required to continuously replenish the population inversion of the gain medium by a constant pump source. In some laser media, this is impossible. These lasers cannot work in CW mode.

Pulsed operation of lasers refers to any laser not classified as a continuous wave so that the optical power appears in pulses of a certain duration with a certain repetition rate. The most important characteristic of a pulsed laser is the ability to store and release energy very quickly, that is, on a nanosecond scale, so that the laser output can reach tens of kilowatts to megawatts of peak power. Some materials, such as excited dimers (excimers) of a noble gas with a halogen, such as ArF and XeCl, maintain laser action for only a short period of several nanoseconds. Other lasers, such as Nd or Yb diode-pumped solid-state (DPSS) lasers, can be both CW and pulsed. Other lasers, such as laser diodes (LD) or Optically Pumped Semiconductor Lasers (OPSL), are not suitable for pulsed operation. Pulsed lasers are especially useful for a wide range of manufacturing processes. The high peak power allows ablative processing of materials in which a small volume of material on the surface of a workpiece can evaporate if it is heated in a very short time, whereas if the power is supplied gradually then the piece absorbs heat without reaching a

sufficiently high temperature at a determined point. The high peak power can also cause several non-linear optical processes, i.e., processes which are based on the interaction with matter of more than one photon at a time.

In a nanosecond pulsed laser, techniques such as Q-switching are used to build and produce short, energetic pulses. Q-switching can be conceptualized as a two-mirror cavity with an optical gate located between one of the mirrors and the laser medium. The key is to store pump energy in the atoms or molecules of the laser medium avoiding laser gain and the amplification process. Then when the stored energy is at its maximum, the laser action is quickly enabled: the stored energy results in extremely high laser gain (amplification), and a giant pulse is formed. A fraction is coupled by the partially transmissive mirror. The result is a pulse with a typical duration of 1 to 200 ns. Q-switching lasers (commonly used in industry) can produce average powers of up to tens or hundreds of kilowatts and repetition rates from 10 Hz to 200 kHz. Most industrial processes are in the tens of kilohertz regime. The Q-switch device is an acousto-optic modulator (AOM) or an electrooptic modulator (EOM). Both use crystals where an applied electric field produces some disturbance of the optical properties of the crystal.

Another method of achieving pulsed laser operation is to pump the laser material with a source that is itself pulsed, either through flash lamps, or another pulsed laser.

An entirely different type of laser is ultrafast lasers, which generally produce pulses in the range of 5 fs to 100 ps generated by mode-locking. In industrial applications, ultrafast amplified pulses are increasingly used in material processing applications that require ablation or materials modification without any residual thermal effect, such as thin-film modeling in the production of flat panel displays or to cut tempered glass for touch screens. Femtosecond's laser pulses have two advantages over picosecond pulses for materials processing. First, the interaction with the material involves many simultaneous photons and becomes reasonably wavelength insensitive, as opposed to linear absorption in nanoseconds. Second, short pulses and non-linear interaction mean that fs pulses can deliver even better edge quality and precision than ps pulses.

The optical bandwidth of a pulse cannot be narrower than the reciprocal of the pulse width. In the case of extremely short pulses, this implies the use of lasers at a considerable bandwidth, quite the opposite of the very narrow bandwidths typical of CW lasers.

Laser technology is a diverse field, using a wide range of very different types of laser gain media, optical elements, and techniques. The workhorses of industrial laser applications are Nd:YAG, CO2, fiber, and laser diodes [51].

Semiconductor lasers can be pumped electrically or optically. They can generate efficiently very high output powers with a deficient beam quality or low output power with good spatial properties (e.g., for use in CD and DVD), or pulses with very high repetition rates (e.g., for telecommunications applications). Special types include quantum cascade lasers and surface-emitting semiconductor lasers (e.g., VCSEL). Direct

diode lasers offer the lowest cost per watt of any type of industrial laser, as well as the lowest operating costs, due to their high electrical efficiency. Direct diode lasers predominantly serve low brightness applications such as heat treating, coating, and some welding applications. On the downside, high-power laser diodes or arrays cannot deliver anything like the limited diffraction beam provided by other types of lasers.

Solid-state lasers based on crystals or glasses doped with ions (doped insulator lasers) pumped with discharge lamps or laser diodes, can generate high output power or lower powers with a very high beam quality, purity, and spectral stability or ultrashort pulses with durations of picoseconds or femtoseconds. Common gain media are Nd:YAG, $Nd:YVO_4$, Nd:glass, Yb:YAG , Yb:glass, Ti:sapphire, etc.

A special type of ion-doped glass laser is fiber lasers, based on glass optical fibers doped with ions in the core. Fiber lasers can reach output powers of up to kilowatts with high beam quality, allow broad wavelength tunable operation width narrow linewidth.

Gas lasers and excimer lasers are based on gases normally excited by electrical discharges. Frequently used gases include CO_2, argon, krypton, and gas mixtures such as helium-neon. Common excimers are ArF, KrF, and XeF. These lasers are also called molecular lasers.

Figure 5 shows laser types with distinct laser lines (above the wavelength bar), and lasers that can emit in a wavelength range (below the wavelength bar).

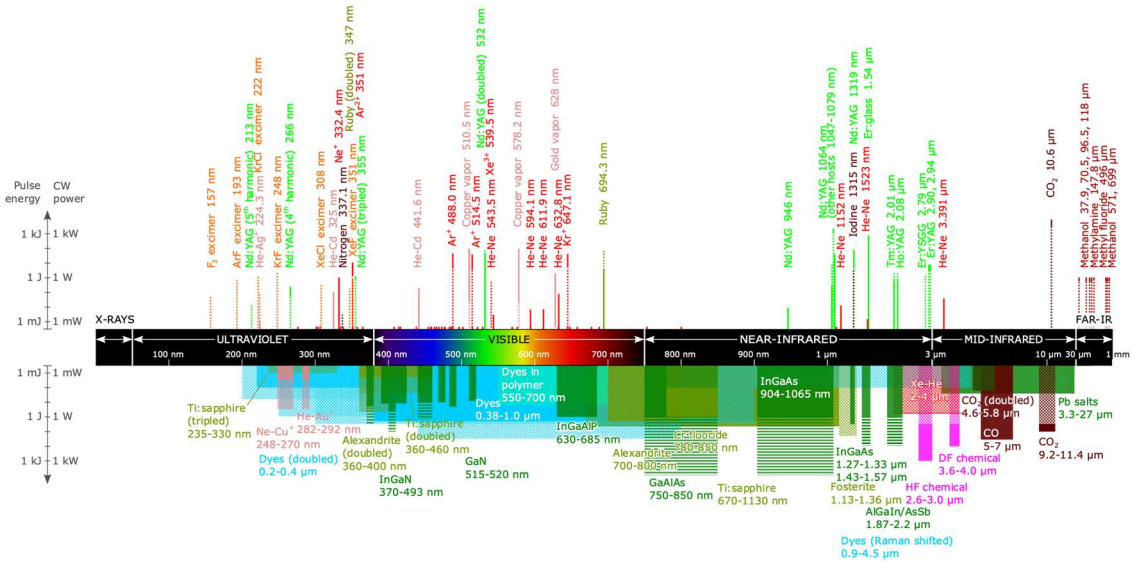

Figure 5: Overview of the wavelengths of commercially available lasers.[52]

2.2. Introduction to embedded computing in laser marking and printing

Laser marking and printing systems are usually controlled by software programs running on a PC or on an embedded system connected with a scanning card (Figure 6) that converts the received data to motion information that is sent to the printhead [53][54]. Existing laser marking machines based on PC and Windows operating systems are large and uncomfortable to manipulate; moreover, they cannot operate in some industrial environments.

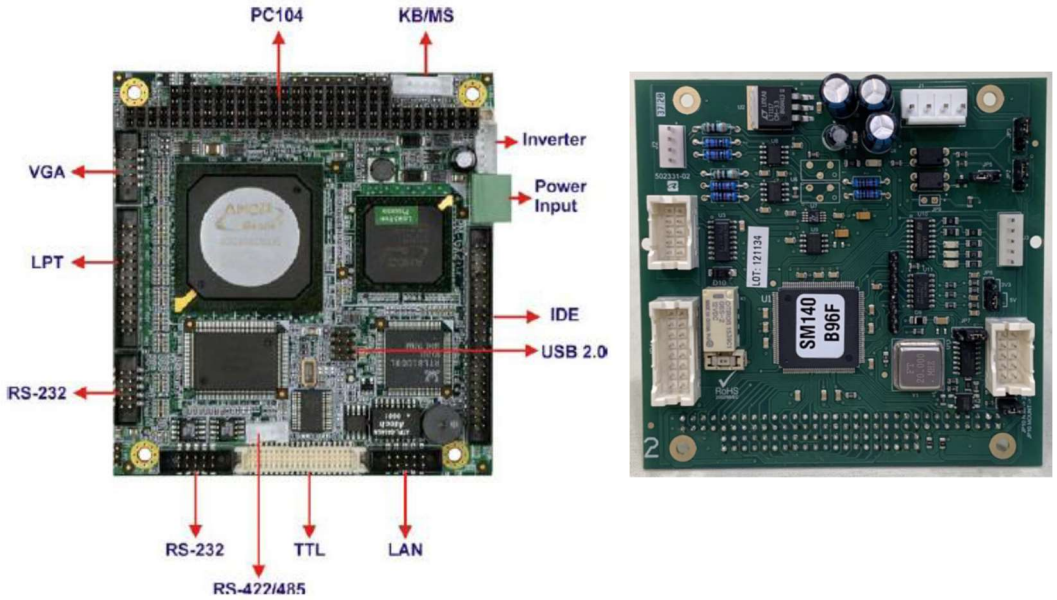

Figure 6: Embedded system and scanning card based on PC104 standard used in Macsa's low-cost laser marking systems

Embedded systems have been used widely in printing systems. For example, in [55] a printer controller for supplying dot data to a printhead module is based on embedded systems, being the printer controller configurable.

Embedded controllers are more convenient, but almost all existing laser marking algorithms are based on PCs and require a very high processing speed that is not easy to reach in an embedded controller. It is therefore required to develop suitable methods for achieving the required marking quality and speed. As an example, in [15] the use of multiple soft-core processors allows independent control of multiple printheads. With a multi soft-core architecture, a particular programming model, and several good design decisions, the factor of use of the laser beam (as a measure of efficiency) can be increased.

Processors used in embedded systems may be types ranging from general-purpose, digital signal processors (DSP), specialized in a particular class of computations, or even custom-designed for the specific application. Since the embedded systems are

dedicated to specific tasks, they may be optimized to reduce the size and the cost of the marking control system and increase reliability and performance.

Figure 7: Embedded system and scanning card based on Q7 standard module and customized motherboard used in Macsa's laser marking systems

Some laser marking controllers are based on ready-for-use embedded single board computers. These embedded computers have low energy consumption, small size, large temperature operating ranges, and low cost per unit. PC/104 and PC/104+ are examples of standard formats for single board computers intended for low volume and small systems. Most of these computing platforms are based on the x86 Intel architectures. Another implementation model uses the back-plane approach composed of: (1) standard high-performance computing module (e.g. SOM format) that contains peripherals and processors on one high-density chip, external flash memory for storage, and DRAM for runtime memory, and (2) a custom motherboard (Figure 7), with hardware designed specifically for the application [56]. The complex modules are manufactured in high volume by specialized companies that provide the software stack (including the operating system -usually Linux-) while the custom back-planes can be produced at much lower volumes.

Embedded systems in laser marking controllers communicate via peripherals, such as Serial Communication Interfaces (SCI), RS-232, RS-422, RS-485; Synchronous Serial Communication Interfaces (I2C, SPI); USB; networks (Ethernet); field buses (CAN, ProFiBus, ProFiNet); and include computational resources like storage (SD cards, Compact Flash); timers (PLL); General Purpose Input/Outputs (GPIO); Analog to Digital and Digital to Analog Converters (ADC & DAC); Debugging: JTAG, etc.

The embedded software must be customizable also for the resulting hardware platform. The largest part of the embedded software functions is initiated and managed by the machine interfaces, not through human interfaces. The software has fixed requirements and fixed hardware capabilities, and the addition or update of hardware or software is strictly controlled so that the embedded software should include at the deployment time all the drivers and stacks for the specific hardware implemented and the resources that ensure the real-time working condition. Embedded systems need software components as networking protocol stacks (CAN, TCP/IP), storage management (FAT),

etc. The software is highly dependent on the CPU and the selected specific chips/platforms.

Development tools for embedded software design can come from several sources. The main ones are open-source (i.e., GNU); embedded board providers (i.e., BSPs), or embedded software providers. The tools include compilers, assemblers, debuggers, and other high abstraction level tools (such as math workbench to simulate the mathematics for the systems that use digital signals processing). Software development requires the use of a cross-compiler, which runs on a computer and produces executable code for the target device, but also can be used some more specific tools as emulators, in-circuit debuggers, prototyping platforms, etc. More sophisticated tools as virtual platforms can be also used [57]. One of the advantages of using a virtual prototype over real hardware for the development and testing of embedded software is the ability of some simulators to take checkpoints of their state. This can result in an important gain in productivity, especially working with complex SW stacks.

Debugging can be interactive resident debugging, using the simple shell provided by the embedded operating system; or external debugging using logging or serial port output to trace operation using either a monitor in flash or using a debug server; or in-circuit debugger (ICD), a hardware device that is connected to the microprocessor via JTAG, allowing to control the operation of the microprocessor externally. Debugging the microprocessor-centric part is different to debug the processing performed by DSPs, FPGAs, or coprocessors. To verify the data traffic on the bus between the processor cores requires debugging at signal/bus level, with a logic analyzer. Some techniques used to recover the system from software errors (memory leaks), or hardware errors are using watchdog timers that reset the system unless the software periodically notifies that it is active or designing with Trusted Computing Base (TCB) architecture that guarantees a highly secure and reliable system environment.

Embedded software architectures alternatives include:

- Simple control loop where the loop calls to subroutines, which manage a part of the hardware or software.
- An interrupt-controlled system where different types of events trigger the tasks performed by the system; an interrupt may be generated, for example, by a timer in a preset frequency, or by a serial port that receives a byte.
- Cooperative Multitasking. The programs cooperate to share the processors. The program that has the control or uses the processor must provide the same processing opportunities as the other programs.
- Preemptive multitasking or multi-threading where the access to the data sharing must be controlled by some synchronization strategy, as messages queues, or semaphores.
- Microkernels of the operating system that assigns memory and CPU to different threads of execution. User-mode processes run important functions such as file systems, network interfaces, etc. Generally speaking, microkernels are successful

when task switching and inter-task communications are fast and fail when they are slow.

- Monolithic kernels have sophisticated capabilities and allow very productive development but require considerably more hardware resources and can be less predictable and reliable. For example, embedded Linux, VxWorks, and Windows CE.

Working with architectural structuring of the embedded software (Figure 8) facilitates the application of agile methods in firmware development, reusing entire functional blocks of firmware, minimizes dependence on hardware, and accelerates software development. In addition, an embedded software architecture provides debugging, manufacturing, and maintenance strategies, and allows more traceability [58].

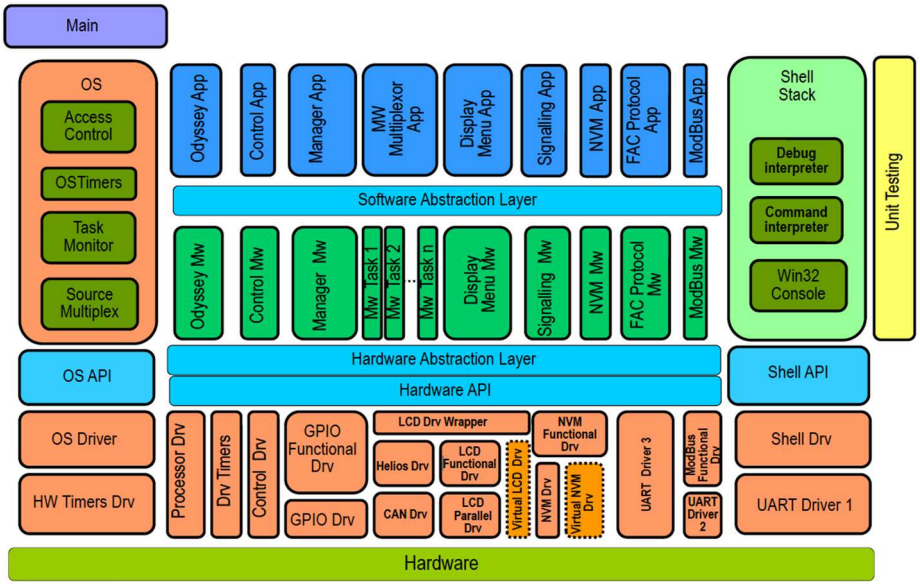

Figure 8: Example of architectural structuring of the embedded software

Hardware resources in embedded systems tend to be tailored to the cost and computational requirements (model of computation, performance, energy, real-time condition) and application domain. Consequently, the design of the operating system should have a similar reduced scope (opposed to the general-purpose systems) also adapted to achieve the required operation for the specific application which is usually statically packed in a single executable image, nowadays often connected to the cloud. Depending on the method used for managing tasks under the required real-time condition, the OS is considered a real-time operating system (RTOS) [59]. Examples of embedded current RTOS are QNX, WinCE, and VxWorks [60]. Bare-metal techniques can emulate multitasking without the RTOS benefit related to pre-emption, improvement in maintainability, reusability, and software complexity reduction.

Embedded systems in laser marking and printing have, of course, real-time computational requirements. The model of computation includes both dataflow and reactive systems. The marking and printing environment is receiving data (image and others like coding algorithm, etc.), transform them according to the laser system

parameters (type and number of lasers, resolution, quality, timings, etc.) some of them provided by sensors (quality, motion sensors, temperature, etc.), and providing control to the actuators (lasers, production line, alarms, etc.). Everything, fast enough to produce markings according to the real-time conditions of the production lines (latency, throughput, jitter). The tasks to be performed by embedded systems controlling laser marking and printing can be classified as:

- Hard Real-time tasks in which losing a deadline implies a system failure. Laser marking systems are installed on production lines; if the marking is delayed, the product in the production line could be out of the range of the laser, leaving the product unmarked; furthermore, the laser could damage the production line or a person.
- Soft Real-time tasks for which the usefulness of a result is degraded after its deadline, so it degrades the system's quality of service, while it does not produce any damage.

Embedded systems implement a range of different hardware architectures and technologies from the classical single-core microcontrollers (MCUs) or Digital Signal Processors (DSPs), to the modern multi-and many-core processor systems (either homogeneous or heterogeneous) or to other approaches such as GPUs or tailored systems whose hardware is implemented in FPGA devices (or reconfigurable cores).

Reconfigurable computing (implemented in FPGA devices) combines part of the flexibility of software (since they can embed many processing cores in the market) with the high performance of the hardware (either custom made or using available cores) to meet the flexible high-speed computing requirements.

The main difference of FPGA compared with the use of instruction-set processor platforms is the ability to make substantial changes in accelerating the data path by increasing the computational parallelism to adapt to the flow control. On the other hand, the main difference with custom hardware (i.e., implemented by application-specific integrated circuits or ASICs) is the possibility of adapting the hardware either off-line or at runtime by loading a new circuit in the reconfigurable structure. On the other hand, FPGA tends to be costly than instruction-set processor platforms. Therefore, FPGAs have been used for complex vertical applications, as are laser marking systems, where the production volume is small, but the companies can pay the extra hardware cost per unit of an FPGA platform to tailor it for different commercial solutions of their catalog.

The horizontalization of microelectronics to design complex systems (in any kind of silicon technology) boost the market of virtual components or intellectual property (IPs) cores that are descriptions of circuit blocks at different levels (from functional or structural descriptions -SoftIPs- up to layouts -hard IPs-) usually verified and optimized.

Contemporary FPGAs also automate the implementation of "system on a programmable chip (SoPC)" that extends the Systems-on-a-chip (SoC) and Multiprocessor Systems-on-a-Chip (MPSoC) paradigms. Examples of these devices are

FPGAs that integrate multi-core ARM architectures implemented as silicon hardIP cores with fully configurable hard processor systems (HPS) that allow tailored concurrent hardware architectures [61]. That hardware acceleration can be also shared with the processor by using hardware-software co-design techniques [62].

Similar MPSoC approaches can be implemented using softIP processor cores (such as Xilinx' MicroBlaze or Altera's Nios II [63][64]) that can be downloaded into the configurable building blocks. The advantage of the soft-core processors lies in that they are significantly faster for some applications due to their ability to change their internal architecture up to changing the instruction sets that allow adding new computational resources in the functional units or as a coprocessor. This compensates for the lower frequency of operation and area requirements compared with hardIP cores directly implemented in silicon inside the FPGA chip.

To define the behavior to be implemented in the FPGA, a hardware description language (HDL) should be used for the HW part embedded in the electronic design automation (EDA) toolchain. It will allow modeling, simulation, logic and physical synthesis, bitmap generation and download, and also in-circuit emulation and testing using hardware-in-the-loop technologies. The most common HDLs are VHDL and Verilog (currently the most popular). To reduce the complexity of the design in HDL, the abstraction level can be raised using system-level design languages such as System Verilog or SystemC or OpenCL (Open Computing Language) that allows the complete path from a high-level language (similar to the SW programming languages such as C or C++) down to the implementation in FPGAs [65].

As a result, FPGAs allow tailoring of the processor(s) core architecture, to select only the required I/O peripherals, to create customized I/O interfaces, and to develop accelerators for tasks computationally intensive. The current development of EDA both for modeling, verification, and synthesis, and the heterogeneous SoC development and integration tools for FPGA devices, allows reducing the additional design effort required to implement prototypes and industrial solutions.

All this technological progress allows programming larger and more complex algorithms in an FPGA. The connection of one of these FPGA to a modern CPU via high-speed busses allows that the configurable logic to act more like a coprocessor than as a peripheral. This has led reconfigurable computing into the high-performance computing sphere. The High-Performance Reconfigurable Computing (HPRC) combines accelerators based on reconfigurable computing as FPGAs with CPUs or multi-core processors. FPGA devices with sufficient resources to implement multiprocessing systems with soft-cores can implement solutions for High-Performance Reconfigurable Computing in hard real-time. Adequate models of parallel programming and efficient methods must be used to optimize the designs. For example, Castells [66] implemented a system that uses a tasks isolation approach to meet the computing requirements of an industrial laser marking system, which should make real-time safety-critical tasks.

Complex computing problems often can be divided into several simpler subtasks whose results are combined once completed. Parallel computing allows performing simultaneously many calculations or processes. In concurrent computing, the various processes could address related tasks, in this case, the separate tasks may have a varied nature and often require some communication between processes during the execution. Parallel computing algorithms with high concurrency are more difficult to write than sequential ones since concurrency can introduce several kinds of errors in software. Inter-process communication and synchronization tend to be some of the bottlenecks to obtaining the optimum performance of the parallel program.

Segmented hierarchical buses for MPSoCs and Networks-on-Chip (NoC) are proposed as a feasible, efficient, scalable, predictable, and flexible solution to interconnect IP blocks in one chip when the number of cores is large (hundreds). NoC-architectures allow embedded computing with maximum system platform composability and flexibility using pre-designed IP cores [67],[68].

To later estimate the computational requirements for the embedded systems facing laser writing and marking applications, I introduce Amdahl's law (Eq. (4) that sets a theoretical upper limit for the speedup of a single program because of parallelization [69]. $S_{latency}$ is the theoretical speedup of the execution of the whole task; s is the speedup of the part of the task that benefits from improved system resources; p is the proportion of execution time that the part benefiting from improved resources originally occupied.

$$S_{latency}(s) = \frac{1}{(1-p)+\frac{p}{s}} \quad (4)$$

Also, Gustafson's law (Eq. 5) gives a less pessimistic and more realistic assessment of parallel performance as:

$$S_{latency}(s) = 1 - p + sp \quad (5)$$

2.3. Laser marking and digital printing

Digital printing refers to methods for direct printing from a digital image directly to the media (without any printing plate or intermediate artifact). It allows on-demand printing and modification of the image used for each impression. The most popular digital printing methods include inkjet printers, which deposit pigment on substrates such as paper and cardboard, and various laser printing systems [70]. The most common method of laser printing is based on electrostatic charges. A laser beam repeatedly passes back and forth over a negatively charged cylinder called a "drum" to define a differentially charged image. The drum then selectively collects electrically charged ink powder (toner) and transfers the image to the paper, which is then heated to permanently fuse the images onto the paper. As with digital copiers, laser printers employ a xerographic printing process [71]. In a variety of laser digital printing, digital images are exposed on laser-

sensitive paper. These prints are photographs and have continuous tone in image detail. The print quality can be as high as that of the photopaper used.

The current methods used in digital printing (for example inkjet or xerography) are very expensive at an industrial scale because they use expensive consumables (specific inks and specially coated substrates) for the printing process [72]. An alternative method to laser digital printing is LIFT technology. Laser-Induced Forward Transfer (LIFT) of inks from a donor ribbon or roller to substrates enables the use of inexpensive inks and paper (commonly used in industrial gravure or offset printing). The challenge of this approach is to develop a fast direct laser writing unit that can cover an area of more than 1 m^2/min with a resolution of 300 dpi to 600 dpi and that allows a precision better than 4 μm, for 8-bit gray scale pixels. Due to the large area and high desired printing speed, the average laser power should be within a range of a few hundred watts; at a laser modulation rate of 20 to 25 MHz; and at laser scanning speed from 800 to 2116 m/s in a scan field length of 530 mm.

Some marking machines could be considered a form of digital printing. They are used to print lot numbers, expiration dates, and other information on labels, cardboard boxes, bottles, or any solid surface [73]. These machines usually work automatically in the production line together with other machines. They can be contact or non-contact. The non-contact type of coding uses a laser or ink spray to mark. Moving products are detected by a sensor and give a signal to the machine that responds immediately with printing. Some examples of these non-contact marking machines are industrial inkjet coding machines and laser marking systems. Inkjet printing recreates a digital image by driving ink droplets onto substrates [74]. They are the most common type of marking machine.

The term laser marking is used as a generic term covering a broad spectrum of surfacing techniques including printing. Some review works of the different laser marking techniques are available in the literature: Han et al. [4], Lazov et al. [3], Patel et al. [75]. To create visible marks on a surface with a laser beam requires that the beam provide a certain optical power density that triggers physicochemical processes. After the process starts, the integration of the irradiance during a period can increase the intensity of the effects or trigger additional different effects.

As depicted in Figure 9, a laser marking or printing system is typically composed of four main parts: (1) a laser beam source, (2) a beam deflector system, (3) a surface of the object to be marked, and (4) a control system to manage all components. The laser source is controlled to generate beams with some desired features, and the deflecting system directs the beams to the areas of the surface that need to be marked. The productivity of the system depends on features from all four elements.

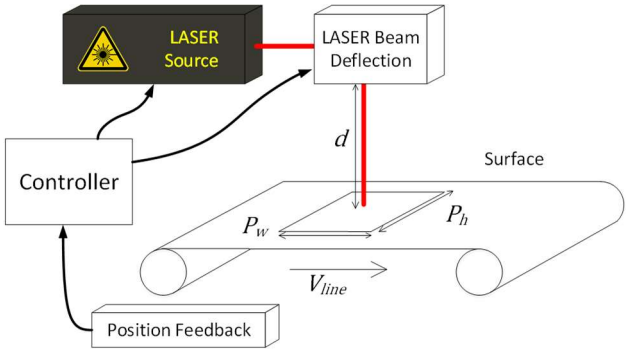

Figure 9: Typical Laser Marking system containing a laser source, a beam deflection system, a conveyor where the marking surface is transported, a system to inform about the position, and a controller

The surface material requires a minimum irradiation time to show a visible change and reacts differently depending on the power of the beam. Beam effects are also affected by the movement created by deflection systems. We will analyze how each part influences the performance of the marking system in the following sections.

2.3.1. The marking surfaces

The interaction of materials with laser beams is a vast multidimensional area of research with many open questions. Reasonably strong absorption of laser light by the marked material is the key to efficient, cost-effective, and aesthetically appealing markings. On the one hand, there exist thousands of different materials and new ones are regularly being synthesized. On the other hand, laser beams can have different wavelengths, power levels, and temporal dynamics. Despite this complexity, the interaction of some of the most common materials with currently available laser sources has been studied to some extend.

In the visible and infrared bands, this interaction is usually based on thermal processes. For them, the important factors are irradiance (I, also known as power density) and fluence (F, also known as fluence). Beam irradiance is directly correlated with the induced heat, which usually triggers vitrification, vaporization, melting, carbonization, and oxidization processes in many materials. The interaction time is controlled to select the intensity of the visual effect caused by the process, which is the final interest in marking applications. Metals require a high-power density beam in the orders of GW/cm^2 to create visible marks. As described by Qi et al. [76], the typical processes involved are vaporization, melting, and oxidization. Ceramic, glass, and plastic react at lower power density values in the order of kW/cm^2. Vaporization and melting are the main processes used for creating visible marks. There are many examples of their industrial use. Noor et al. [77] already reviews their use to mark encapsulated integrated circuits on plastic or ceramic packaging. Deprez et al. [78] study the marking of glass, which is more challenging due to the material transparency. Organic surfaces react at lower power densities of just some W/cm^2. They also can vaporize as other materials, but instead of melting they usually carbonize. This is used in many industrial processes like marking

QR codes or best dates in all kinds of foods. marking of QR codes or best date in all kinds of foods. Chen et al. [79] described their application for marking on eggshells, and Nasution and Rath [80] on a banana skin. Paper and cardboard are also organic, Bravo-Montero et al. [28] recently described a method to mark it with minimal debris generation. Textile materials can be organic, inorganic, or a combination of them. In this case, the required power density can range from W/cm^2 to kW/cm^2, and the triggered processes depend on the nature of the fibers. Angelova et al. [81] analyzed the benefits of laser treatment for leather and textile manufacturing. Table 1 shows the fluence threshold (F_{th}) range required to produce visible changes on the material (for every material family) together with a brief list of the main triggered processes. We also include the irradiance order most frequently used to mark each kind of material.

Table 1 Processes triggered by different power densities in different material surfaces

Surfaces	Typical Irradiance order	Typical fluence threshold ranges (J/cm^2)	Triggered Processes	Examples
Metals	GW/cm^2	10^{-1} – 10^{1}	Vaporization, Melting, Oxidization	[76][6][82][83]
Ceramic	kW/cm^2	10^{1} – 10^{3}	Vaporization, Melting	[77][2][84][80]
Glass	kW/cm^2	10^{0} – 10^{1}	Vaporization, Melting	[78]
Plastic	kW/cm^2	10^{-1} – 10^{1}	Vaporization, Melting	[77][85][86]
Textile	kW/cm^2	10^{-3} – 10^{-0}	Vitrification, Melting, Carbonization	[81]
Food	W/cm^2	10^{-4} – 10^{-3}	Vaporization, Carbonization	[79][80][87]
Paper	W/cm^2	10^{-1} – 10^{1}	Vaporization, Carbonization	[28]
Thermochromic ink	W/cm^2	10^{-1} – 10^{1}	Color change	[88][27]

As we can see in Table 1, object surfaces react in different ways to laser beams. The impact of the laser light on a surface triggers different processes depending on the wavelength of the beam, its power and modulation frequency, and the absorption of the irradiated energy by the different molecules of the material. Figure 10 shows examples of microscope images of how the same laser source, used in the development of this research work, affects different materials differently. Figure 11 shows an SEM microscopy image of how the same laser source affects differently the irregularities on the same surface.

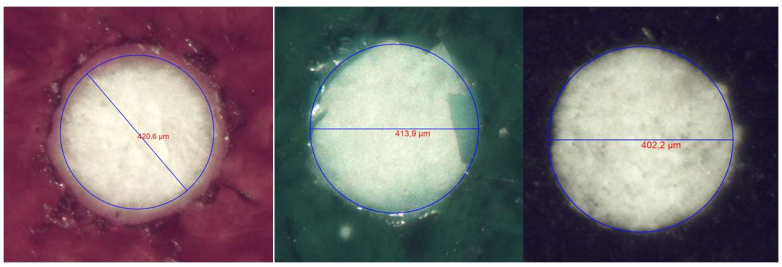

Figure 10: Effect on different surfaces of a laser pulse with (HP f-LDA prototype) 975nm wavelength, 400µm beam diameter, 30µs width, and 240W power over substrates from different customers.

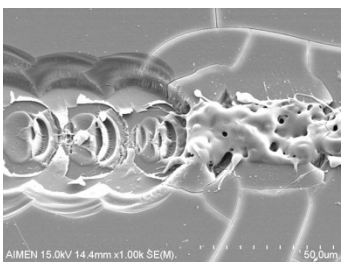

Figure 11: Effect on a non-uniform surface of superposed UV fs laser pulses to evaluate laser effect on different transparent substrates.

The laser beams could be used to expose thermochromic ink/labels or can cause ablation on the material, or pyrolysis or carbonization. Table 2 shows the fluence threshold (F_{th}) range and the irradiance order of some processes triggered by different power densities in different material surfaces used in this work.

Table 2: Processes triggered by different power densities in different material surfaces used in this work

Surfaces	Typical Irradiance order	Typical fluence threshold ranges	Triggered Processes
Thermochromic ink	W/cm^2	(mJ/cm^2)	Photochemical transformation
Ink	kW/cm^2	(J/cm^2)	Ablation
Cardboard, paper	W/cm^2	(J/cm^2)	Pyrolysis, Carbonization

Micromachining with lasers, where the target material under laser irradiation absorbs energy and transforms into either a liquid or a vapor, requires material removal through the ablation process. Additionally, other processes such as heat conduction, radiation, and plasma expansion are associated with the laser-material interactions.

When the laser energy is deposited in a surface layer, the thickness of the layer is given by the optical penetration skin depth (δ_p) Eq. 6

$$\delta_p = \frac{1}{\alpha} \tag{6}$$

where α is the absorption coefficient. Another characteristic length called the heat diffusion length during the laser pulse gives the heat penetration depth due to the thermal conduction. This diffusion length is given by Eq. 7

$$L_D = \sqrt{D\ \Delta t_p} \tag{7}$$

where D is the heat diffusion coefficient and $\Delta t_p$is the laser pulse duration. For long pulses, $L_D > \delta_p$, materials are heated by the laser pulse and the temperature is determined by the heat diffusion length during the laser pulse. On the other hand, for a short pulse laser, $L_D < \delta_p$, the skin depth determines the heated volume during the laser pulse, instead of the heat diffusion length [89][90].

In industrial applications of laser marking on the packaging, the most used materials are organic: paper, ink, cardboard, etc. In the following paragraphs, we study with more detail the laser marking on paper and cardboard, which has a special interest for our applications.

For longer wavelengths, the energy of the laser beam is transferred into heat. Some applicable simplified heat transfer models can be derived from the Stefan-Boltzmann radiation law as modeled in [91].

For wavelengths in the ultraviolet (UV) range and shorter, the energy of the beam is not only transferred into heat but also can break the molecular bonds between atoms, degrading the organic materials. This degradation of the material is the reason why UV lasers have been discarded by some authors (as [92]) to produce discoloration in organic materials.

Being all organic materials, paper, cardboard, and organic textile fabrics share a similar chemical composition. They all contain a high percentage of cellulose, a lower amount of hemicellulose, and an even lower amount of lignin. Lignin contributes to brownish color, so it is usually removed in the high-quality white paper, but not from eco-paper and cardboard

The processes involved in color response and color change are complex and its study involves many different disciplines. A lot of them are explained in detail in [93]. Temperature changes are one of those phenomena that can cause reversible or irreversible color changes in materials. Every organic compound found in paper, cardboard and fabric have a different response when heated. Some of those processes involve an irreversible color change.

In [94] and [95] Chen et al. study the reaction of paper when heated. They do a thermogravimetric analysis and a color analysis. From the weight loss perspective, they identify 4 different temperature zones: A, B, C, D. In the first A zone (below 100ºC) weight loss is caused by water evaporation. In their case, this accounts for 10% of the weight loss. In the B zone, almost no weight loss occurs. C zone spans approximately from 260ºC to 320ºC for hemicellulose and from 315ºC to 380ºC for cellulose. This is where more weight loss happens due to pyrolysis. At the end of the process, 70% of the weight is lost. The final phase above 400ºC is where carbonization occurs producing a blackening effect.

Oxygen should be avoided to prevent combustion. Paper autoignition is often reported to happen at 233ºC. However, other research [96] shows that when irradiated with infrared radiation the required threshold surface temperature is 376ºC. In absence of oxygen, pyrolysis occurs, and the previously described zones can be exploited for industrial interest.

The color change of paper is not only induced by heat. Paper turns yellow at ambient temperature by the effect of oxidation and photooxidation at a very slow rate. However, heat can accelerate this yellowish discoloration. This process is studied with more detail in [97], [95], and [98].

In the C zone, the pyrolysis processes usually produce liquids (bio-oils, such as tar), solids (char and coke), and gases as the biomass volatilizes. Biagini et al. [99] study

the devolatilization of biomass fuels. On the other hand, Pan et al. [100] study other volatilized molecules with mass spectrometry. They find out 24 different volatile compounds and classify them in order of toxicity. Most toxic products are produced between 400ºC and 600ºC.

Although some by-products are created during pyrolysis, the number of debris is orders of magnitude lower than the amount of residue generated by alternative ink-based printing.

The initial attempts to print without ink were based on the deposition of special coatings containing diacetylene compounds over the paper substrate [19]. Those compounds react easier to heat induced by the laser beams. One of the benefits of this technology is that multiple compounds can be added reacting at different wavelengths enabling color printing [101]. However, it has the drawback of the additional coating process and its environmental impact.

Although there exist some early patents of direct laser printing on the paper surface without any additives ([102],[103]). the methods were not mature enough for industrial success. Some of the problems of such technologies are the risk of combustion, and the required processes to handle debris.

A more recent patent [104], describes a more feasible method to print without ink. The method includes a preheating phase so that the additional heat to carbonize the paper is reduced. It is known that gradual preheating favors the marking process [105] as heat is more uniform and quality is increased due to the reduction of temperature gradients.

To avoid the liberation of devolatilized by-products they dispose of a coating transparent layer immediately after carbonization to adhere the volatilized molecules to the printing surface. This has the drawback of using other consumables for this fixing process.

Other works ([106]) analyze how the pyrolysis effects depend on the speed of marking. The speed contributes to lower heat flux, working in the C zone, modulating the intensity of the discoloration of the paper. The authors claim that working in the pyrolysis range before carbonization occurs [100] is environmentally safer because the number of undesired volatilized molecules is reduced. However, the observed printing contrast does not meet industrial requirements.

To the best of our knowledge, there is still a need to provide a laser inkless printing system having a high contrast mark where post-treatment steps are avoided to reduce the economic costs of other known methods.

Two key factors in the interaction of materials with laser beams are power density and time of interaction. The power density of a laser beam, also known as Irradiance (I), is the radiant flux (Φ) per area, which is typically approximated by a circle, that can be varied by optical means. The intended output of most lasers' radiance profile is described

by a fundamental (or TEM00) transverse Gaussian mode. However, for the simplification of this analysis, I will consider the mean Irradiance value on the circle that is determined by Eq. (8)

$$I = \frac{\Phi}{a} = \frac{4\Phi}{\pi {d_{spot}}^2} \quad (8)$$

The integration of the power density over a period of time is equivalent to the irradiated energy density, known as fluence (F). The control of the interaction time selects the degree of a visual effect caused by the process, which is the final interest in marking applications.

Since materials are characterized by a certain fluence threshold (F_{th}) which is required to produce a visible change, then the minimum time to make a mark will be determined by Eq. 9.

$$t_{mark} = \frac{F_{th}}{I} \quad (9)$$

Further complexity appears because F_{th} is not constant since it depends on the wavelength and the pulse duration of the laser. An example of how large this variability can be is shown by Preuss et al. [107]. However, the marking time can generally be reduced by increasing the beam irradiance (I).

As fluence threshold plays such an important role in determining the performance of a marking system, there is a great industrial interest to create materials that require lower power densities, shorter interaction times, or both. Such materials might be added to the objects of interest in coating layers. Jarvis et al. ([27],[108]) describe an ink with these goals.

Laser beams based on higher energy photons in the ultraviolet band can break molecular bonds without introducing heat in a process known as ablative photodecomposition (APD). It has been successfully used to mark metals ([109]) and plastics ([85]). Shorter wavelengths allow smaller spot sizes, providing power densities in the order of GW/cm^2.

The shape of the surface can also affect performance. Regular surfaces (e.g., planar) are easier to mark because appropriate lenses can be used to correctly focus all points of the surface. Marking irregular surfaces is also possible, but the beam needs to be dynamically re-focused for each point of the marking area. Chen et al. [79] take advantage of the known details of the surface to precompute the required focus and minimize additional delays. However, if the surface position or orientation is unknown, a pre-scanning of the 3D surface is needed. Current scanning technologies are much faster than the tens of seconds reported by Diaci et al. [110], but the introduced delay would still be significant.

2.3.2. Laser sources

The power of a laser beam (or radiant flux Φ) is determined by the number of photons n_{ph} per unit of time and the energy of each photon, which depends on the Planck constant (h) and the photon frequency v (see Eq. 10). Q_e is the radiant energy.

$$\Phi = \frac{\partial Q_e}{\partial t} = \frac{n_{ph} E_{ph}}{t} = \frac{n_{ph} h v}{t} \quad (10)$$

As seen in the previous section, in laser applications, an important factor is power density. We will use the simple approximation of a uniform distribution on a circle called spot. The minimum spot diameter is inversely correlated with photon frequency with some factor k, so d_{spot}= k/ v. Hence, combining Eq. (8)

with Eq. 10, the maximum power density (Irradiance I), is determined by Eq. 11.

$$I = \frac{\Phi}{a} = \frac{4\Phi}{\pi {d_{spot}}^2} = \frac{4 n_{ph} h v^3}{t \pi k^2} \quad (11)$$

Note that the beam power has a linear relation with the photon frequency, but its power density has a cubic relation with photon frequency. Therefore, high-frequency systems require less power than low-frequency systems to obtain the same power density and the same visible effect. Table 3 shows the typical light wavelengths bands used by laser marking systems.

Table 3 Light Wavelengths used in Laser Systems

Acronym	Name	Wavelength
UV	Ultra-Violet	10- 400 nm
VIS	Visible	400- 700 nm
NIR	Near Infrared	700 nm -2.5μm
MIR	Mid-Infrared	2.5μm-15μm

As seen in section 2.1.1, the material whose atoms are subject to the stimulated photon emission is known as lasing material. Not all materials are suitable as lasing medium and laser sources are usually identified by the lasing medium they use, which produce specific wavelengths and may require a certain type of stimuli (such as flashing light or electrical discharges) to bring atoms to excited states and perform the optical pumping. Table 4 lists the most common laser types found in the industry for laser marking and printing and their typical operating parameters.

Table 4 Most popular Laser types in industrial applications for laser marking and printing

Type	Power	Efficiency	Pulse duration	Wavelength
Gas	10W-400W	5%	CW - μs	MIR
Fiber	10W-100W	30%	CW – ns	NIR
Solid State	1W – 100W	25%	ns – ps	NIR, VIS, UV
Semiconductor	0.5W – 200W	50%	CW - μs	NIR, VIS

Some laser applications use continuous wave (CW) laser beams whose output power Φ_{CW} is constant over time. Pulsed lasers are based on different principles. Energy may be stored and released periodically, allowing short laser pulses to be generated with peak powers far more than the constant power deliverable by CW lasers. Peak power (Φ_{peak}) is determined by Eq. 12. where Φ_{avg} is the average power of the system, Δt_p is the pulse width, and f_p the frequency of pulses (or repetition rate). This is often used to create different intensity levels or even colors in the mark [111].

$$\Phi_{peak} = \frac{\Phi_{avg}}{\Delta t_p f_p} \tag{12}$$

The product of pulse width and repetition rate can be interpreted as the duty cycle of the pulsed signal. Although the power levels are very different, a CW laser modulated with a PWM signal responds to the same Eq. 12. Figure 12 represents this operation.

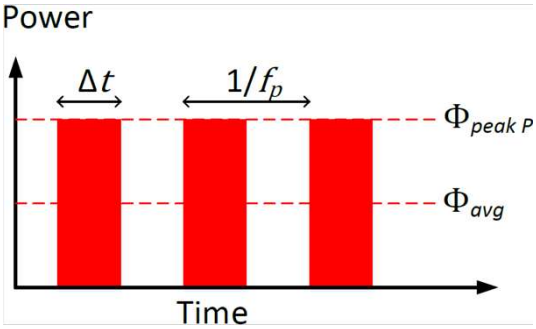

Figure 12: Power delivered by modulated CW lasers or pulsed lasers

To understand how these parameters affect the performance of a marking system, we must define the concept of laser scribing speed, which is the speed at which we move the laser beam relative to the object (or vice versa) while producing a visible mark. When there is a movement (either of the object or the beam) the radiant power (Φ) does not change but the area affected by the irradiance (I) and Fluence (F) increases. Figure 13 illustrates this effect for non-modulated CW systems. The area covered by a moving beam is determined by Eq. 13. If the scribing speed ($V_{sc\,CW}$) and the scribing time (t) are high enough ($V_{sc\,CW}t \gg d_{spot}$) the area can be approximated by a simple rectangle if we ignore the Gaussian energy distribution of the beam, (right side of Eq. 13)

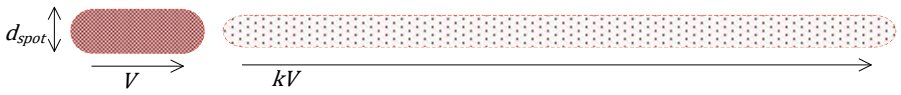

Figure 13: Left) mark with a scribing speed V Right) mark with a faster scribing speed by factor k. The same power and energy are distributed along a larger area, resulting in lower irradiance and fluence applied to the material

$$a = \frac{\pi {d_{spot}}^2}{4} + d_{spot} V_{sc}\, t \approx d_{spot} V_{sc}\, t \tag{13}$$

Hence, the energy density (fluence) for continuous wave lasers is simplified to the expression shown in Eq. (14)

$$F_{CW} = I\ t \approx \frac{\Phi_{avg}}{d_{spot} V_{sc\ CW}} \quad (14)$$

The maximum scribing speed (Eq. (*15*) will be the maximum speed that ensures that fluence is higher than the material fluence threshold (F_{th}).

$$V_{sc\ CW} < \frac{\Phi_{avg}}{d_{spot} F_{th}} \quad (15)$$

Pulsed and modulated lasers both have in common that the beam is interrupted during periods of time. The area irradiated by the pulses will depend on spot diameter (d_{spot}), the pulse duration (Δt_p), the pulse repetition rate (f_p), the scribing time (t) and the scribing speed (V_{scp}). Adjusting those values allows different marking effects on the material. For example, Figure 14 illustrates the irradiated area effect produced when marking continuous lines by pulse overlapping.

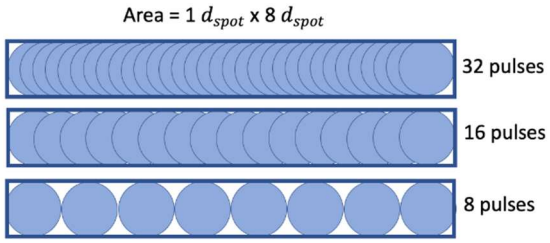

Figure 14: Irradiate area by overlapping pulses at different $\frac{f_p}{V_{sc\ p}}$ ratios

As an example, to vary and study the effect of the overlap degree, lines are processed on the material, maintaining a frequency at 5kHz and varying the speed of the beam on the surface. It starts at 500mm/s, varying the pulse energy from 100% to 5%. Microscope images show the differences between the finishes of the lines made with low (Figure 15 left) and high (Figure 15 right) percentage of overlap, but with the same pulse energies per line, and always the same pulse frequency.

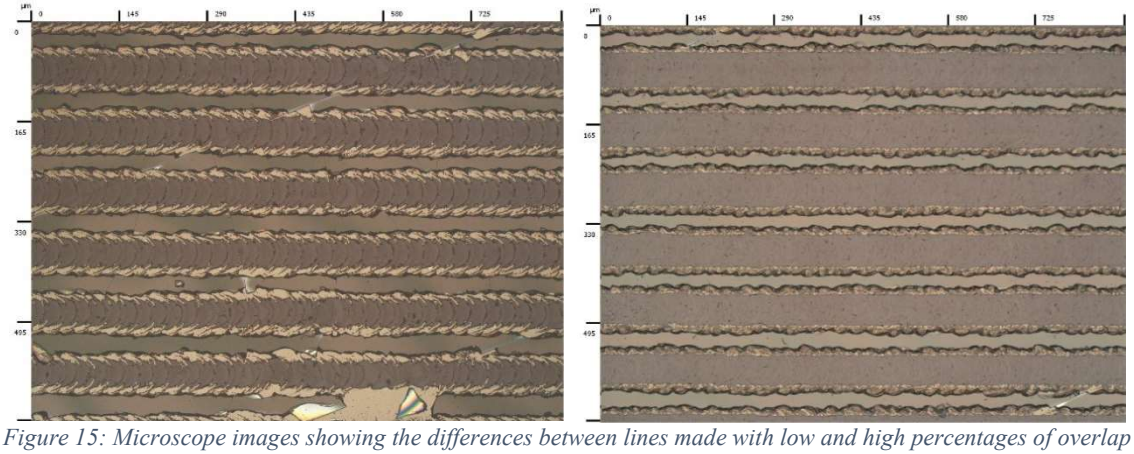

Figure 15: Microscope images showing the differences between lines made with low and high percentages of overlap

Images show how the resulting surface is much more homogeneous in the case of high overlap. The improvement in the roughness of the material is also observed in SEM images. Figure 16 shows the general area (left) and a detail of a channel (right) in

which the look of the generated channel is much better. In the case of channels made with less overlap, the size of the spot and the degree of overlap are more distinguished. In the case of the larger overlap, the width of the channel is reduced since the breaks of the material at the edges are made smaller thanks to said overlap.

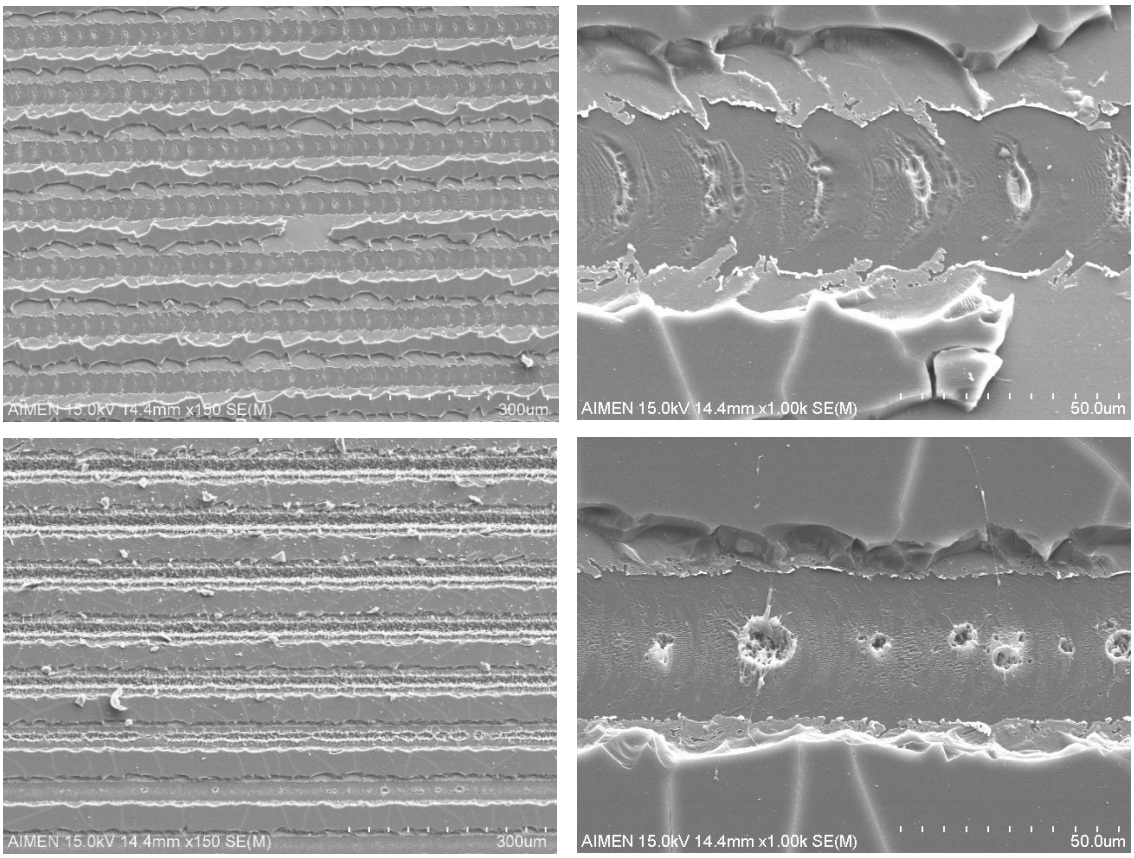

Figure 16: SEM images showing the finish of the generated channels

The area covered by a moving beam is simplified by Eq. 13. The mean energy density for the active areas will be simplified by Eq. (16)

$$F = \frac{\Phi_{peak}\Delta t_p f_p t}{\frac{\pi d_{spot}^{\ 2}}{4} + d_{spot} V_{sc} t} \tag{16}$$

From where we can deduce the maximum speed in Eq. 17

$$V_{scP} < \frac{\Phi_{peak} f_p \Delta t_p}{d_{spot} F_{th}} - \frac{\pi d_{spot}}{4t} \tag{17}$$

The distances between pulses (x_{pitch}) is determined by Eq. 18

$$x_{pitch} = \frac{V_{sc\,P}}{f_p} \tag{18}$$

Combining equations 17 and 18, we get Eq. (19). The maximum scribing speed will be determined by the maximum pitch distance that the application can tolerate, or the

maximum frequency of laser pulses, or the combination of values that makes the mean fluence higher than the threshold.

$$V_{scp} < min\begin{cases} x_{pitc}\ f_p \\ \frac{\Phi_{peak} f_p \Delta t_p}{d_{spot} F_{th}} \_ \frac{\pi d_{spot}}{4t} \end{cases} \quad (19)$$

In these equations, we find the relationship between the parameters of the material we want to mark (fluence threshold F_{th}); the requirements of the application such as the resolution or distance between points (x_{pitch}) and the scribing speed (V_{scp}); the parameters for the optical design such as spot diameter (d_{spot}) and laser power (Φ_{peak}); and the electronic control parameters: pulse duration (Δt_p), pulse repetition frequency (f_p) and marking time (t). In the case of a considerable length of overlapping pulses, the maximum scribing speed can be obtained by Eq. (20)

$$V_{scp} < min\begin{cases} x_{pitch} f_p \\ \frac{\Phi_{peak} f_p \Delta t_p}{d_{spot} F_{th}} \end{cases} \quad (20)$$

Adjusting the values of the variables of equation (19) we can also print individual spots. If the distance between pulses x_{pitch} is higher than the diameter of the spot ($x_{pitch} > d_{spot}$), the irradiated area of individual spots resembles Figure 17.

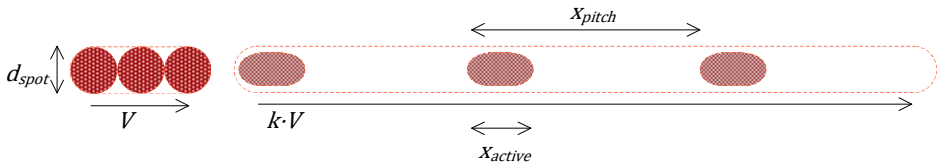

Figure 17: Left) mark produced by a pulsed laser with a low scribing speed V. Right) mark with a faster scribing speed by factor k. The pulsed operation creates areas without irradiance.

In this case, the scribing time (t) is the pulse repetition period ($\Delta t = \frac{1}{f_p}$) and the max scribing speed is defined by Eq. (19) considering $t = \Delta t$. In this scenario, the aspect ratio (width/height) of the area irradiated by the pulses is determined by Eq. 21.

$$AR_P = \frac{d_{spot} + V_{sc\,P} \Delta t_p}{d_{spot}} \quad (21)$$

For very short pulses, the movement for the pulse duration (Δt_p) will be irrelevant, and the aspect ratio will be 1. For longer pulses from modulated continuous-wave lasers, the mean Fluence on the active area will also be proportional to Δt_p. Increasing the duty cycle ($\Delta t_p f_p$) to 100% (CW) will get the maximum mean fluence in that scenario. The Fluence will be simplified by Eq. 22 if $\pi {d_{spot}}^2/4 \ll d_{spot} V_{sc} \Delta t_p$.

$$F \approx \frac{\Phi_{peak}}{d_{spot} V_{scp}} \quad (22)$$

For certain applications, the maximum pulse time on the moving beam to prevent deformation of the printed dot is derived from AR Eq. 21 and shown in Eq. 23.

$$\Delta t_p < \frac{d_{spot}\cdot(AR_p-1)}{V_{scp}} \tag{23}$$

And using equation (16)

the mean Fluence is determined by equation 24.

$$F = \frac{\Phi_{peak}\,(AR_p-1)}{d_{spot}V_{scp}\left(\frac{\pi}{4}+AR_p-1\right)} \tag{24}$$

Combining with the pitch info (Eq. 18), we get Eq. 25. The maximum scribing speed will be limited by the maximum pitch distance and the maximum aspect ratio that the application can tolerate, and, if none is required, by the continuous wave equation. As depicted in Figure 18, for a fixed resolution (constant x_{pitch}) the scribing speed of modulated lasers can be increased by increasing the pulse repetition rate up to the AR limit. Note that this threshold is a fraction of the absolute maximum speed determined by the continuous wave fluence equation.

$$V_{scp} < min\begin{cases} x_{pitch}f_p \\ \dfrac{\Phi_{peak}\,(AR_p-1)}{F_{th}\,d_{spot}\left(\frac{\pi}{4}+AR_p-1\right)} \\ \dfrac{\Phi_{peak}}{F_{th}\,d_{spot}} \end{cases} \tag{25}$$

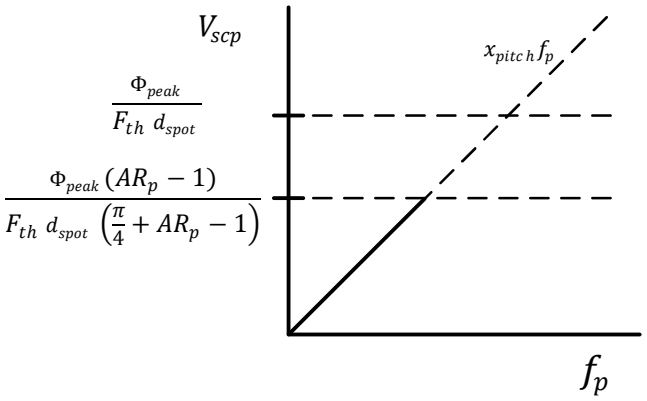

Figure 18: Plot of the maximum scribing speed (Vscp) as a function of modulating frequency for pulsed and modulated lasers.

When using thermal-based phenomena for marking, a method to reduce the laser power requirements is to use an alternative method to preheat the surface below the fluence threshold. Restrepo et al. [105] applied this technique to reduce the energy required to mark bricks, and Bravo-Montero et al. [28] followed a similar approach with paper and cardboard. If this is done, the laser beam provides an additional irradiance to jump above the fluence threshold needed to produce a visible mark.

In section 2.3.1 we have seen that the material's fluence threshold will be the most limiting variable to increase marking speed. If the system requires a certain speed,

material selection would be the first decision to take. Later, other important decisions (like selecting the laser source characteristics) should be taken. Since the beam power has a direct relation with scribing speed (as shown by Eq. (19) and subsequent), the industry has an obvious interest in increasing it. But this increase in power density should be achieved while reducing the total power consumption as much as possible because it has a direct impact on the economic cost. Therefore, there are many incentives to research new methods that increase the efficiency of transforming electric energy into radiant flux to reduce the need for heat dissipation. This is extremely important as the analysis of Goffin et al. [112] reveals that the cooling system takes an important part of the power budget of the whole system.

Another important aspect of laser sources of industrial interest is their maintenance requirements (as explained in [4]). The laser source is often the most critical component for the reliability of a laser marking system. In designing a laser marking system, the lifetime of the laser source must be carefully evaluated. Assessing lifetime expectations for lasers sources is a complex activity typically involving several tests for very long times. Usually accelerated lifetime tests are preferred since they allow to estimate very long lifetimes in real operating conditions based on much shorter tests than the expected lifetime.

2.3.3. Beam deflecting methods

Marking applications require the beam to be applied to a certain area. Either the beam is static, and the object is moved, or the beam is deflected concerning a static object. In any case, the movement of the beam concerning the object must follow a path that covers all the positions to be marked. Alike other computer-generated drawings, the images marked with laser beams can be created by using either raster or vector graphics. Vector graphics are defined in terms of 2D points, which are connected by lines to form polygons. Raster graphics are based on dot matrices which represent a rectangular grid of pixels. Several path planning strategies are possible depending on the type of images to mark, either raster or vector graphics. In production lines, the objects to mark are generally transported by conveyors. Therefore, the laser beam must be moved to mark a moving object. The production line is already creating a scan movement in one axis. In this context, only a single-axis scanner is indispensable. Nevertheless, using 2D scanning is still effective to avoid slowing down the production line. If the objects to mark are spaced in the line as shown in Figure 19 ($X_{sep} > A_w$), the time window to do the mark is longer than if only the marking area (Aw) is considered

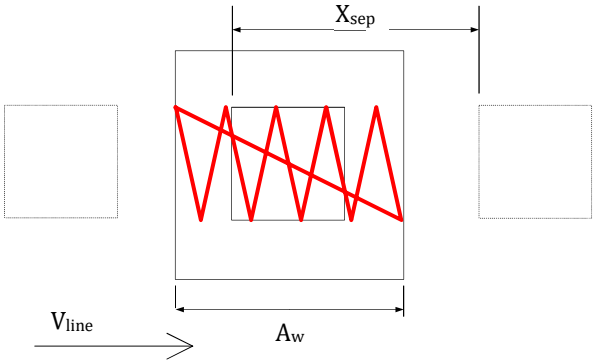

Figure 19: 2D scanning path for marking objects in a production line

The maximum line speed (Eq. 26) is determined by the scribing speed, the width of the marking area, and the length of the scan path (l_{pat}).

$$V_{line} < \frac{V_{sc} A_w}{l_{path}} \qquad (26)$$

Production lines are designed to work with a certain maximum constant speed (ideally). Nevertheless, unexpected events might require slowing down the line, or even reverse it for short periods of time (as shown in Figure 20). Thus, in practice, laser marking systems must support a variable production line speed, and therefore, they require positioning information feedback in real-time to avoid marking defects.

Figure 20: Possible variability of production line speed

Most laser beams can be deflected using optical systems like mirrors, lenses, or optical fibers. There are several methods to deflect the laser beam to scan the desired marking surface. The usual deflecting methods found in the industry are based on electro-mechanical (Polygonal Mirrors – PM [113], Galvo Scanners – GS), acousto-optic (AOD), or electro-optical systems (EOS). Their behavior can be characterized by some important parameters (listed in Table 5).

Table 5: Important features of beam deflecting systems

Symbol	Description	Units
θ_{max}	Maximum deflection angle	rad
ω_{max}	Maximum angular speed	rad/s
$\Delta\theta min$	Resolution of the angle values	rad
A	Aperture	mm
I	Moment of inertia	kg m^2
T	Transparency / Efficiency	%

The maximum deflection angle determines the deflection range, and the deflection angle resolution determines the number of resolvable locations of the beam. It is necessary to have a minimum resolution that allows visiting all the pixels of the raster. The angular speed usually determines the maximum scan frequency but, depending on the system, the moment of inertia will reduce this frequency value, as it prevents a fast change of direction of the deflected beam. Aperture is related to the size of the device. This is important in 2D systems because the range of beam positions from the first axis device needs to fit on the entrance of the second axis device. Transparency or efficiency is the percentage of optical power that goes through the deflecting system. The more transparent the system, the better, to avoid losing laser power. Otherwise, the absorbed power is transformed into heat that must be evacuated by additional cooling systems.

2.3.4. Reflective Deflection

Mirrors deflect laser beams with high efficiency, losing a small amount of energy in the process. They can be attached to electromechanical actuators to control their deflection angles at will. One of the most popular such systems is mirror galvanometers (GS). They are fast and have good resolution, as their position depends linearly on the current applied to their coil. They are usually combined in pairs (as shown in Figure 21a) to cover a target 2D surface. Their typical maximum angular speeds are around 200 rad/s. By design, the resolution of galvanometers degrades at extremes, so they are usually created to work in a maximum deflection angle lower than +/-20º. Due to the usual degrees of freedom, they are good to work in raster and vector modes. Although they react fast to electric control, the attached mirror has a relatively important mass that creates some inertia. This inertia favors the design of systems that maintain constant speeds and smooth trajectories. Figure 21 b) shows such an adequate trajectory for raster marking. A thorough analysis of the most convenient scanning regimes is analyzed by Duma [21].

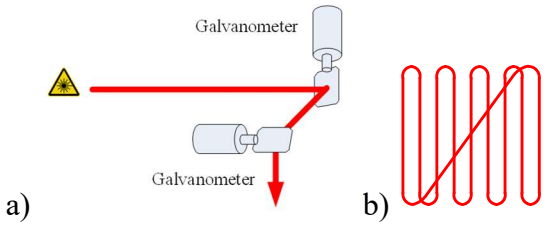

Figure 21: Galvanometer-based scanners a) disposition of the two-axis galvanometers. b) optimal scanning path for printing raster images

Other mechanical systems are polygonal mirrors (PM). They consist of a rotating polygon that rotates at a constant speed (see Figure 22 a). The laser beam is deflected with different angles depending on the rotation angle of the polygon. The constant rotation speed reduces the artifacts of raster scanning but makes it impossible to use them for vector marking. Since their maximum deflection angles are so large, they need special optics to minimize the nonlinear response of beam position with deflector rotation. Their resolution is good but is difficult to set them up to mark a 2D plane. Therefore, they are

usually combined with other means for the second axis (see Figure 22 b) to do bidirectional scanning. PMs might have important inertia, but it does not affect their scanning speed because the direction of movement is never altered. PM is commonly used in laser printers. The fastest laser printers using PMs are around 1m/s, while dot time is about 9.5 ns.

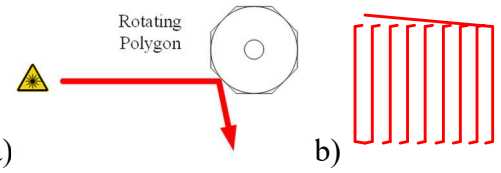

Figure 22: Polygonal mirrors. a) system disposition, only the rotating polygonal mirror is showed, an additional deflecting system is required for the other axis b) typical scanning path for a printing raster image.

Fast steering mirrors (FSM) are other possible deflecting devices. They are constructed by mounting a mirror on top of a structure that can be deformed at will. For instance, some piezoelectric columns can be expanded or contracted by an electronic control system using the piezoelectric effect (as depicted by Figure 23). These systems are usually faster than GS but have a limited angle of deflection. They have been implemented in 1D by Xiang et al. [22] and 2D by Wei et al. [23]. In the last paper, the authors reach 2.5º x 4.4º for maximum angles and 1036 and 654 Hz on each axis, allowing scanning above 100Hz. They can be integrated into Micro-Optic-Electro-Mechanical Systems (MOEMS). Other electrophysical effects, such as electrostatic attraction, are alternatively used in MOEMS. MOEMS have a lower aperture and usually have a limited deflection angle as reviewed by Holmström et al. [11].

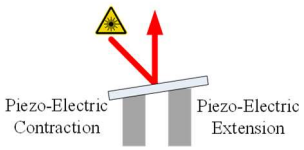

Figure 23: Piezo-Electric Mirrors

2.3.5. Refractive Deflection

Laser beams can also be deflected taking profit from the refraction that occurs when light passes through a different medium. Risley prisms (Figure 24) use this principle. They are usually combined in pairs so that they allow scanning a 2D area. Each prism can produce a deflection in one axis, by rotating both prisms the points in a surface can be addressed. Their efficiency is also high. Li et al. [114] demonstrate how they can get up to 120º of maximum deflection angle and 3000 rpm (314 rad/s). One of the problems with this scanning technique is that they have a blind zone in the center of the surface and the deflection angle is not linear with the prism's rotation, requiring a much more complex controller.

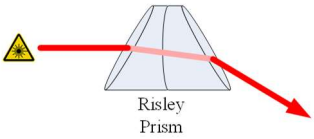

Figure 24: Risley prism

Acousto-Optic modulators (AOM) and Electro-Optic modulators (EOM) are different types of refractive deflectors. As described in detail by Römer and Bechtold [24], they are based on a change of the refractive index of a material induced by different means. Figure 25 illustrates how, in AOMs, the change of the refractive index is induced by sound waves. In EOM, the change is induced by an electric field which can be used to modulate the amplitude, phase, or polarization of the beam. Deflection angles are lower than GS and PM and their resolution is significantly lower. For instance, the EOM-based system described by Scrymgeour et al. [115] only reports 17 resolvable spots. Nevertheless, they are much faster. Their efficiency is also lower, in addition to the power devoted to maintaining the deflection of the beam, the beam power can also be attenuated by the physical phenomena they are based on. AOMs typically have a transparency value between 60% and 80%. Combining two AOMs to create a 2D scanning system would result in a transparency value between 36% and 64% making them impractical for 2D scanning.

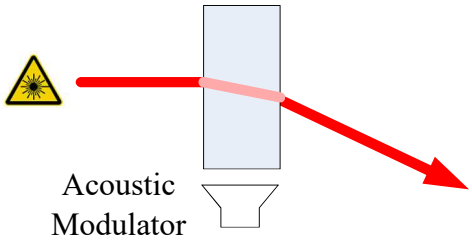

Figure 25: Acousto-Optic Modulator

In summary, GS is currently the most popular deflection method as they provide a more complete mix of properties. Table 6 summarizes the characteristics of the reviewed deflecting mechanisms.

Table 6: Typical Key Parameters for Scanning Systems

Technology	**A (mm)**	$\boldsymbol{\theta max}$ **(rad)**	$\boldsymbol{\Delta\theta_{min}}$ **(rad)**	$\boldsymbol{\omega_{max}}$ **(rad/s)**	$\boldsymbol{I}$ **(kg m²)**
GS	5–50	±0.3	10^{-5}	10^{2}	medium
PM	2–12	±0.7	10^{-4}	10^{4}	high
FSM	5–30	±0.05	10^{-6}	10^{1}	medium
AODs	0.5–5	±0.05	10^{-6}	10^{5}	-
EODs	0.1-5	±0.08	10^{-3}	10^{5}	-

The beam deflection mechanism has an impact on the achievable scribing speed. The best option also depends on the characteristics of the image to transfer. The beam

deflector is usually placed at a distance *d* of the marking surface (as shown in Figure 26). Lower deflecting angles will be used to mark small objects while large objects will require great distances or higher deflecting angles.

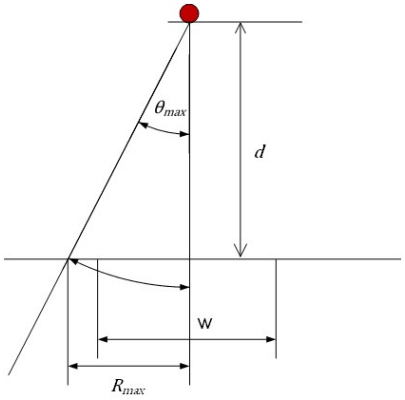

Figure 26 Effects of the beam deflecting geometry

When no lenses are used to correct the angular nonlinearity, the linear resolution will be approximated by the values at extremes. Thus, the linear resolution will be given by Eq. (27).

$$\Delta X_{min} = d\ (sin(\theta_{max}) - sin(\theta_{max} - \Delta\theta_{min})) \tag{27}$$

In addition, Nguyen et al [116] observed that the scanning speed of two-mirror deflection scanners can also be limited by the update frequency of the position coordinates allowed by the scanning head controller. Eq. 28 gives the maximum linear scribing speed according to the deflection system.

$$V_{sc\ def} < min\begin{cases}\omega_{eff\ max} d \\ \Delta X_{min} f_{ctrl}\end{cases} \tag{28}$$

Table 7 shows some of the highest scribing speeds (in m/min and m/s) achieved with different technologies reported in the literature.

Table 7: Scanning speeds achieved with deflecting systems reported in the literature.

Ref.	Year	Deflector Type	Wavelength (nm)	$V_{sc\ def}$ (m/min)	$V_{sc\ def}$ (m/s)
Hosaka et al. [117]	1987	AOD	514	600	10
Endo et al. [118]	2005	AOD	9200	2400	40
Hartwig et al. [119]	2010	GS	n/a	900	15
Park et al. [120]	2012	FSM	n/a	60	1
Exner et al. [121]	2012	PM	1070	18000	300
Exner et al. [121]	2012	GS	1070	1200	20
Wetzig et al. [122]	2019	GS	10600	1000	16

2.4. Summary of the chapter and discussion

The reaction of materials irradiated by moving laser beams is very complex, and many variables are affecting the final quality of the mark. In the previous sections, we have simplified many of the involved processes to a very high degree to build a coarse-

grain analytical model. By using it, we will foresee the limits of current technologies, and point out future challenges.

The three main aspects that limit the speed of production lines are laser-surface interaction, scanning, and the bandwidth and computing requirements of controllers. In the laser-surface interaction, the fluence threshold is a key feature. Although apparently, it is a fixed value, special coatings can be applied to the surfaces to provide a lower threshold and, consequently, increase the scribing speed. However, this is a one-time improvement. A more scalable alternative is to increase the irradiance provided by the laser source. However, the economic cost of high-power lasers becomes a de-facto limit for many industrial needs.

Nowadays, industrial laser marking systems are dominated by single beam systems. While not being the fastest option, GS is the most popular beam deflecting system due to its performance, flexibility, and cost. The problem with single-beam systems is that they quickly reduce the line speed by a factor of *1/x* as the width of the marking area increase.

Figure 27 depicts the relation between the laser power, the marked size, and the maximum achievable V_{line}. If the mark width is a single point, like in laser cutting applications, the line speed is the same that the scribing speed, which increases linearly with laser power (see Eq. (15), (19) and subsequent). For a single point, since deflection is not required, the limiting factor would be the ability to switch on and off the laser source. But as multiple points are required a deflection system is required to move the beam on the axis perpendicular to the conveyor. The deflection system introduces the maximum scanning speed as a limiting factor ($V_{sc\ def}$ Eq. 28). When this speed is reached no further power increases can contribute to faster V_{line} speeds.

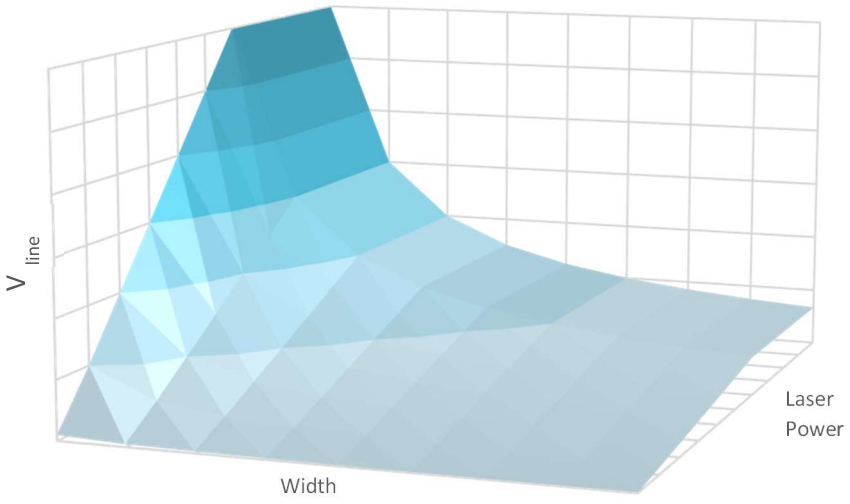

Figure 27: Relation of irradiance and size of marking area with the maximum line speed of single beam laser marking systems

Many industries have been dealing with these trade-offs for more than 20 years in different situations. As a result, we can create a category of marking scenarios (see Table 8) derived from the trade-off between marking area height (A_h) and line speed (V_{line}). Bruton [123] already proposed a similar classification.

Table 8: Current common laser marking scenarios for single-beam systems

Scenario	A_h order (dots)	V_{line} order (m/min)
High-speed coding (marking)	10^1	10^2
Labeling (high-speed printing or marking))	10^2	10^1
High-resolution printing	10^3	10^0

We predict that future industries will demand a gradual increase in many production lines' speed above 10 m/s. In addition, one of the basic pillars of the Industry 4.0 concept is the traceability of goods and their composing parts (as detailed in [124]). Direct Part Marking (DPM) plays an essential role in it and will probably make laser marking ubiquitous in future industries, increasing the demand for their associated technologies.

Higher line speeds will increase the demand for higher scanning speeds of single beam deflecting systems, but those having mechanical parts will probably be not able to fulfill the requirements as down-time and maintenance costs will increase. Operation time is an important part of the Overall Equipment Effectiveness (OEE) [125]. This justifies that, even with higher acquisition costs, industries will be investing in laser marking machines requiring less maintenance, higher operation time, and higher productivity because of the overall economic benefits.

All this will not be possible without a computation and communication system fast enough so that the control is not the limitation of the speed, resolution, or area of the printing system. More independent beams will lead to parallel computing, while the flexibility to design modular and scalable systems that can adjust the number of beams required by the application, leads to the use of reconfigurable architectures implemented in FPGAs.

3. Building multibeam laser marking systems

This chapter introduces the basic concepts that will cause a disruptive change in laser marking and printing: the evolution from single bean to multibeam. Based on this principle, I propose and develop in the following chapters, several architectures and implementations targeting application domains with different tradeoffs between printing speed, printing quality, paper width, and other parameters. I planned my thesis as a combination of Research (original ideas and theoretical and practical development to discover new knowledge in the technological field) with Development (application of research results for the implement new production systems to demonstrate its validity) and with Technological Innovation (advance in obtaining new methods that will produce better functionality and performance). The result should be a relevant improvement in technology with objective novelty (scientific-technological advance for the sector).

3.1. Laser Marking Systems Research and Development

Figure 28, shows the innovation process of the company dealing with the technologies developed in this thesis. It is relevant to mention that the research starts from Demand-Pull. This means that the rate and direction of technological changes are by-products of the company's economic activity; in particular, the inventions associated with this thesis are commercialized through investments in production plants and industrial equipment. This model is combined with the Science-Push model; in other words, we also invest in industrial basic research that leads to inventions (and related patents), then to innovation (first commercialization), and later to dissemination among potential clients.

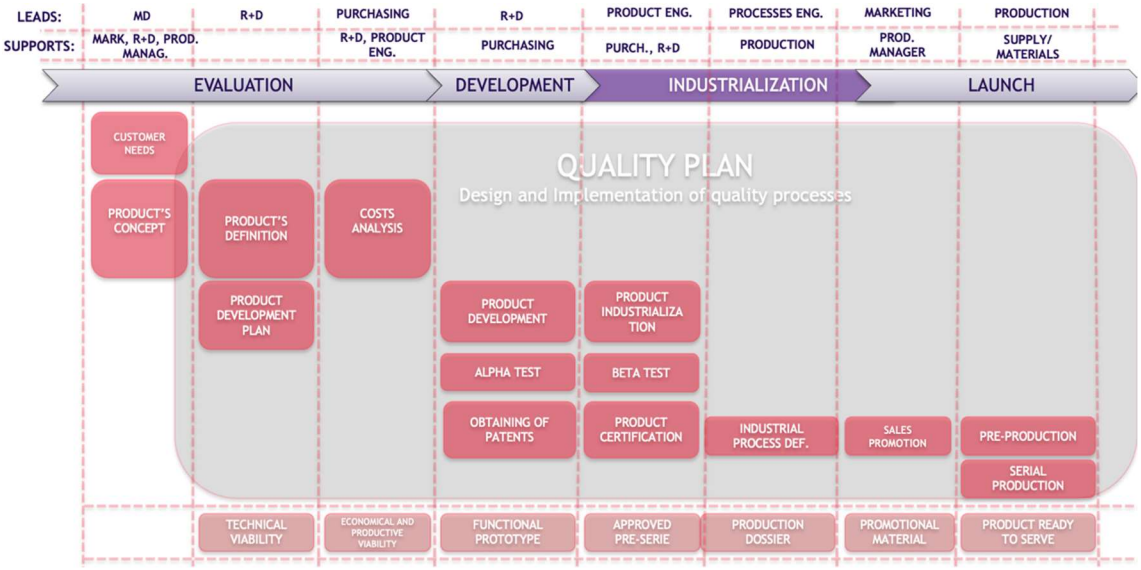

Figure 28: Complete innovation process, associated with the technologies developed in this thesis

It is an application-focused model, similar to the model proposed by Par Lab[1] at the University of California, Berkeley: driven top-down, applications first. At Par Lab, they select applications up-front to drive research and provide concrete goals and metrics to evaluate progress. They select each application based on some criteria such as compelling in terms of likely market and involvement of a committed expert application partner to help design, use and evaluate the technology [69]. I have tried to apply this model in this Thesis.

The process includes building prototypes and testing them experimentally, corroborating that, under the same conditions in which current systems fail to meet the requirements of high-performance production lines, the systems I propose can meet these requirements. Committed expert application partners evaluate the technology and verify that developed equipment can print the required information at the required speed. Thus, developed prototypes are accepted by the customers that validate the solution.

My focus is the proposal and development of new laser marking and printing systems for industrial environments, which includes a robust laser design for reliable operation, compact, and moderate cost of installation, lifetime, and maintenance together with the complementary ICT solution in terms of SW (system and embedded) and embedded HW.

The research work takes into account the main components of any laser marking system:

MARKING SURFACE: A material (thermo-chronic additive, paint, etc.) sensitive to certain wavelengths, requiring the smaller possible energy (E) of activation.

LASER SOURCE: A laser with the appropriate wavelength and enough power (P) to deliver the required energy ($E = P \cdot t$) to activate the material in a time (t) small enough to achieve the required speed

MARKING METHOD: covering the laser activation of the surface on the required area, with the required speed and resolution, using a laser beam deflection system or multiple laser beams

COMPUTING: We need to use embedded computation and communication systems, fast enough so that the control does not limit speed, resolution, or printing area.

In the following lines, I present some example problems related to laser marking systems in industrial environments. :

Example of a problem and solution related to the MARKING SURFACE: The packaging and consumer goods sector must produce and distribute products that are easier to recycle and use clean coding and marking technologies to print on modern, recyclable materials. There is a need in the industry to create solutions that optimize profitability and production while reducing the impact on the environment. Today's secondary packaging coding solutions require generating a large amount of non-recyclable waste (label and

[1] http://parlab.eecs.berkeley.edu/

backing paper and ribbon), and use consumables, solvents, and inks. Current coding solutions do not allow the 100% material separation to achieve optimal packaging recycling and have a high maintenance cost. Research here should focus on laser printing directly onto secondary packaging cardboard with no special pre-coating on the substrate required. The aim is to offer a solution for coding and marking boxes quickly and sustainably. In chapter 4 I will detail my proposal to design, develop and patent a method and system for marking paper, cardboard, and/or fabric [126][127] comprising the following steps: (1) pre-heating the surface of the material utilizing a heat source to a temperature lower than a temperature at which the visual appearance of the material changes; (2) marking the heated surface employing a marking laser so that the laser beam raises the temperature on the surface of the material enough to change the visual appearance of the surface.

Example of a problem and solution related to the LASER SOURCE: The current laser apparatuses have a complex structure and a high price. This limits their application and extension to certain fields in which costs are relevant. To solve this problem, I detail the proposal to provide a laser apparatus that has simple features because of its structure. The laser apparatus of the present invention [128][129][130] has a main extruded aluminum base where is possible to mount the laser cavity, as well as its electronic assemblies and optics, reducing the number of components. The laser source is formed by a laser cavity incorporated directly on the extruded base in a chamber of the latter, with the aid of lateral and base spacer elements that enable mounting in such a way as to allow expansion differences between the cavity and the extruded support without generating mechanical or thermal stresses on the cavity, which could alter the functioning of the laser. The structure of the apparatus allows the laser cavity to be placed at a level very close to the mounting surface of the equipment, avoiding expensive solutions such as periscopes, articulated optics, etc. Other features of the laser apparatus of the present invention comprise the increase in the heat-radiating surfaces. The new laser apparatus is solid and stable, mechanically as well as thermally and electrically, so that marking is reliable. The structuring of the apparatus allows the placing of the different electronic assemblies electromagnetically insulated employing metal walls that prevent disturbances from the RF power supply. This invention can be applied for the systems described in chapter 4.

Example of a problem and solution related to the MARKING METHOD: According to the state of the art, a laser marking system can be used to print a set of vector or raster data on a working area. The speed of the moving object concerning the stationary working area is determined by the needs of the production line, but not by the needs of the laser system, which, having a stationary working area, must adapt to the speed imposed by the production line. Thus, when the object enters the working area, the system begins to mark the product. If the marking system can obtain the position of the object in real-time, even though the production line does not have a constant speed during the marking process, the laser system could follow the object. To allow this variability in speed, it is necessary to have hardware and software to correct or convert the two-dimensional vector data or the corresponding raster data so that the laser can mark in real-

time by consequently moving the laser beam on the surface of the object. If the production line exceeds a critical speed, the object is not marked in its entirety because it leaves the working area before all raster or vector data can be marked. I contributed to the design, development, and patent of a device and process to mark a moving object using a laser system [131][132][133][134] with the ability to mark within a working area characterized in that the position of the object to be marked is obtained utilizing a sensor, and the laser system varies the speed of the object depending on the relation between the position of the object and the working area and/or the position of the laser beam within the working area. This invention can be applied to the systems described in chapter 4.

Example of a problem and solution related to the CONTROL SYSTEM: A problem in high-speed marking or printing is adapting the laser marking system to changes in the printing of the image or characters to be marked on the surface of the product. I contributed to the design, development, and patent of an invention [135][136][137][138] intended to be applied in those cases where various images, which share some common aspect, are to be marked on the surface of an object, and consists of optimizing the control method by dividing the image for marking into a fixed portion of the image (which corresponds to the common points among the variations in the image) and a variable portion of the image (which corresponds to the points of differentiation among the variations in the image). Given that the images to be marked normally have different variations, with the method according to the invention it is not necessary to process the entire image in each marking operation. The control system transforms said variable and invariable portions of the image into a variable matrix and an invariable matrix respectively. Said two matrices are then combined to form a complete NxM matrix of dots to be marked. Subsequently, if there is a new variation in the image it is only necessary to process the variable portion of the image, which is transformed into a new variable matrix. Said new variable matrix is combined with the previously calculated fixed matrix to form a complete N'xM' new matrix of dots to be marked for the new variation of the image. Optimization of machine control is achieved using said control method which reduces the modification time and therefore also reduces the marking time. The image to be marked can therefore be modified without increasing the marking time. This invention can be applied to the systems described in chapter 5 and 6.

Example of a problem and solution related to the LASER SYSTEM AS A WHOLE: Owing to the great variety of laser marking applications, the possible combinations of components in a piece of laser-marking equipment are very great. Consequently, versatility in the production of laser marking equipment is limited due to the heavy dependence on the application for which the equipment is intended, meaning that on-demand production entails a long lead time, it requires a sufficient stock of components to be available, changes of specifications once production has begun requires to start production of a new piece of equipment from the beginning, once the laser marking equipment has been assembled and configured, and it is complicated and costly to modify its functionality to adapt it to another application. Because of the above, I have contributed to the design, development, and patent of an invention [139][140][141][142] to overcome these drawbacks of the known laser marking equipment. This invention

discloses a method for producing equipment for marking products by a laser that comprises having various types of modules in which equipment components are grouped, selecting modules from each of the different module types, and removably attaching the selected modules, as will be demonstrated in chapter 5 and 6.

Example of a problem and solution related to the INDUSTRIAL ENVIRONMENTS: The cooling systems of the laser marking devices known in the prior art take in air from the front area of the appliance, this being the area that usually houses the lens through which the laser beam is projected towards the exterior of the device and cause this air to pass through the interior of the device. A problem with this type of cooling system lies in the fact that the front area of the device is the area that tends to contain the most dust and dirt due to its operation so that the air that enters the appliance is dirty. Despite the use of filters, according to the IP (Ingress Protection) indices, the entry of dust and/or dirt into the device is inevitable, and this results in a reduction of its durability. Additionally, the lens of a laser marking device tends to accumulate dirt during the operation of the device. Consequently, in many cases, this can result in it being stopped during its operation for marking or engraving products in a production line. Given the above, I contributed to the design, development, and patent of an invention [143][144][145] to solve the disadvantages of the known systems for the cooling of laser marking devices. The invented device comprises an outer casing defining internal volumes including a laser beam generating source, optical systems, and electronic and control means. The casing has air outlets and fans for generating cooling air flows between air inlets and air outlets, wherein the air inlet is more distant from the laser output than the air output. The most sensible optics and electronics parts are cooled through an air-to-air heat interchanger that isolates completely these components from the aggressive industrial environment. This invention can be applied to the systems described in chapter 4.

3.2. Parallel processing using multibeam laser systems

Within the framework of this development process for new laser marking and printing systems for industrial environments, several years ago, we started pioneering technologies for parallel processing using multibeam laser systems.

The examples of problems that I contributed to solving using multibeam laser systems are:

Laser marking apparatus with diode laser matrix (detailed in chapters 5): In the state of the art, it is known to use systems for marking moving objects, for example, a marking system using a CO_2 laser and an acousto-optic deflector. Although this type of system operates perfectly, it has the drawback that the system is very expensive, the CO_2 laser tube has very large dimensions, so it is difficult to site it in production lines and the acousto-optic deflector has high losses by absorption. On the other hand, laser diodes have a very small size, they can generate a laser beam with a considerable power level and with very low energy consumption. At that time, no marking system employs laser

diodes to produce the marking according to an N×M matrix of dots, which would be a system with a smaller volume and lower costs. To overcome the above-mentioned drawbacks and deficiencies, I contributed to the invention [146] consisting of a new marking system using a plurality of laser diodes and optical means producing laser beams that are focused on the surface to be marked. A marking control unit produces control signals which are applied to the plurality of laser diodes to thereby produce a controllable N×M matrix of laser beam dots, wherein selective illumination of the dots in the matrix produces a predetermined marking on the surface to be marked. If multiple lasers are used, their power can be combined with a concentrator to produce a single beam with a higher power and provide for simplified control over the beam's power.

Marking procedure through laser beams by images projection (detailed in chapter 6): Currently, the operative base for laser marking systems known so far is point-to-point printing in a matrix or vector way, but always defining a limited matrix of points. We developed an invention [8] that aims to achieve the impression of a complex image on a determined surface printing all the points simultaneously through optical techniques. To carry out this invention, advanced optical techniques (phase spatial modulation with Fourier Optical Transform) will be used. The procedure involves at the first stage the formation of the image to be marked in a computer, then transforming the image in a matrix NxM of non-coherent laser beams that are submitted to a spatial phase modulation diverting in an angular manner the individual laser beams for its digital conversion and a system of zeros and ones corresponding to the no diverting and diverting positions of the individual laser beams, then doing the concentration of the selected signs on the object to mark, marking at once all the selected marking image.

At the time that I contributed these pioneering technologies, the devices required to efficiently implement that technology were not available, e.g., laser diodes were bulky and not very powerful, optical fibers had high insertion loss, micro-optics did not allow high integration densities, component costs and availability were doing difficult the economic feasibility of applications. Currently, several laser companies developed high-power laser components, enabling fiber and direct diode laser systems for material processing while other companies developed color-change materials for laser coding, and equipment companies, such as Macsa, have developed truly disruptive in-line digital printing solutions.

3.2.1. Theoretical formulation of laser marking

For the simplification of the analysis, in section 2.3., I considered that the mean Irradiance value on a circle is determined by Eq. (8)

. When there is relative motion between the substrate and laser marking emitter in the x-direction, with speed V_{sc} , the area covered by a moving beam, assuming circular symmetry, and ignoring the intensity distribution of the beam, I consider it is determined by Eq. 13.

In practice, with the relative movement between emitter and substrate, dots become thinner on the transverse axis and more stretched on the longitudinal axis. In a more detailed analysis, I could consider that the beam of each emitter has an intensity distribution in the focused or image spot that may be represented by Eq. (29):

$$I(x,y) = I_0 e^{-2(|x|^s+|y|^s)/{w_0}^s} \tag{29}$$

When *s* is lower than 2 this distribution tends to be narrower and more peaked than the Gaussian distribution and may be described as pseudo-Gaussian, when *s* is equal to 2 the intensity distribution is Gaussian, and when *s* is higher than 2 the intensity distribution becomes flatter and tends to a "top hat" intensity distribution as *s* becomes larger. When *s* is equal to even integers and is higher than 2 the distribution is described as super-Gaussian. The parameter w_0 characterizes the beam size or spot radius [147]. Integrating this intensity distribution on the axis perpendicular to the movement can be obtained the parameter I_y, Eq. (30):

$$I_y = \int_0^\infty e^{-2|y|^s/{w_0}^s}\, dy \tag{30}$$

Considering a certain fluence threshold (F_{th}) which is required to produce a visible change, considering a relative motion between the substrate and laser marking emitter in the x-direction, with speed V_x, considering the power parameter Φ for the emitter, and assuming circular symmetry, the line width *lw* of a marked line will be determined by Eq. (31)

$$l_w = 2w_0 \left\{-\frac{1}{2}\ln\left[\frac{2F_{th}V_x I_y}{\Phi}\right]\right\}^{\frac{1}{s}} \tag{31}$$

Let *lwi* represent the line width measured at emitter power parameter Φ_i. Then from equation (31), for the power parameter Φ_1, can be written as Eq. (32):

$$e^{-2\left(\frac{l_{w1}}{2w_0}\right)^s} = \frac{2F_{th}V_x I_y}{\Phi_1} \tag{32}$$

A similar expression may be written for the line width l_{w2} measured at power parameter Φ_2. Dividing Eq. (32) as written in terms of Φ_2 by equation (32) as written in terms of Φ_1 and solving for w_0 results in Eq. (33):

$$w_0 = \frac{1}{2}\left\{\frac{l_{w2}^s - l_{w1}^s}{\frac{1}{2}\ln\left[\frac{\Phi_2}{\Phi_1}\right]}\right\}^{\frac{1}{s}} \tag{33}$$

Making another measurement of line width l_{w3} at power parameter Φ_3 will allow us to derive an equivalent relation to equation (33) linking Φ_2 and Φ_3. Combining the relations of equation (33) for Φ_1, Φ_2 and Φ_3 it is possible to derive the following relation Eq. (34):

$$l_{w3}^{s} - l_{w2}^{s} = A'(l_{w2}^{s} - l_{w1}^{s}) \tag{34}$$

Where the parameter A' is determined by the three power parameter values used for the line width measurements and is given in the following Eq. (35:

$$A' = \frac{\ln\left[\frac{\Phi_3}{\Phi_2}\right]}{\ln\left[\frac{\Phi_2}{\Phi_1}\right]} \tag{35}$$

Equation (34) may be solved to determine the value of '*s*' by using numerical or analytical methods. Having determined '*s*' from a solution to Eq. (34) the emitting aperture parameter may be determined from Eq. (33) and the parameter F_{th} may be determined from equations of the form Eq. (36):

$$F_{th} = \frac{\Phi_n}{2V_x I_y} e^{-2\left(\frac{l_{wn}}{2w_0}\right)^s} \tag{36}$$

The average optical density OD for the line in question is proportional to the integral of the energy density received above the threshold across the width of the image line. If A_{th} represents the area in question I may write Eq. (37).

$$A_{th} = \int_{-\frac{l_w}{2}}^{\frac{l_w}{2}} \frac{\Phi}{2V_x I_y} e^{-2|y|^s/{w_0}^s}\, dy - F_{th} l_w \tag{37}$$

Since average optical density is proportional to A_{th}, to find a power parameter Φ to balance the A_{th} value for each line, it is necessary to rearrange equation (37) to obtain Eq. (38):

$$\Phi = \frac{2V_x I_y (A_{th} + F_{th} l_w)}{\int_{-\frac{l_w}{2}}^{\frac{l_w}{2}} e^{-2|y|^s/{w_0}^s} dy} \tag{38}$$

The line width relation of equation (31) may be rearranged for Φ to give Eq. (39):

$$\Phi = 2F_{th} V_x I_y e^{2\left(\frac{l_w}{2w_0}\right)^s} \tag{39}$$

Equating equation (38 with equation (39 and rearranging provides the following relation (Eq. (40):

$$A_{th} = F_{th} e^{2\left(\frac{l_w}{2w_0}\right)^s} \int_{-\frac{l_w}{2}}^{\frac{l_w}{2}} e^{-2|y|^s/{w_0}^s}\, dy - F_{th} l_w \tag{40}$$

During variations in substrate speed, the optical density of the marked image will vary. Intuitively and as seen in the different mathematical models, the optical density decreases as the speed of the substrate increases. For parallel processing using multibeam lasers, the average optical density of the image depends on the density of individual points, the narrowing of points or lines, and the elongation of points as product movement

increases. The spaces between points, in the direction of movement, can be made smaller, the region between adjacent transverse points can become less dense and widen, the optical density of individual points or lines can be reduced, and therefore the average optical density of the image can be enlarged or decreased with the substrate speed. The result of these interactions is that the appearance of an image can become lighter or darker as the speed of the substrate changes. The effects depend on the specific marking settings defined by parameters such as pulse duration, longitudinal pitch, resolution, dot size, etc. Marking and printing results on different substrates with multi-beam laser systems show a non-linear and non-intuitive variation in optical density as pulse duration and substrate speed vary, although they do show a trend in which optical density decreases as substrate speed increases.

It is very challenging to predict the resulting optical density for any given marking substrate and it is outside the scope of this thesis to create an exact model that explains all possible factors that affect the speed/optical density ratio, like the temperature of the substrate or variations in the emitter irradiance profile. The increase in the complexity of the mathematical model used to explain the relationship between speed and optical density does not substantially increase precision on the predictions in the experimental results, so I decided that the model for the calculations and the theoretical basis used in this thesis will use that simple and generic approach.

3.2.2. Multiple homogeneous beam systems

The performance of a single beam marking system is influenced by the scribing speed, which is limited by the interaction of the beam with the surface (Eq. (*15* and Eq. 25.) or by the deflection method (Eq. 28).

The maximum scribing speed values found in the industry are generally lower than few meters per second. When marking several dots per column the speed of the production line is reduced even more (Eq. 26).

The empirical production line speed limit achieved so far is around 8 m/s [118], printing few dots per column on surfaces with coatings that are sensible to the laser wavelength.

An option to creating multiple independent beams (beamlets) is to project a single beam into a micromirror array (MMA) or a spatial light modulator (SLM). Sans et al. [8] patented an imaging laser beam marking procedure using an SLM. Kuntze et al. [148] successfully used an MMA in combination with an Excimer laser source to mark on paper and plastic surfaces. By using an array of mirrors, different parts of the beam can be deflected to follow different trajectories (as shown in Figure 29). MMAs orientate each mirror independently. Typically, the allowed orientation positions are only two.

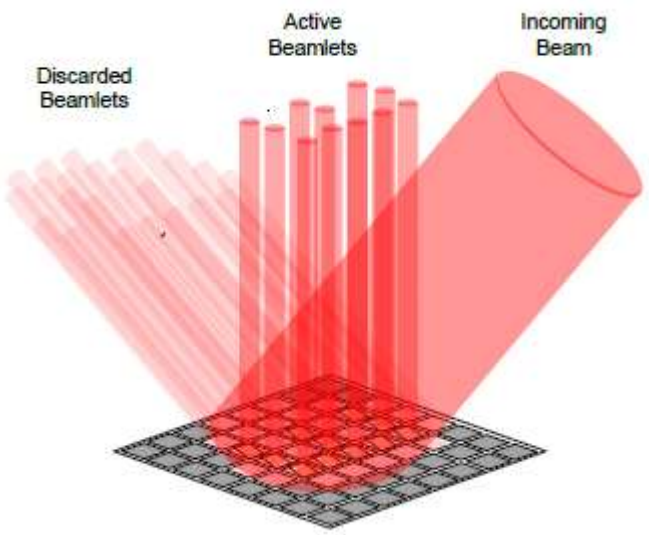

Figure 29: Beamlets created by radiating a beam on an MMA device. Some of the beamlets will be actively used to produce the mark, while the rest will be discarded.

As stated in section 2.4, it is usually desirable to reduce the beam diameter to increase the irradiance and fluence in the marking plane. However, when using MMAs, an optical path is required to expand the beam so that it covers a certain area of the MMA and later reduces it again before hitting the surface. The irradiance delivered by the beamlets is typically small. The scribing speed will be derived from the irradiance of the beamlets reflected by the individual micromirrors (as derived from Eq. 11).

An alternative to surpass this limit and increase the production line speed is to use multiple independent lower-cost laser sources (such as laser diodes) and eliminate the dynamic beam deflection systems. Even though duplicating laser sources has an important economic cost. Sans et al. [146] patented the use of multiple laser diodes for marking. Figure 30 depicts an array of laser sources.

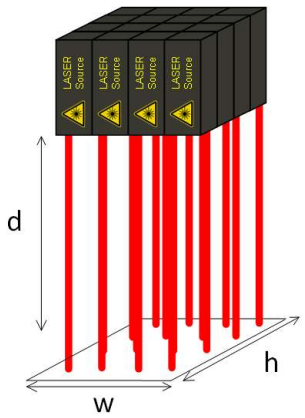

Figure 30: Diode Matrix marking system.

In this case, the density of the marked dots becomes the main problem as it is severely limited by the physical dimensions of the devices. Large laser diodes have an

efficiency of around 50%, so they also need an important area for heat dissipation. Kataoka et al. [149] overcome this problem by generating the laser beams in a distant location with a lower power density and later concentrating them in the printing head using optical fibers.

Integrated circuit technologies allow integrating several laser diodes on the same chip. Vertical Cavity Surface Emitting Lasers (VCSEL) have been used by Mukoyama et al. [1] to create a system with 32 beams and power of 3mW with up to 2400 dpi. and, according to Kowalski [150], diode arrays are increasingly being used for printing applications. The marking performance of a diode array that covers the entire surface to mark with columns of LDs is determined by the scribing speed because all pixels would be activated at the same time.

Assuming a simple system with diode array columns orthogonal to the product movement on the production line, and assuming uniform process direction resolution is maintained, and printed dots pitch is equal to diode array pitch (X-process direction resolution), then Eq. (*41*).

$$V_{line} = V_{sc} \tag{41}$$

determines the speed of the production line (V_{line}) for a system with just one column of LDs (see Figure 31a).

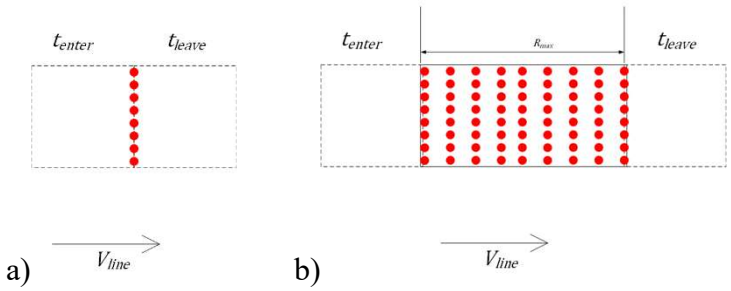

Figure 31 a) Dynamic marking with just one diode column b) Dynamic marking with several columns

In the case of an LD matrix, the columns can be marked in reverse order from the direction of the conveyor. The LDs of different columns could be used as the object is moving to accumulate the light hitting a given object point. The laser-on time would then be shared among columns. The maximum value would be the result of all columns contributing. This allows increasing the speed at will, with the only limits imposed by the tolerances in aspect ratio (given by Eq. 21), the physical dimensions, and the economic cost of the additional laser sources.

$$AR_P = \frac{d_{spot} + V_{sc\,P}\Delta t_p}{d_{spot}} \tag{42}$$

Eq. 43 determines the speed of the production line for a system with multiple columns of LDs, where L_C is the number of the laser diode columns.

$$V_{line} \approx V_{sc} L_c \quad (43)$$

The diodes can be away from the marking surface (where convenient cooling is provided) and connected by optical fibers. The benefit of this approach is that the imaging speed is independent of image content.

The individual laser diodes from these marking systems comprising multi-source laser arrays are modulated based on the image requirements to generate an array of dots or pixels in the substrate. The modulation of individual laser diodes to achieve a given optical density can be through the modulation of the input current to control the output power emitted by the diode or varying the pulse duration of the emitter, or the duty cycle of the emitter, or the relative speed of the substrate relative to the emitter. Any or each of these inputs together defines a marking setting that relates to the target optical density in the marked image.

There is natural variation between the output power, and variation in the emitted beam intensity distribution and spot size for each laser channel. Furthermore, some marking substrates will have relatively significant differences in response to variations in laser power, intensity distribution, or spot size. It is very challenging to predict the resulting optical density for any given marking substrate and adjust such differences consequently to equalize the individual laser channels to provide a method of calibrating such laser marking systems [147][151][152][153].

One possible method of calibrating is marking individual lines on a substrate for each emitter at a plurality of different marking settings, creating a calibration test pattern; measuring the line width of each line in the pattern; and thereby calculating a relationship between the marking setting and the marked line width. For each emitter with a given marking setting and beam intensity distribution there exists a relationship (Eq. (40) between line width and the sum of the excess energy above the threshold for marking received across the width of the line (A_{th}). As the sum A_{th} is related to the optical density of the line, this method provides for the calculation of a relationship between the marking setting and the output optical density for each emitter. The marking setting may be defined by any one or more power parameters of the emitter; pulse duration of the emitter; duty cycle of the emitter; and the relative velocity between the emitters and the substrate. A laser marking system can make use of a look-up table of settings wherein the table is populated using the calibration method. Section 3.2.1 provides the equations and theoretical basis for the interpolation calculations relating to marking setting and optical density *OD*.

3.2.3. Multiple heterogeneous beam systems

Lasers are widely used for labeling and marking purposes. Typical applications include writing barcodes. Different companies offer such systems which are controlled by computers and can produce various types of labels with high flexibility [154][17] Laser marking is one of the environment-friendly technologies. Laser marking decreases waste creation in comparison with the other classical marking technologies [18].

As we have seen in the previous section, multiple similar laser beamlets can contribute to the fluence provided to a dot of the marking surface. Another option is to combine different types of beams to contribute to reaching the fluence threshold as required by the application.

Laser marking on paper and cardboard packaging has a special interest for industrial applications. In paper and cardboard, we have seen that using different laser types can provide additional benefits. Chapter 4 details the implementation of the novel method to print on paper and cardboard without ink. The method is based on the carbonization of paper by a combination of lasers working on different wavelengths. It aims to reach the carbonization stage in two phases to minimize the generation of debris. In the first phase, a certain area of the surface is preheated below the temperature threshold in which visible changes are manifested. In the second phase, a short wavelength laser injects the additional required heat to produce visual marks while triggering polymerization of some of the volatilized compounds, thus reducing the debris.

3.2.4. Proposed printing method using thermochromic coating

The information printed on the packaging has different uses, requires different qualities, and can be done at different times in the life of the product. Brands and logos that decorate a package can remain constant for years, while other critical information such as batch numbers, unique sequential identifiers, variations on country-specific regulations and languages, etc., changes frequently. To accommodate this more dynamic information, one method that packagers use is to overprint variable information on pre-printed packages during manufacturing or filling.

Additionally, there is a demand for more information at the late process stages. New coding and marking regulations are driving changes to font sizes for more readable formats. This is going to require printing technology that can print more information, coupled with graphics that boost visual appeal and readability.

Until now, no coding and marking technology has been of sufficient quality to print high-resolution graphics and logos, small fonts, and various forms of barcodes at high speeds. I contributed to this research that has supported by the consortium composed by Macsa I.D., S.A, DataLase Ltd., and Xerox Corporation working with Palo Alto Research Center (PARC), that implemented a disruptive digital laser packaging print technology that enables high-quality printing of complex information in the last stages of product packaging [155][156]. This method takes a novel approach: using no ink or toner, but a patch of pre-printed thermochromic materials that are activated by a series of laser beams. The heat from the laser causes thermochromic pigments in materials to change to predetermined monochrome color.

This inkless, laser-based Inline Digital Printing (IDP) is a printing method that combines laser-reactive materials and multi-laser arrays [157]. Laser-reactive materials are specialized coatings that change color in areas exposed to laser light. The multi-laser array forms images on laser-reactive materials. Used together in the inline digital method,

these two technologies can address the current challenges of package printing: speed, resolutions, reliability, and endurance. IDP is a clean, dry process and is more manageable than processes dependent on inks, powders, or waxes. Lasers, which use no liquids, ribbons, or labels, rarely malfunction. Lasers are one of the most long-lasting, consistent marking technologies. IDP is a combined application of chemical and advanced optical technologies. The coating is applied to a substrate as part of the packaging. The coating is white or colorless and, when irradiated with a laser, undergoes a chemical reaction, and turns black (or another color as determined by the coating formulation).

Process steps are as follows (Figure 32):

1) Substrate and Coating Matching: the converter selects a laser-reactive coating suitable for the target substrate. Possible substrates include Polyethylene, Polypropylene, BOPP, paper, Polyolefin, foil films, corrugate, folding cartons, and others. A pack or product is conventionally printed by flexography, gravure, or lithography.
2) Coating Application: the converter applies the coating to the substrate using a standard flexographic, gravure, screen, or other print processes. Thermochromic materials are applied to specified areas on the product or pack in the form of a clear or white ink patch containing the laser-sensitive materials.
3) Finishing: the coating dries or is cured. It is now ready for imaging at the converter replacing flexo or gravure processes, on a filling line, or at a retailer.
4) IDP uses a multi-laser array to create images. Objects coated with laser-reactive material pass beneath the array and turn black (or another color) in areas exposed to the laser beam. By selectively pulsing the lasers on and off, the array can choose which areas change color and which areas remain white/colorless. The combination of colored areas and whitespace form a monochrome image.

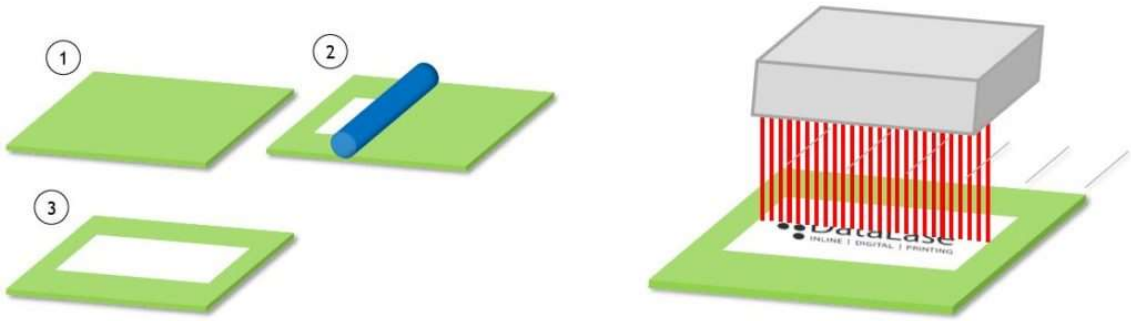

Figure 32: Process steps for the inkless, laser-based Inline Digital Printing (IDP) method

Multiple implementations of the different components of the Inline Digital Printing (IDP) method have been made by various manufacturers.

Ricoh specifies in [153] that a thermosensitive recording medium, to which image recording is performed once, can be used and a thermoreversible recording medium, to which image recording and image erasing can be repetitively performed, can be also used. The thermosensitive recording medium includes a support and a thermosensitive coloring

layer and may further include other layers according to the necessity. Each layer may have a single-layer structure or a laminate structure. The thermosensitive coloring layer includes a material that absorbs the laser light and converts it into heat (photothermal conversion material) and a material that causes a change in hue or reflectance with heat. Examples of these materials known in the art are a combination of an electron-donating dye precursor and an electron-accepting color developer used in the thermosensitive paper. Moreover, the change of the material includes a complex reaction of heat and light, such as a discoloring reaction due to solid-phase polymerization of a diacetylene-based compound caused by heating and UV irradiation. Reference [153] provides multiple examples of the electron-donating dye precursor and the electron-accepting color developer, as well as the photothermal conversion material. The last ones are preferable those whose absorption of light in the near-infrared region is large and absorption of light in the visible region is small. The photothermal conversion material may be used alone or in combination and may be included in a thermosensitive coloring layer. The photothermal conversion layer includes the photothermal conversion material, a binder resin, and other possible materials. The support may be a single-layer or a laminate structure. Other possible layers include a protective layer, a UV ray-absorbing layer, an oxygen-barrier layer, a backing layer, an adhesive layer, etc. Additionally, reference [153] provides several examples for the production of the thermosensitive recording material, coloring layer coating liquid, and support to produce a thermosensitive recording medium as a recording target.

DataLase Ltd.'s core business is thermochromic coatings and they have multiples patents that protect their implementations. For example in [108], they protect an ink formulation comprising: (a) a near-infrared absorbing system; (b) a color change agent; and (c) a binder. This patent also provides alternative ink formulations for laser marking, a method of forming an image using the ink formulations and a substrate coated with them. Reference [108] claims that these ink formulations have good laser imaging efficacy and a negligible impact on the background color of the coating. DataLase Ltd. also protects in [158] an ink formulation comprising a marking component, e.g., ammonium octamolybdate, and a metal salt that absorbs laser irradiation at 780-2500 nm, e.g. reduced indium tin oxide and thereby causes the marking component to change color. And they also claim improvements in or relating to laser marking in [147], where the emitter may be operable to emit light with any suitable wavelength, including visible or near-infrared (NIR) wavelengths, specifically in the ranges: 390 to 460nm, 500 to 550nm, 620 to 660nm, 900 to 1100nm and 1400 to 1600nm. The substrate comprises a color change material operable to change color in response to illumination by the emitters and a NIR (near-infrared) absorber material. The NIR absorber material may be operable to facilitate the transfer of energy from a NIR laser to the color change material.

Figure 33 shows the thermally driven color change induced by laser absorption in thermochromic print media.

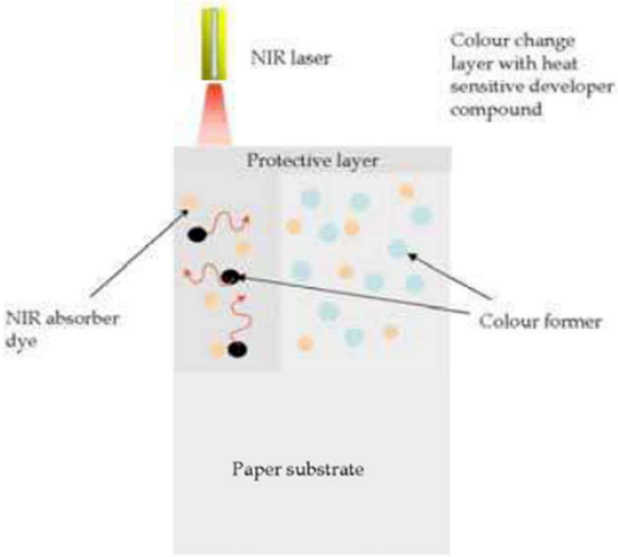

Figure 33: Thermally driven color change induced by laser absorption in thermochromic print media [150].

This inkless, laser-based Inline Digital Printing (IDP) method has many advantages over inkjet and thermal transfer [155][156].

- Laser technology avoids the use of consumables (ribbons and inks) in the fulfillment area, reducing inventory management as well as health and safety issues.
- This new method offers the potential to eliminate printing and affixing labels by printing directly onto the packaging.
- Replacing consumables incurs higher costs, and there are maintenance issues when equipment is shut down due to ribbons, labels, or dried-ink blockage.
- Productivity is higher, as it uses no consumables that require refilling or replacement and cleanup.
- Reliability is greater. The lasers maintain high-resolution printing when fired from long distances from the packaging, reducing the likelihood that a printhead will be struck and misaligned during production.
- Running costs are lower, particularly when assembly line shutdown frequency is considered.
- Digital laser printing is easier to read and has better durability than inkjet printing. Print quality and durability match that of the flexo and offset presses used for early-stage printing, enabling a broader range of late-stage applications with high-resolution graphics and logos, grayscale, small fonts, bar-codes, 2D codes, variable product information, etc.
- High-quality barcode and QR code capability allow for a unique serial number for each product sent out that can tie in with product security and track and trace features.
- By using the solution to print such variable information as ingredients, languages, and country regulations, manufacturers and converters can reduce their inventory and SKU levels, saving on warehousing and picking.

- Manufacturers using IDP can switch seamlessly between different customers' label requirements and adjust quickly when those requirements change.
- Inline digital printing is also central to new eCommerce marketing strategies. Online retailers can personalize each box to reflect one-off items or to market new products based on customers' ordering patterns.
- By introducing new applications, such as ads printed onto shipping cartons customized to the profile of the recipient, manufacturers and converters can develop new, sophisticated marketing-driven revenue streams, for example, real-time promotional efforts, such as content or graphics around a recent Olympic medal winner on the packaging.

3.2.5. Proposed printing method by ablating the surface material

Very high-speed laser marking on the packaging is of great interest for high-performance production lines. In the equations Eq. (41 and Eq. 43 I have shown that with multi-beam laser marking systems, the maximum production line speed (V_{line}) is limited in a direct proportion to the marking scribing speed (V_{sc}.), and in the equation Eq. (17) I have shown that the maximum scribing speed (V_{sc}) is directly proportional to the duration of the laser pulses (Δt_p)

$$V_{scP} < \frac{\Phi_{peak} f_p \Delta t_p}{d_{spot} F_{th}} - \frac{\pi d_{spot}}{4t} \qquad (44)$$

Laser marking of materials can use various marking methods, for example, ablation. Laser ablation or photoablation is the process of removing material from a surface by irradiating it with a laser beam [159]. For materials processing, ablation requires the highest power densities and the shortest interaction times (Δt_p), while other processes require lower power densities and longer interaction times [160]. When selecting a laser marking method for a particular application, there are many factors to consider: (a) irradiance; (b) thermal factors: thermal conductivity, heat capacity, melting point, and heat of vaporization; (c) reflectivity: material, wavelength, and temperature. In ablation, the laser removes a coating layer. The underlying base material is visible in the mark. Generally, laser ablation refers to the removal of material with a pulsed laser, but ablation with a continuous wave laser beam is possible if the intensity of the laser is high enough [159].

Chapter 5 and chapter 6 will detail the digital laser marking of packaging method, based on ablative processes, that allows the marking of unique information at high speed [161]. This method uses high-power laser diodes (HPLD) to ablate packaging materials. The high irradiance of the laser beams causes various ablative processes in coatings of different materials, making visible the substrate under the coating. Absorption of beam energy by the irradiated coating must be as much efficient as possible to achieve maximum coating removal and maximum contrast between the area unaffected by the beam and the substrate that appears once the coating is ablated. I conducted laser markings under different combinations of process parameters: pulse duration, pulse

power, and scanning speed of the laser beam. I have studied how different laser parameters affect the surface texture and color change of materials while creating minimal waste. The morphological characterization of surfaces has been carried out using optical microscopy and scanning electron microscopy (SEM).

At low laser flux, the material is heated by absorbed laser energy and evaporates or sublimates. With a high laser flux, the material is typically converted to plasma. In the marking process, the energy density used is usually high enough that the desired vaporization is completed within microseconds. A series of vaporized craters on a surface generally alters its appearance. The marking contrast depends on the chemistry of the material, the surface finishing, and the color. A good definition of the mark edge can be achieved, and the depth and width of the mark are controllable.

The depth at which laser energy is absorbed, and therefore the amount of material removed by a single laser pulse, depends on the optical properties of the material and the duration of the laser pulse and wavelength. The total mass removed from the target material per laser pulse is often referred to as the ablation rate. Characteristics of laser radiation such as the scanning speed of the laser beam and the coverage of the scanning lines can significantly influence the ablation process [159]. Laser pulses can vary over a very wide range of duration (milliseconds to femtoseconds) and fluxes and can be precisely controlled. When a beam of pulses of sufficient intensity is incident on a surface, the absorbed energy can melt and/or vaporize the material on the surface [160]. Depending on the energy source and the surface material, this can occur by photochemical ablation or by photothermal ablation. Organic materials can be marked by photochemical ablation because organic compounds tend to absorb ultraviolet radiation efficiently. Photothermic ablation can occur by normal vaporization, by normal boiling, or by phase explosion. There are no models that fully describe explosive laser ablation processes [162]. When a high-powered, short-pulse laser beam is focused onto any solid target, some of the material instantly explodes into vapor. The laser irradiance (power density) and the thermo-optical properties of the material are critical parameters that influence these processes.

Normal vaporization refers to the transformation of the condensed phase (solid or liquid) to the vapor phase as atoms or molecules are emitted from the extreme outer surface [160]. It can occur with any fluence and pulse duration, and there is no temperature threshold. The surface temperature is not constant since the vapor pressure is not zero. The contribution of normal vaporization to ablation is negligible on timescales less than 1 ns and for very low temperatures. When the duration of the laser pulse is microseconds or more and the irradiance is less than approximately 10^6 W/cm^2, vaporization is likely to be a dominant process influencing the removal of material from a target [162].

Normal boiling requires a relatively long pulse period. The normal boiling process occurs within the optical penetration skin depth (δ_p) Eq. 6 where α is the absorption coefficient.

The surface temperature is constant and the same as the vaporization temperature corresponding to the pressure at the surface [160].

At higher irradiance, beyond 10^9 W/cm^2 with nanosecond and shorter laser pulses, focused on any material, an explosion occurs. Phenomenologically, the surface temperature is instantly heated beyond its vaporization temperature through linear one-photon absorption, multi-photon absorption, dielectric breakdown, and other undefined additional mechanisms [162]. This explosive interaction has been described as "non-thermal" and melting is often not observed around the crater. Fractional vaporization should be negligible. Nevertheless, during an ablative interaction, a plasma is initiated in the sample. Plasma temperatures are above 10^4 K and radiative heat transport can establish a plasma-material interaction. The duration of the plasma is microseconds, which is long compared to the short laser pulse. Fractional vaporization can occur during this plasma-material interaction, and to a greater extent than in the case of direct laser vaporization interaction.

The power densities given are approximate. Power densities in the range 10^6-10^9 W/cm^2 can cause vaporization, boiling, phase explosion, all these processes simultaneously, or additional mechanisms that have not yet been identified. The existence of shock waves is easily confirmed by the sonic boom of a focused short pulse laser that explodes a target material at atmospheric pressure. For the interaction of long pulses laser with the material, the processing can be very unstable due to the complicated laser ablation mechanisms that have been studied. Figure 34 [163] shows the complexity of a microsecond pulse laser ablation. The diffusion of heat is sometimes associated with the formation of surface shock waves. These shock waves can give rise to irregular crater shapes during solidification [164].

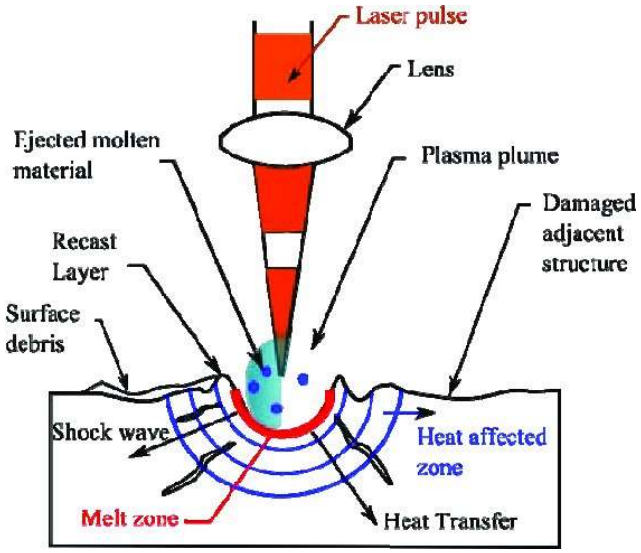

Figure 34: Microsecond pulse laser ablation [163]

The microscopic mechanisms of the fluence threshold behavior in laser ablation of organic solids have been defined [87]. Below the threshold, it is identified that

evaporation occurs, and mainly individual molecules are desorbed. Above the threshold, collective expulsion or ablation occurs in which large molecular clusters make up a significant part of the ejected plume. Laser-induced pressure build-up and phase explosion due to overheating of irradiated material are identified as the key processes that determine the dynamics of laser ablation [87]. Threshold behavior has been found in laser ablation of a wide variety of organic solids; this is the case for most packaging materials. The threshold where visible changes manifest depends on the chemical components of the material. To know these thresholds, I have performed multiple tests with multiple packaging materials, varying multiple parameters of laser irradiation.

Since currently available high power laser diodes (HPLDs) are limited to a maximum power density on the order of 10^5 W/cm^2, most applications of HPLDs to process materials are limited to surface treatments such as marking [165]. High contrast marks have been generated using HPLDs in the marking and etching of various materials through heating, melting, or material removal mechanisms. The color of materials was found to influence beam absorption. Light-colored material reflects more of the laser beam.

3.3. High-Performance Embedded Systems

The operation I want from the control system is as follows: A specific design software application is used in an external host to compose the images to print, ranging from few tens up to several millions of pixels, and from few mm2 up to several hundred cm^2. It allows the definition of fixed and dynamic parts of images, which is used to reduce the image transfer time (preferably in the order of ms) from the host to the controller. The external host sends both parts of the image to the controller through Gigabit Ethernet, which is fast enough for the required bandwidth. The controller is responsible to manage each print in synchronization with the production line. Figure 35 shows the intended possible content for the printing covering all the applications.

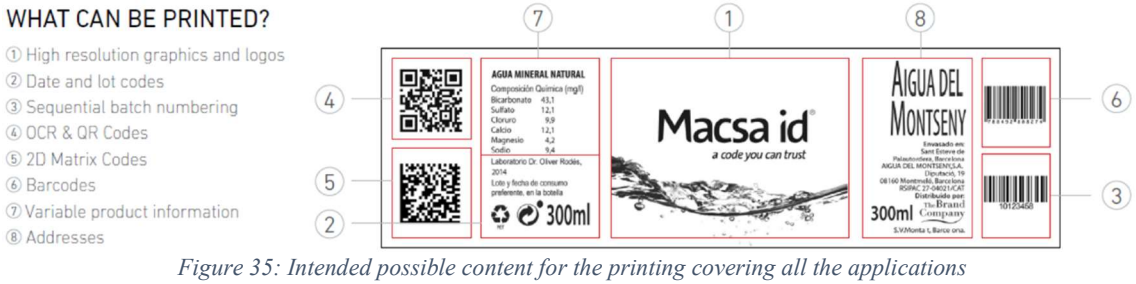

Figure 35: Intended possible content for the printing covering all the applications

3.3.1. Computing requirements

In a digital printing system, a Digital Front End (DFE) accepts a print file and converts it into a format that the print engine can use to place the content in the substrate. In raster printing, the DFE is the raster image processor (RIP) and performs other functions depending on the printing system. The functions of the RIP begin interpreting the incoming file to generate the corresponding bitmap at the required resolution. The last step is to apply sets of algorithms to create the screened file ready to be used by the print engine.

DFE's can support complex functionality to manage grayscale, print speeds, variable data, process automation, and two-way communication with other workflow processes, even enabling sensors to participate in the process. Variable data printing [166] is a form of digital printing, including on-demand printing, in which elements such as text, graphics, and images may be changed from one printed piece to the next, without stopping or slowing down the printing process and using information from a database or external file. For example, a set of personalized products in a production line, each with the same basic layout, can be printed with a different code on each product. Variable data printing in production lines can be used for special marketing promotions campaigns, customer relationship management, advertising, or traceability. Assuming that the DFE can compute the next image in parallel to marking the current one, I evaluate the computing requirements.

The controller system is the computing part that controls the different parts of the system. As depicted in Figure 9, Section 2.3, it receives the information of the dynamics of the production line, typically with an encoder and activates the laser beam, and controls the beam deflecting system for a proper marking of images. In digital printing, images can be different for each mark. If this is the case, an external computing system could transfer each image to the controller using a network. The minimum bandwidth requirements for transmitting uncompressed images between the DFE and the print engine are defined by Eq. 45 and assuming that the system is marking an image of $I_w \times I_h$ pixels over an area of $P_w \times P_h$ physical dimensions and using bpp bits per pixel (to account for its grey level).

$$BW > \frac{bpp\, I_w I_h V_{line}}{P_w} \tag{45}$$

The bandwidth requirements could be reduced by compressing the image with some lossless compression algorithm. However, in product marking, a part of the image to print will likely be common for several products, and another one will contain a unique mark to identify the marked product. In this case, the common part can be transmitted once, and the variable part (e.g., identifiers) can be transmitted for each product or even generated in the same controller.

In any case, the image in the controller will be processed to generate the final output. The latency of the control process that has to handle the feedback information is

important since when marking a moving object, a significant delay would produce marks in undesired locations.

This imposes a maximum process latency (L_{max}) as defined by Eq. 46. Where ε_{max} is the maximum acceptable position error.

$$L_{max} = \frac{\varepsilon_{max}}{V_{line}} \quad (46)$$

Computing Throughput (CT, expressed in billions of operations per second - GOPS) must also be considered. If every pixel of the image needs a number (m) of computing operations to be processed, then the necessary throughput is defined by Eq. 47.

$$CT = \frac{m\, I_w I_h V_{line}}{P_w} \quad (47)$$

In some cases, the processing can be irregular on the different pixels, but I can estimate the total number of operations *M* required for the image. Then, I could rewrite Eq. 47 as Eq. 48.

$$CT = \frac{M\, V_{line}}{P_w} \quad (48)$$

A problem in high-speed marking and printing is adapting the laser marking system to changes in the printing image. A solution for this problem is presented in [137]. This common scheme separates two types of information. On the one hand, there is a piece of constant repetitive information plus a design template (brand design, space allocation, background for variable information, etc.). On the other hand, there is variable information and design that could contain predefined variables (2D codes, barcodes, legal information, variable text, traceability code, images, etc.) plus real-time variables (counters, batch data, time data, expiry date, customer personalization, random codes for promotions, etc.).

By separating these information sources, I can reduce the processing and communication time between the printing of one image and the next one (with common elements to the first one). I can reduce the latency and increase the throughput by a separate parallel process that handles the minimum variable information needed between printing sequential images thus achieving better performance in real-time. This parallel processing, often implemented in FPGAs, prevents bandwidth limitations and computing redundant information among images.

3.3.2. Computational architectures

Unlike the traditional approach of making hardware the main element on which the architecture of the control system of laser marking systems is based, the approach of the architectures for control systems developed in this industrial doctorate is based on applications, in a similar way to how it was proposed in Par Lab [69].

In recent years, industrial equipment has undergone an extraordinary transformation from purely mechanical or electromechanical systems to "mechatronic"

systems. This transformation applies to devices of all types and sizes, including equipment installed on production lines, such as industrial marking and printing systems. Their control systems were revolutionized by highly flexible programmable microcontrollers (MCUs), embedded systems taking part in cyber-physical systems are regularly used in complex control loops where hard-real time requirements are usually found [66], yet compared to their consumer product counterparts, industrial devices are still several evolutionary steps behind [167]. The control subsystem of an industrial marking system is responsible for monitoring and controlling the I/O; to manage the user interface; and communications with external systems. The separation of the control subsystem into other subsystems responsible for each of these functions in a modular and scalable configuration provides several advantages to system designers, for example:

- Distributed processing and software reduction, which enables features such as real-time sequencing of events and safety interlock capabilities.
- Software partitioning, allowing independent software maintenance, evolution, and scalability.
- Separation of component technology that allows the control subsystem to operate on higher technology PCBs while other subsystems can remain on cheaper technologies.

For the control systems architectures developed for the key laser systems developed in this industrial doctorate, I use a fully decoupled subsystem topology that enables subsystem-level scalability across different products, easier testing of a simpler subsystem unit during design and manufacturing, and more effective machine assembly and maintenance. The System-on-Module (SoM) deployment model turns highly complex subsystem design challenges into much simpler off-the-shelf subsystem integration challenges. I combine these modules with hardware specifically designed for each of the applications. One of the modules we have used the most is the standard Q7 module and a custom motherboard. Some examples of hardware we use are synchronous serial communication interfaces (preferably I2C), USB, SD card storage, Ethernet, field buses (preferably ProFiNet); timers (PLL), general-purpose inputs/outputs (GPIO), analog-to-digital and digital-to-analog converters (ADC/DAC) and debugging using JTAG. The FPGA part of the designs has been synthesized for the Intel Altera Cyclone series devices, and the whole system has been implemented in a sandwich of several PCBs.

Software is a strategic element and a business differentiator. Software is key to our laser marking systems and is critical to the success of our products. Current embedded software architecture can profit from open software ecosystems. Our reference SW has been extended to the new multibeam systems and evaluated based on several quality attributes [168]. While it does not fit perfectly, it does have the fundamental mechanisms required for the new laser marking platforms.

In short, the control system should complete the following main processes: to input the marking contents (text, image, barcode, etc.) and monitor the operational status by the human-machine interface; sensing the velocity of the production line; trigger the

marking when detecting the workpiece, and control the timing and power of multiple laser beams.

Although all controller processes are subject to a real-time constraint, I classify them into hard real-time and soft real-time, which helps us make first design decisions defining strategies that can be used to divide the work between the different computing elements.

In soft-real-time processing (HMI control, marking data processing, image processing, communications, etc.) we use FIFO buffers for improving throughput (hundreds of MOps), although extra buffers may hurt latency (up to ms). A real-time operating system is a possible tool around improving latency and especially jitter; anyway, I have preferred to adapt a Linux distribution, controlling latency and jitter within acceptable margins (enough if they are in the order of ms), and increasing controller usefulness. For these latency and jitter values in soft real-time processing of our applications, microprocessors or microcontrollers are feasible.

Instead, it needs to be considered that laser pulses are in the order of a few μs and has hard real-time requirements; alike, an encoder (speed and position) and trigger signal readings must be quickly and accurately integrated to activate every laser beam in the correct position; then, for these kinds of processes, hardware is mandatory.

Pixels are grouped in rasters. All the pixels of a raster must be activated at the same time, with tolerances in the order of nanoseconds, and all rasters must be activated sequentially avoiding time gaps in the order of nanoseconds.

In all our applications, a pulse is generated for every image pixel. Pulses duration and power level determine grayscale level. A certain duration and power produce a maximum contrast dot, and a minimum threshold duration is required to produce a minimum contrast. For some applications, we need 256 gray levels. The difference between the minimum and maximum pulse duration must be divided by 256 to obtain the resolution at which we will produce grayscale colors. In this case, we need to control differences of a few ns in pulse length.

The combination of high-throughput (up to 1GOPS) and low-latency and jitter requirements (in the order of ns) makes FPGAs good candidates to implement such Embedded High-Performance Computing (EHPC) system. I demonstrated how to benefit from FPGA computational resources[15] by using multi-soft-core to control multiple beams. The concept of the task-isolation mechanism is further analyzed in [66] to create independent non-cooperating high-performance tasks.

This reasoning leads us to decide the most outstanding controller components: (1) internal processor, (2) FPGAs, (3) production line control, and (4) signals distribution.

Despite the wide range of process parameter values required by our applications (detailed in chapters 4, 5, and 6), I can define common processes for all applications:

- The controller receives via Ethernet, TCP/IP socket, the information in a .xml format describing the static and dynamic part of the image.
- The method of controlling the matrix of lasers beams includes the sequential transformation of images to be marked into a series of marking commands according to an N x M matrix of dots. It comprises the following phases: (1) division of a first image into a fixed portion of the image and a variable portion of the image, (2) transformation into a fixed matrix and a variable matrix, (3) combination of fixed and variable matrices, forming the complete N x M matrix of the dots to be marked, (4) laser marking of the first matrix on the surface to be marked, (5) processing of a second image, obtaining a new variable matrix which is added to the previously fixed matrix, producing a complete new N' x M' matrix corresponding to a new image, (6) laser marking of the second matrix on the surface to be marked.
- There are four printing modes: (1) Static printing - Object does not move (2) Dynamic standard - Object moves along X-Axis (3) Dynamic Distance - prints are done at a predefined distance (4) Static-Dynamic - Object moves alone X-Axis, the message is printed at the exact location where it is drawn on the screen. Print modes support either left to right, or right to left printing, which is covered with a software switch. The setting of the system manages the proper 'top to bottom' orientation of an image.
- System-ready status is monitored via Ethernet. The internal processor has access to all interlock and machine status signals: system ready status, interlocks, temperature, refrigerant flow, etc. Status is apparent from the control panel so that an operator can determine the reason for the system not being ready.
- The product-sensor and encoder inputs are interfaced through an interface board which can be adapted for all sensor configurations.
- The different values of resolution (from 50dpi up to 300dpi), width (from 10 up to 100mm), gray levels (from 2 up to 256), and velocity (from less than 0.5m/s up to more than 10m/s) of the different applications (very-high-speed coding, high-speed printing, and high-resolution printing), force to use different hardware for image forming (laser diode arrays, MMAs...) and different control architectures.

3.4. Overview of the key laser systems developed in this work

This industrial doctorate has involved the research, development, and implementation or use of various laser marking and printing systems, in which we have experimented with different multiple lasers beams parallel processing architectures, and different printing and marking methodologies, different laser sources, on different materials and using different physical principles.

I can classify the laser systems analyzed in this thesis based on the architecture of the laser hardware and the marking methods (Table 9). In Annex B an overview is given, in a schematic way of each one of them.

Table 9: laser systems analyzed in this thesis based on the architecture of the laser hardware and the marking methods

	Laser Hardware		
Marking Method	**Different Wavelengths**	**Laser Diode Arrays**	**Projection Based**
Carbonization	Paper/Cardboard printing		
Thermochromic pigments		f-LDA labeling	MMA labeling
Ablation		HP f-LDA	SLM coding

3.5. Summary of the chapter and discussion

In this chapter, I detailed the foundations for the implementation of multibeam systems that will be considered in the following chapters for the implementation devoted to different application domains.

It includes the theoretical foundations; the relations with the different elements of the laser printing process: marking surface; laser source; marking method and computing, and the development environment together with the research proposals that end up in patents in which I contributed.

4. Laser Inkless Eco-Printing on Paper and Cardboard

In the current industrial and commercial printing scenario, the importance of secondary packaging has grown exponentially, especially facing paper and cardboard as their main substrates. Therefore, a solution that allows coding this type of packaging efficiently and cleanly is key for the printing equipment manufacturers in providing to the industry an eco-marking system that respects the environment without losing productivity in manufacturing processes.

4.1. System Overview

In the previous section 3.2.4, I explained the existing methods for marking or printing on cardboard and paper that use thermochromic pigments and in section 3.2.5 methods that ablate inks and paints.

Laser marking can be also used for that purpose in a way more sustainable and respectful with the environment, although the existing solutions up to date do not produce enough contrast since the usual result is a brown color on the cardboard or paper surface (Figure 36).

Figure 36: Direct laser marking on cardboard.

Also, in previous section 3.2.3, I proposed a new laser marking method that allows obtaining maximum contrast directly on cardboard and paper, again without requiring polluting inks or other additives. In addition, this proposal reduces costs for both consumables and time in production processes (product drying, replacement of consumables, etc.)

The process is optimized with the most efficient absorption of beam energy by the irradiated surface. The main component of the organic surfaces is cellulose, which has a characteristic abortion profile to radiation (see [92]) with three local maxima at the ranges 2.86 μm – 2.94 μm, 8.30 μm – 10 μm and 14.9 μm. CO2 laser working at 9.3 μm wavelength lie on the second maximal range showing a good absorption efficiency (Figure 37).

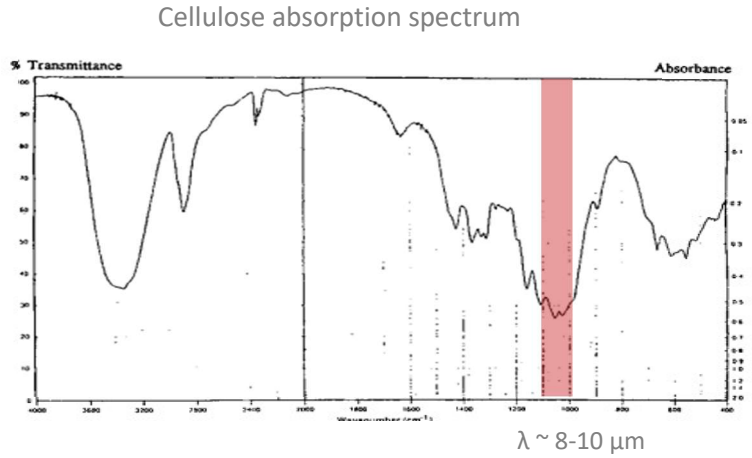

Figure 37: Cellulose absorption spectrum

The threshold where visible changes are manifested is dependent on the chemical components of the material. To find out those thresholds for standard office white paper and brown cardboard, the darkening effects are analyzed when the surfaces are irradiated with a 9.3 µm CO2 laser beam with a beam spot diameter of 5mm. Relative lightness value L* is used to measure the darkening effect intensity. A value of 100% corresponds to the lightness of the original white paper, while a value of 0% is the lightness of the reference region printed with black ink. For cardboard, the 100% value is still the lightness of white paper, so the surface baseline lightness level is already around 60%. The works [94][95] use a similar approach to report lightness versus the surface temperature. In our case, I use lightness versus fluence, which is easier measured in the context of laser technology.

Figure 38 depicts the obtained profiles for paper and cardboard when irradiated with the CO2 laser. Fluence is the integration of irradiation over time, which is the main driver of temperature increase that causes visible marks on the irradiated surface. When irradiated with low fluence, the paper does not show any visible effect, but when fluence is bigger than 5 J/cm2 a yellowing effect starts to manifest, and it progressively increases going to a dark brown color but not reaching a desired black color. Moreover, above 12 J/cm2 the probability of perforating the paper is highly increased, so the effective minimum achievable blackening is above 20%.

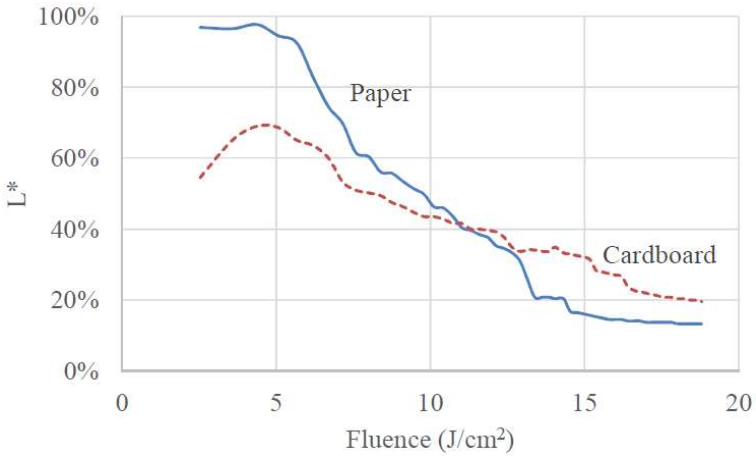

Figure 38: Relation between Fluence and relative Lightness (L) of white paper and brown cardboard marked with a 30-Watt CO2 laser.*

Cardboard reacts differently. For lower fluence below 7 J/cm2, the cardboard becomes brighter in a process known as photo-bleaching. Above that threshold, the material is blackened quite linearly with fluence. The minimum achieved lightness is around 20-25%. The higher thickness of cardboard makes it easier to gradually increase the darkening effect preventing the perforation of the material.

When observing the irradiated paper at the microscope (Figure 39 left) it is clear that the yellowing discoloration is not uniformly affecting the surface, but selectively affecting some of the cellulosic strands imbricated in the paper.

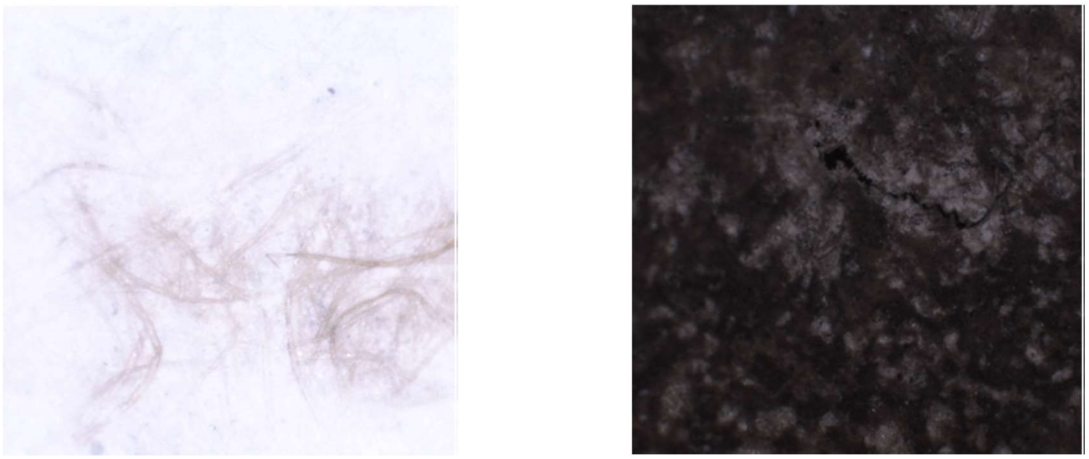

Figure 39: left) magnified view of the yellowing effect on a 1 mm2 area after low fluence radiation. (right) magnified view of the darkening effect on a 1 mm2 area after high fluence radiation. A surface perforation can be observed as a darker crack in the center.

This suggests that there are gradients in temperature caused by some strands absorbing more radiation than others. When the discoloration starts, the effect is accelerated for those strands, since darker strands have higher absorptivity than brighter ones. On the other hand, the larger darkening effect caused by carbonization does not

produce a strong black color but a dark brown with a relative lightness of 20%. Similar findings are reported by [94][95]. Due to the irregularity of the surface, higher fluence can easily cause perforation, such as seen in (Figure 39 right) or ignite combustion.

The same test is repeated with a laser working on the lower wavelength laser of the blue visible spectrum (around 480 nm) with a 6 Watts laser source. In this case, the beam spot is smaller, around 200μm. The small beam spot increases the irradiance of the beam and reduces the time required to get the fluence levels reached in the previous experiment. The shorter irradiation time creates higher temperature gradients on the heated surface increasing the unpredictability of the effect Figure 40 depicts the reaction of the whitepaper and cardboard surfaces to the lower wavelength laser beam. The fluence thresholds are higher than for CO2 lasers. For paper, there is a much sharper threshold between marking and no marking. For cardboard, the level of blackening is significantly higher than when using CO2 lasers.

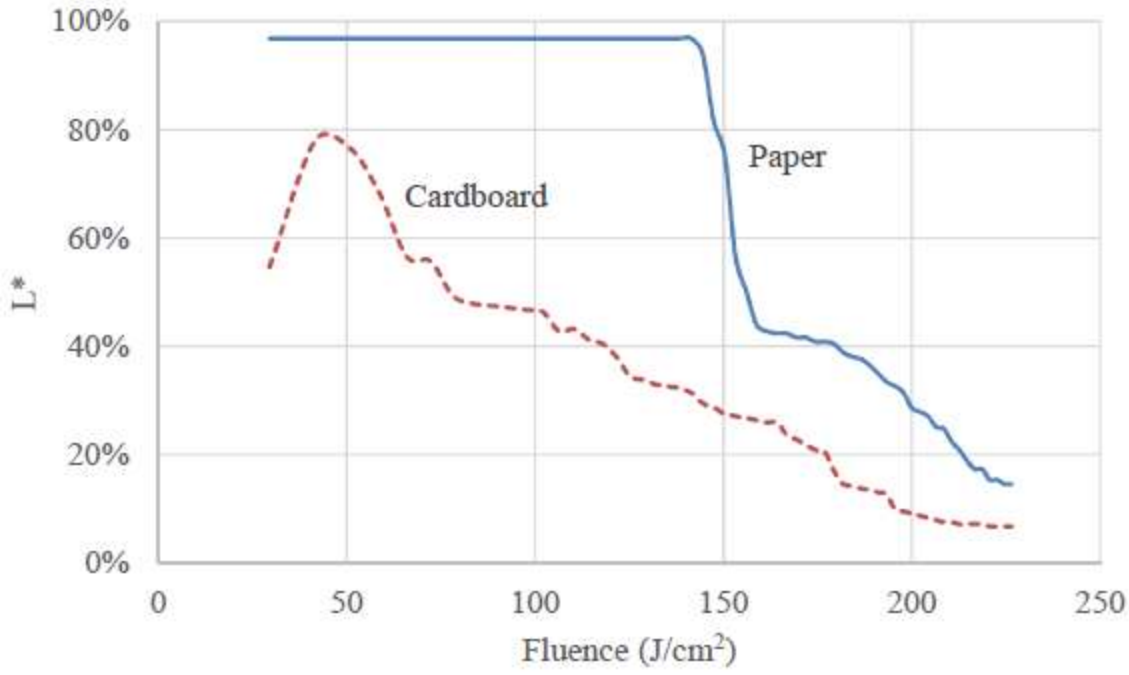

Figure 40: Relation between Fluence and relative Lightness (L) of white paper and brown cardboard marked with a 6-Watt Blue Visible Light laser.*

Our goal is to preheat the surface to a certain level that does not produce a visible change, so I keep the fluence below the 0.1 J/cm2 range. An additional heat injection is added to jump above that threshold for the regions that are marked. The process is depicted in Figure 41.

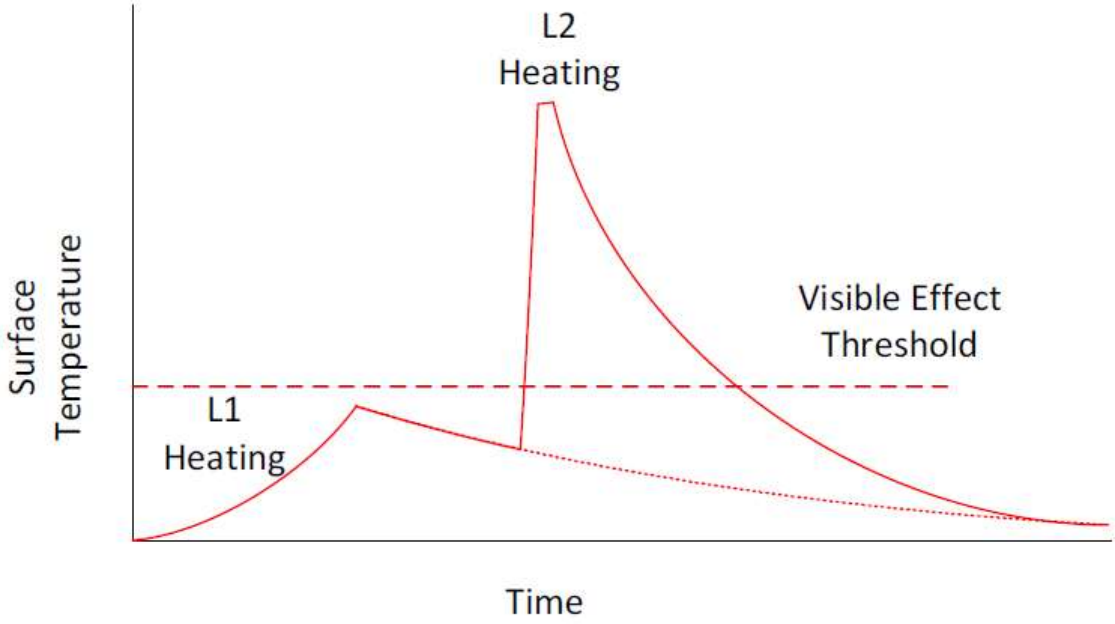

Figure 41: Relative Temperature profile for our 2-phase proposed method

Liao et al. [169] describe the dynamics of combustion ignition also using a CO2 laser as a radiant source. They report two important contributions for our analysis: 1) combustion usually starts because of the ignition of the gases generated by the previous heating 2) the surface temperature ignition threshold depends on the thickness of the surface. Thicker surfaces require more heat to ignite. So, to minimize the risk of combustion the system should be aware of that thickness to reduce the fluence accordingly. On the other hand, heating the volatilized gases should be reduced to prevent combustion.

CO2 lasers are widely used by the marking industry, but their infrared wavelength forces the use of a relatively big beam spot. To increase the contrast and resolution of the marking phase I propose to use lower wavelength lasers with smaller beam spots like visible light and ultraviolet lasers.

However, there is a low wavelength limit I should avoid overpass. Organic materials are based on carbon molecules, being C-C bonds are the most frequent bonds that keep molecules together. Eq. *49* defines the threshold wavelength that breaks a chemical bond, where h is the Planck constant, c the speed of light, N_0 the Avogadro number, and BE the bond enthalpy.

$$\lambda_{th} = \frac{hcN_0}{BE} \tag{49}$$

For C-C bonds, bond enthalpy is 346 kJ/mol. Thus, the required wavelength to break them λ_{th} is 345.7 nm, which is in the UV band. In other words, laser beams with wavelengths greater than 345.7 nm would contribute to heat transfer phenomena, while lower wavelengths would trigger the degradation of materials as reported by [92].

On the other hand, it is known that in these UV and visible bands pulsed lasers can induce photopolymerization [170] of carbonization by-products like tar and volatilized by-products. According to [95], the main volatilized by-products are Levoglucosan ($C_6H_{10}O_5$), Carbon dioxide (CO_2), a-Angelica lactone ($C_5H_6O_2$), Acetol ($C_3H_6O_2$), Propargyl acetate ($C_6H_{10}O_5$), 3,3-bis (hydroxymethyl)-2-Butanone ($C_6H_{12}O_3$), and 2-Allyl-1,3 dioxolane ($C_6H_{10}O_2$.

I hypothesize that either tar or some of these volatilized by-products act as chromophores and contribute to the photo-polymerization of the surface capturing a large number of volatiles, and other residues. Assuming this effect occurs, we have implemented several designs using different laser wavelengths and analyzed the quality of the marks by visual inspection. From the empirical observation is seems that polymerization is taking place since the obtained contrast is higher compared with the contrast obtained with infrared lasers and the generated residue is greatly reduced.

This represents a great improvement concerning alternative current industrial methods. Solid by-products are very bad for the industrial production lines, as they impact the quality of the printing, increasing the risk of introducing debris into the production line which can create defects or event damage to the equipment. With the proposed method there is no need for any additional post-treatment, so the economic benefit is obvious.

The phases of the printing method that allows generating a black color for marking depend on the temperature that is applied to the cardboard (or paper) and the rate at which we apply this temperature (Figure 42).

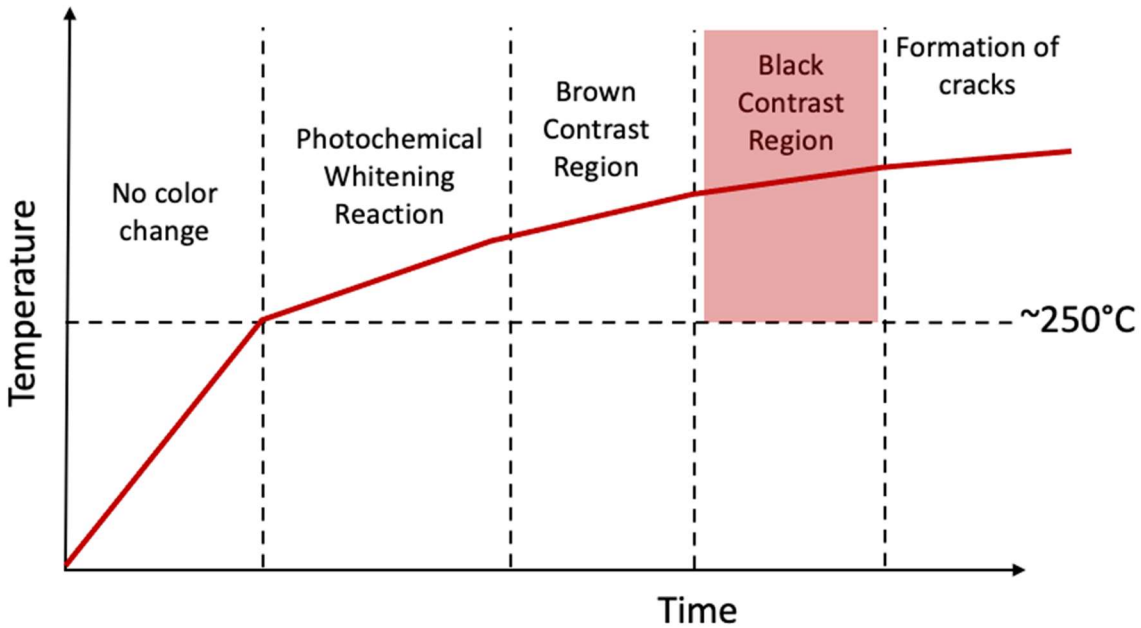

Figure 42: Carbonization process of paper and cardboard

The system that we implemented uses two independent laser sources. First, a 9.3 μm wavelength CO_2 laser (L1) is used for preheating and, second, an ultraviolet or visible light laser performs the marking (L2). Preheating with the IR laser L1 increases the surface temperature sharply. When the moving beam is no longer heating any point of the surface, cooling is dominated by conduction and convection heat transfer effects that reduce the temperature at a much slower rate.

Initially, we preheat a relatively large area to reduce the temperature gradients created in the later marking phase. The dot diameter of the L1 laser is between 5mm and 8mm. As shown in the previous chapter, the irregularities of the surface can contribute to different reaction velocities of the heated cellulosic strands. An unfocused beam contributes to minimizing these effects and the gradual increase of temperature also avoids the creation of volatile by-products.

The second laser L2, acting as a marking laser is designed to rapidly raise the temperature of the surface above the carbonization threshold.

Both lasers L1 and L2 have independent deflection systems and go through different optical paths since, being based on different wavelengths, not all the optical systems can be shared among them. Moreover, their paths over the surface will also be different (due to the different dot diameters) while their beam diameters are fundamentally different also due to their different wavelengths.

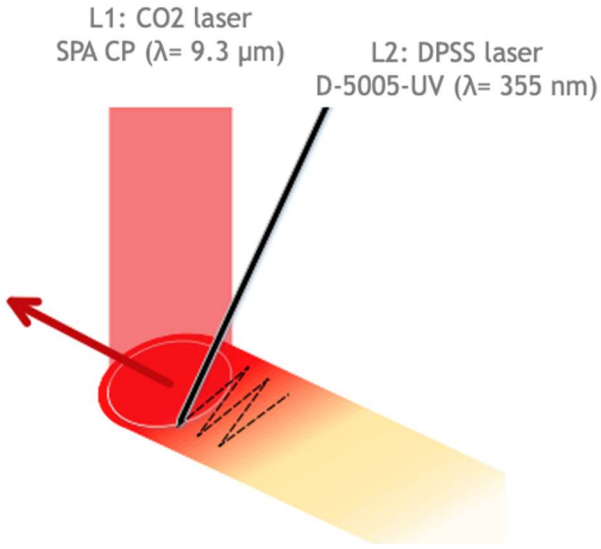

Figure 43: Combination of laser beams for laser printing on paper and cardboard. The CO_2 L1 beam is illustrated in red color while the visible or ultraviolet L2 laser is shown in black color.

Figure 43 depicts how our implemented system operates. We preheat, with the CO_2 laser L1, a wide area. Before the surface is cooled down, we mark the required geometry with the visible or ultraviolet laser of narrower width, to increase the temperature above the carbonization threshold.

The preheating laser L1 follows a straight-line path, while the scribing laser L2 follows the path to produce the required mark. The scribing speed of the second laser is faster than the first one since it must travel a longer path than the first one. We found that the resulting marking has better quality when both lasers have an equivalent average speed related to the preheating axis, to minimize the irregularities produced by the natural surface cooling.

The system is designed so that the mean delay time between the path of the first laser and the second one is around 100 ms. This time ensures that the surface has been effectively preheated and the cooling down process is not that evolved before injecting the L2 radiation.

The beam deflection method for both lasers is based on standard galvanometric mirrors. Figure 44 shows the testing laboratory setup. A Macsa ID SPA 9.3 µm 30W CO_2 laser is used for preheating and Abmark AB-D lasers, with UV and visible wavelengths, are used for marking. Marking laser sources wavelengths range between 532 and 355nm with powers between 5 and 30W. The best results have been achieved with a 30W blue wavelength laser (455nm): CNI Optoelectronics model OEM-KD-455.

The experiments were carried out in a laboratory environment. The marking paths are predefined with independent static marking works. To synchronize the marking process both marking jobs are triggered at the same time with an external electronic trigger.

Figure 44: Testing setup containing a CO_2 laser (right) and a UV laser (left).

4.2. Results analysis and discussion

Through this process, we can obtain black color marking resolutions up to 600 dpi with high contrast in a sustainable way (Figure 45). In addition, this solution allows 100% recyclability of the components involved in the secondary packaging coding.

Figure 45: Examples of direct inkless marking

The main result of this research is the minimization of debris. Compared with the methods presented in [94][94][94][94][94][94], [95], and [104] the proposed method does not produce any visible residue, eliminating the need for any additional treatment process on the marking process.

Moreover, an important requirement for industrial success is the marking contrast. The relative lightness L* achieved is 0%, meaning that it is equivalent to the achieved with black ink. This is a remarkable achievement for proposals [94] and [95] and also compared with the tests presented in section 3.2.3 using only one laser. In those setups, the minimum L* achieved is around 20-25% for the paper using CO_2 lasers without any perforation.

Figure 46 shows the excellent contrast achieved by marking on white and brown cardboard. No free residue was observed during or after printing. Moreover, the quality and resolution of the print are around 600 dpi, as we have defined in the deflection system.

Of course, the economic cost of having two lasers is higher than using a single one, although there is not any existing system that achieves an equivalent contrast at a lower cost than the proposed solution. Alternative proposals either need extra consumables (such as [104]) or provide a significantly lower contrast ([94],[95]).

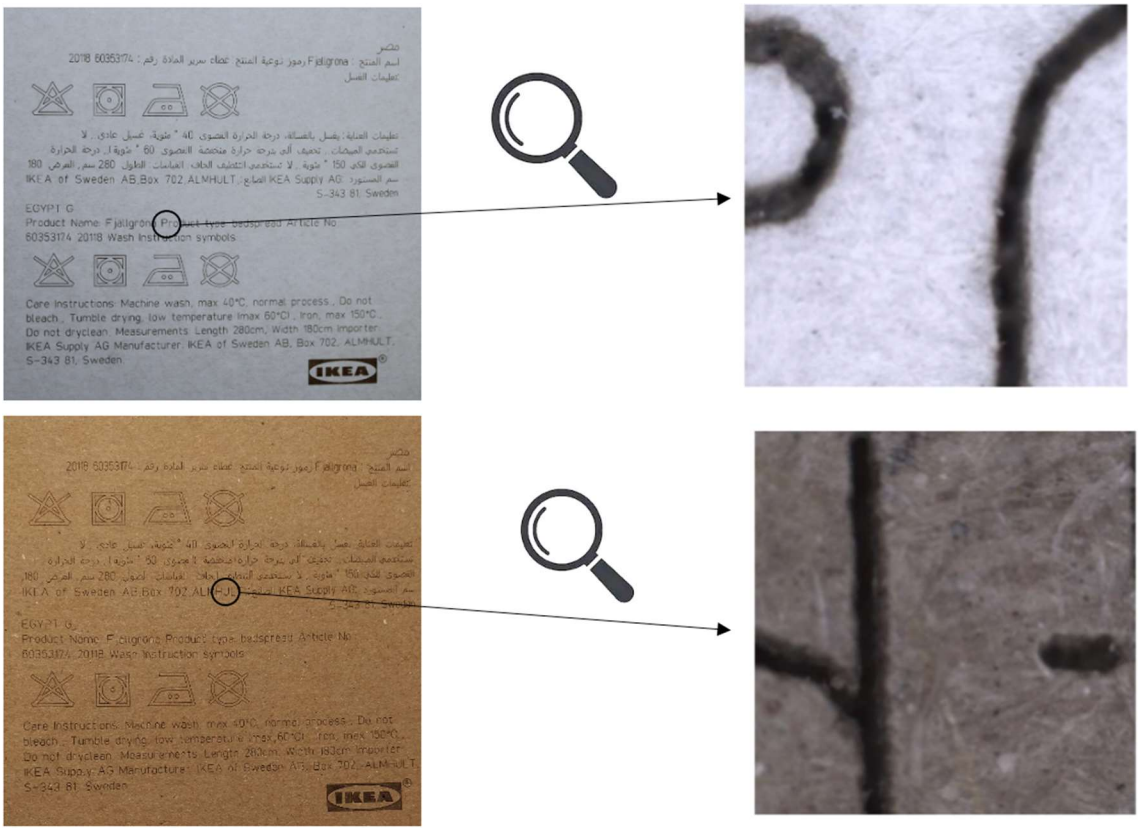

Figure 46: (Top) magnified view of the mark with the proposed method on a 1 mm² area of white cardboard. (Bottom) magnified view of the mark with the proposed method on a 1 mm² area of brown cardboard.

4.3. Summary of the chapter

We have presented a novel method to print in paper and cardboard without ink. The reduction of residue and the cost to treat them is incomparable to any other known method in the literature and industry. Moreover, the printing quality both in contrast and resolution meets the typical requirements of the industrial and office environments. This method will allow a significant reduction of consumables in the packaging world.

Although there is no visible debris, more research is needed to analyze with more detail the nature of the materials involved in the process and the quantification of the generated by-products using mass spectrometry and gas chromatography.

5. High-Speed Implementation using LDA

Laser marking is a common part of many manufacturing processes in the industry, with great importance in the fast-moving consumer goods (FMCG) industry. The speed of production lines is the key determinant of the throughput of many industries, but their scalability could be hindered by some fundamental limits of current laser marking technologies mainly based on irradiation and scanning parameters. In this chapter, I review the limiting factors of the laser marking speed, analyze how future systems could overcome them, and propose real systems that overcome the limits.

The systems we designed and developed are addressing the need of marking product packaging surfaces being transported by high-speed conveyors. They are in-line digital marking and printing systems able to print variable information in real-time across virtually any substrate or width. We base our digital printing solution on a high number of parallelly controlled laser beams covering one axis of the surface while the other axis is covered by the conveyor movement. I have identified three ranges of target applications in the laser marking and printing market that I classify as very-high-speed coding, high-speed printing, and high-resolution printing. Table 10 shows the parameter values for resolution, width, gray levels, and speed associated with each type of application.

Table 10 Parameters associated with laser marking and printing applications

Type of applications	Resolution (dpi)	Width (mm)	Gray levels	Speed (m/s)
Very-high-speed coding	100	25	2	> 10
High-speed printing	200	50	16	2
High resolution printing	300	100	256	< 0.5

All systems presented in the following subsections will be based on laser diode arrays. Laser beams are collected in a print head close to the marking surface with all the required optics for the correct beam spot forming. A photocell and an encoder are required to obtain the information from the movement of the products on the conveyor.

Our laser diode array systems, as many sophisticated industrial systems, are unable to afford significant downtime. This implies that they need high diode reliability at an acceptable cost. Laser diode arrays systems consist of many different modules and components (diode lasers, drivers, embedded electronics, etc.) and every laser marking or printing application should be able to adapt to specific environmental conditions and duty cycles. Therefore, defining its lifetime is not simple at all. Lifetime issues are especially critical for the high-power fiber-coupled laser diode array that I will detail in section 5.3.

5.1. Elementary design of Laser Diode Array (LDA) system

The first proof-of-concept consists in placing the diodes as close as possible to the marking surface, as described in previous works in the literature [150]. As depicted in Figure 47, this system includes the laser print head (embedding the laser diodes), the controller (connected to a host computer through a high-speed bus), the cooling system, the fume extractor, and the acquisition of movement data from the production line (with encoder and photocell).

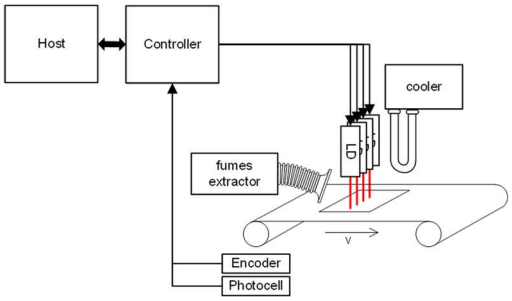

Figure 47: Schematic of the marking system with laser diodes directly applied to the surface

The goal is to create a small print head containing several laser diode (LD) array chips (up to 400 LDs) with a pitch of 125 µm. Considering a laser power per diode of 0.5 W, the maximum total power of the print head will be 200 W. I estimate that this would result in a heat power density higher than 30 W/cm^2 in some points of the printhead, which will require a challenging cooling system.

We can use low fluence threshold materials ($F_{th} \approx 10^{-1}$ J/cm^2) to obtain a higher printing speed. The marked dots pitch (x_{pitch}) should be equal to the diode array pitch to obtain proper printing of raster images at 200 dpi resolution. With these values, the estimated maximum line speed, given by Eq. 25, is 0.81 m/s for AR=1.2.

This limited speed combined with the limited area coverage and resolution of this solution is not very interesting for its implementation in high-speed industrial marking while it could be very interesting in other domains. The small space of the microelectronic laser diodes results in a high-power density. Given this limitation, I decided to analyze this design for the label printing application.

5.2. Fiber-Coupled Laser Diode Array (f-LDA)

As a first market-oriented implementation (see Table 10, High-speed printing), the f-LDA architecture for the label printing application targets both high-speed and high-resolution printing types of applications.

A solution to the thermal density problem that limits the laser power in the LDA design is to increase the area occupied by each LD emitter. Without area restrictions, I propose to use laser diodes of higher power (not as higher as those presented in the next subsection) together with high-performance cooling systems and fiber optics [149][146] to divert the beams to the printhead. Authors in [146] developed a pioneering technology

several years ago but, at that time, the devices required to implement it were not sufficiently advanced. For instance, laser diodes were bulky and not powerful enough, optical fibers had high insertion loss, micro-optics did not allow high integration densities, and component costs and availability made applications using that system economically unfeasible. Currently, several laser industries (as II-VI Laser Enterprise, BWT, etc.) provide high-power laser components, enabling fiber and direct diode laser systems to be used for material processing. Other companies (as DataLase, Ricoh, etc.) developed color-change materials for laser coding, and our company, Macsa, developed several truly disruptive in-line digital printing solutions. Figure 48 shows the updated model of Figure 47, in which a fiber umbilical cable connects laser diodes and printhead.

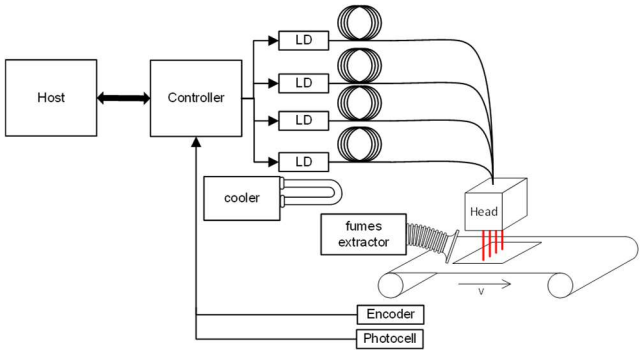

Figure 48: Schema of the system with laser diodes connected to fiber optics that applied coherent light to the surface

With this strategy, the laser diodes and laser drivers can be placed far from the marking surface, providing greater flexibility for the printhead positioning due to its lower mechanical constraints. Figure 49 shows one of the first prototypes with diode stacks (975nm 8W laser diodes from Oclaro II-VI) and fiber umbilical cables (105µm) used for the f-LDA implementation.

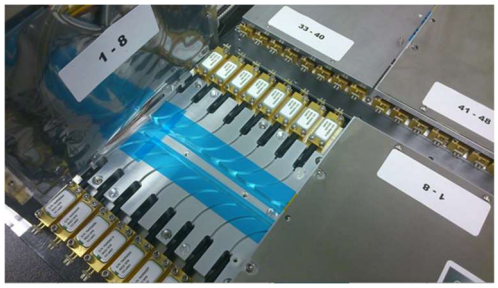

Figure 49: Detail of the f-LDA prototype with diode stacks and fiber umbilical cables

Every diode emits a laser beam which is responsible for marking a single dot per column. The number and size of optic fibers and the required focusing optics limit the resolution and dot dimensions so that a proper fiber placement in the printhead is needed. V-groove distributors are used to spatially distribute the fiber bundle in a correct position. An arrangement of lenses focuses the laser beams on the product surface.

An optical design is sought to image a multimode fiber array at a range of distances. The optical system performing the imaging can vary widely in complexity and cost depending on the performance requirements. It is therefore critical to define the

machine requirements in order not to over-specify them and reduce NRE and production costs. An analysis of the system was conducted, first ignoring aberrations (paraxial) to give a feel of the fundamental system response, then delving into the aberrations which will most affect performance.

The overview of the setup has been sketched in Figure 50. The concept of using a zoom was discarded to simplify the system. This implies that the optical system shall have a fixed focal length. Paraxially has implications with regards to the projected image because spot size and separation will be linearly proportional to the working distance. For example, if the image is projected at 90mm, the spot diameter and the spot separation will be three times larger than if the spot is projected at 30mm.

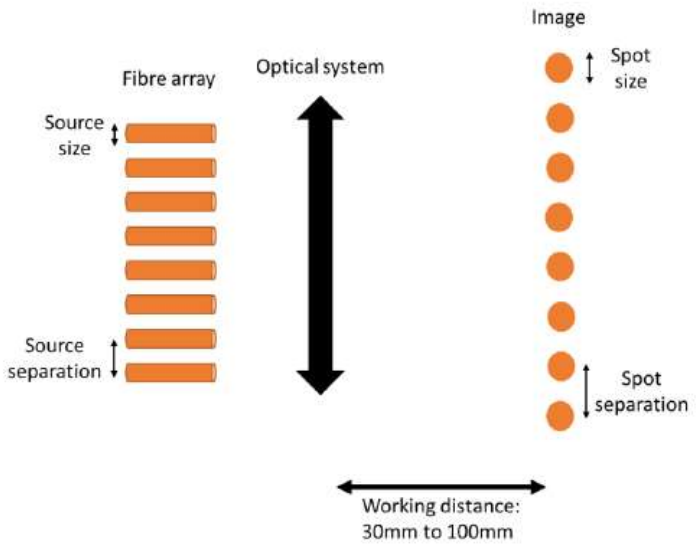

Figure 50: Overview of the optical setup for the f-LDA system

The most prominent aberrations for such optical systems that will affect performance are off-axis aberrations (namely distortion, astigmatism, and field curvature) are shown in Figure 51. Distortion implies that the spot separation is not constant across the image because the distance between the spots typically increases away from the center of the image. Field curvature and astigmatism will act to make the off-axis spots larger and more elliptical. All aberrations can be compensated up to a certain degree during the optical design but each compensation adds optical elements in the design and therefore results in a costlier end-product.

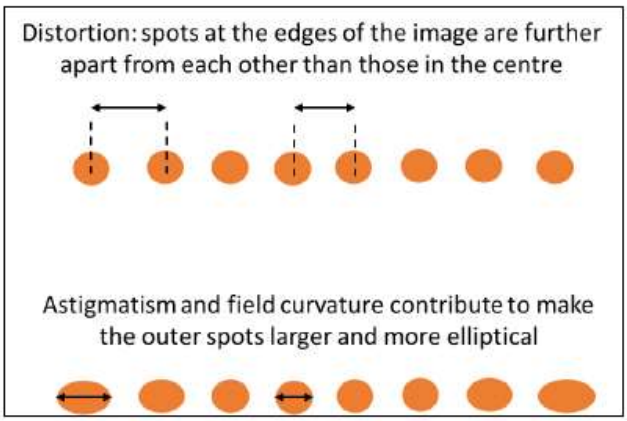

Figure 51: Aberrations that affect performance for LD marking systems

As stated previously, the optical design depends on the specifications of the spot on the marking plane. As spot size must remain nearly the same through the full focus, and spacing variation needs to be reduced, then this forces a more complex lens as distortion and telecentricity need to be tightly controlled. When the spot circularity is important, additional aberration control is required by using aspheric surfaces. I relaxed the maximum ellipticity specification in order not to over-specify the requirements. I have tightened the specifications considering as scope of work, a set of fixed focal lenses without magnification (1 to 1 image) with a focal length around 50mm.

In the first implementation, the pitch between dots was selected to be the same as the dot size ($d_{spot} = 125$ μm) to allow the printing of high-quality raster images with 203 dpi resolution.

We use low fluence threshold materials ($F_{th} \approx 10^{-1}$ J/cm^2) to reduce laser power requirements. Every modulated continuous wave laser diode radiant flux is $\Phi_{peak} \approx 6\ W$ and their wavelength is $\lambda = 980$ nm (quite cost-effective). The system achieves speeds up to 2 m/s. Equation 25 predicts that it is possible to reach higher speeds but then the grayscale resolution will be reduced and marked images lose contrast becoming lighter and blurred.

At 2 m/s, the control system activates the LD at 15 kHz to maintain the horizontal resolution equal to the vertical (125 μm pitch). We can print light grays ($F_{th} \approx 0.5$ J/cm^2) with AR around 1.2, and dark grays ($F_{th} \approx 1$ J/cm^2) with AR around 1.5 (Figure 52 left). For a production line speed above 2 m/s, the laser can increase the frequency and maintain the pitch. The AR will rise to 2 (equivalent to laser activation 100% Duty Cycle) and the laser will print a continuous line of adjacent overlapping dots, leaving no option to print small blank spaces (Figure 52 right). Grayscale can be printed by changing pulse width (Δt_p) or radiant flux (Φ).

Figure 52: Printing 3 black dots, one white dot, and 3 black dots with AR = 1.5 (left) and with AR = 2 (right)

This configuration (200 dpi at 2 m/s) is very competitive in the label printing application scenario. Printing dots with 256 grayscale levels requires 8 bpp. Assuming we want to print an image with the maximum height of the print head (384 dots of 125 µm diameter and pitch) at 2 m/s, the bandwidth required to inject new images on the print engine can be derived from Eq. 45. It predicts a minimum controller bandwidth of 49 Mbps. Ethernet interface could become a bottleneck if errors or collisions occur in the link. Gigabit Ethernet provides a safer margin. The maximum latency of the system is given by Eq. 46. The position control system must work on time. If we are printing at 2 m/s, the pulse period will be given by Eq. *50*

$$\frac{1}{f_p} = \frac{x_{pitch}}{V_{sc\,P}} = 62.5\ \mu s \qquad (50)$$

The maximum allowed displacement is relative to the maximum dot aspect ratio. The maximum latency for printing with AR=1.2 (Eq. 51) must be in the order of µs to avoid artifacts.

$$L_{max} = \frac{\varepsilon_{max}}{V_{line}} = \frac{(AR_p - 100\%)/2 \cdot d_{spot}}{V_{line}} = 6.25\mu s \qquad (51)$$

Regarding computing requirements, we estimate the minimum number of operations performed by the processor per image pixel as 300. Eq. 52 provides the minimum computing throughput.

$$CT = \frac{m\, I_w I_h V_{line}}{P_w} = \frac{300 \cdot 384 \cdot 384 \cdot 2}{48 \cdot 10^{-3}} = 1.8\ \text{GOPS} \qquad (52)$$

Many microprocessors could reach these requirements, but a slight increase in the number of operations per pixel on the input image (e.g. for some variable codes in digital printing) would create a bottleneck on the controller. The latency requirement is driven by the position feedback integration and the required synchronization with the laser activation. A delayed activation would produce skew artifacts. Given the latency requirements and the safety-critical requirements, I propose to divide computation between hard real-time computing and soft real-time computing. FPGAs are the best option to have predictable behavior in the hard real-time part of the system (image forming, laser marking on-the-fly, triggering, speed monitoring).

The power density problem imposes a physical distribution of the diodes close to the pulse control functions. According to the marking system requirements, several FPGAs must be placed closer to groups of diodes to reduce wiring. Figure 53 shows the proposed system architecture. A hybrid CPU+FPGA chip is responsible to coordinate the distributed FPGA boards. The central unit connects the distributed boards via fiberoptic

and TOSlink optical transmitters, to avoid electromagnetic compatibility (EMC) and interference (EMI) issues.

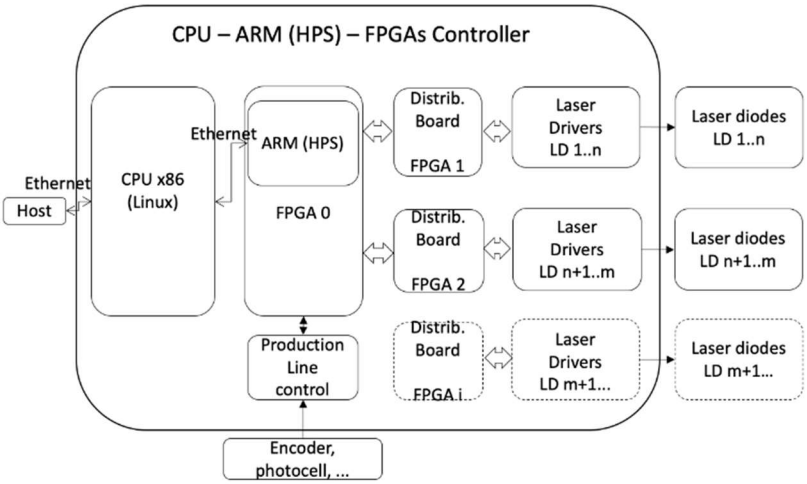

Figure 53: Architecture of the f-LDA platform based on distributed FPGA modules

The soft-real time part of the system includes HMI, control, marking images, and data processing and communications. It is implemented in an x86 CPU running embedded Linux. The CPU's communication with the external world uses Gigabit Ethernet to fetch the marking workloads while the communication with the internal FPGA ARM CPU uses an additional Ethernet port, thus avoiding any possible interference. The Cyclone V SoC from Intel-Altera was selected to implement a Field Programmable Gate Array (FPGA) since it contains both a Hard Processor System (HPS) and an FPGA fabric. Intel-Altera's Electronic Automation Design (EDA) tools used to implement the internal architecture are Quartus Prime and Qsys. VHDL was used to describe the HW subsystem. Table 11 lists the main computing resources of the controller platform depicted in Figure 53.

Table 11: Main components of the controller architecture

	Processor	**Core / Clock frequency**	**External Communication I/F**	**Storage capacity**
CPU	x86 Intel Atom Dual Core	1.86GHz	1 Gb Ethernet	1 GB DDR3
HPS	ARM Cortex-A9 (in Altera Cyclone V)	925 MHz	1 Gb Ethernet	512MB DDR2
FPGA 0	Altera Cyclone V	< 250 MHz	TOSlink	7,880 Kbits

The HPS most relevant blocks of the Cyclone V SoC for this development are the 925 MHz dual-core ARM processor with an Armv7-A Instruction Set Architecture (ISA) and the bridges in the HPS to exchange data between the FPGA fabric and the HPS logic. The bridges use the Advanced Microcontroller Bus Architecture (AMBA) Advanced eXtensible Interface (AXI) protocol based on the AMBA Network Interconnect (NIC-301) [6]. The FPGA's most relevant blocks of the Cyclone V SoC for this implementation are the I/O elements (IOEs) which are used to output the Cyclone V SoC signals. The

ARM processor found in the HPS can run a Linux distribution, which can decrease the development time of an embedded application. This custom Linux provides the control to access the DDR3 SDRAM.

The diode and fiber configuration allow a wide range of implementations with different diode power, dot sizes, and printing widths. Figure 54 shows an implementation of the developed architecture and its interaction with the production line for the f-LDA print system.

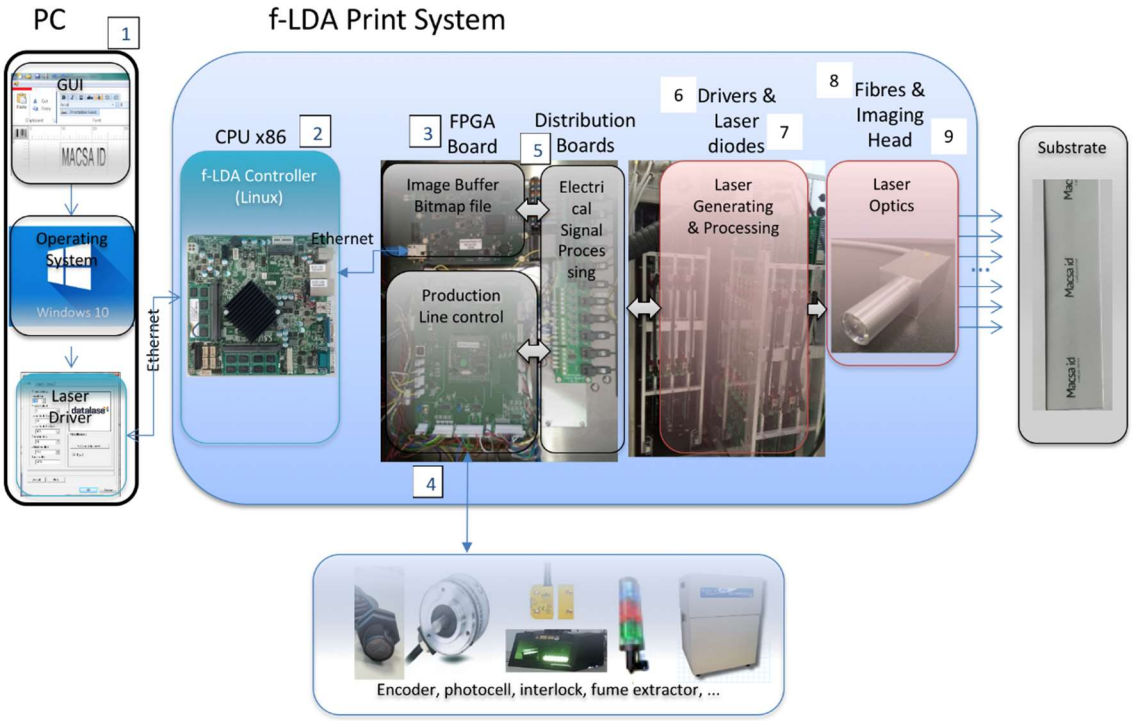

Figure 54: Implementation of the developed architecture and its interaction with the production line for the f-LDA print system.

5.3. High-Power Fiber-Coupled Laser Diode Array (HP f-LDA)

The second market-oriented implementation (see Table 10) is devoted to very high-speed coding types of applications, we have populated 35 high-power modulated continuous wave laser diodes in a system that emits the corresponding 35 laser beams. Its

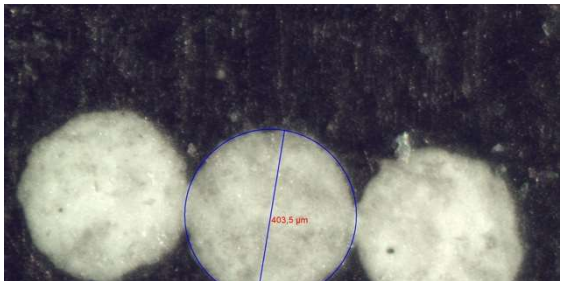

Figure 55: Measurement of dots resulting from the substrate laser ablation

main parameters are: (i) Wavelength λ = 980 nm (quite cost-effective) (ii) Radiant flux $\Phi \approx 240\ W$, and (iii) dot diameter $d_{spot} = 400$ µm (Figure 55).

In this case, the maximum irradiance ($I_{max} \approx 191\ \mathrm{kW/cm^2}$) allows ablation of many materials. All printheads have the same optical architecture described in section 5.2 for Fiber-Coupled Laser Diode Array: a set of fixed focal lenses, any magnification (1 to 1 image), with only one column of laser beams with a vertical pitch equal to the spot diameter, giving a low dot density (63.5 dpi). The picture in Figure 56 corresponds to one of the implementations of the printhead.

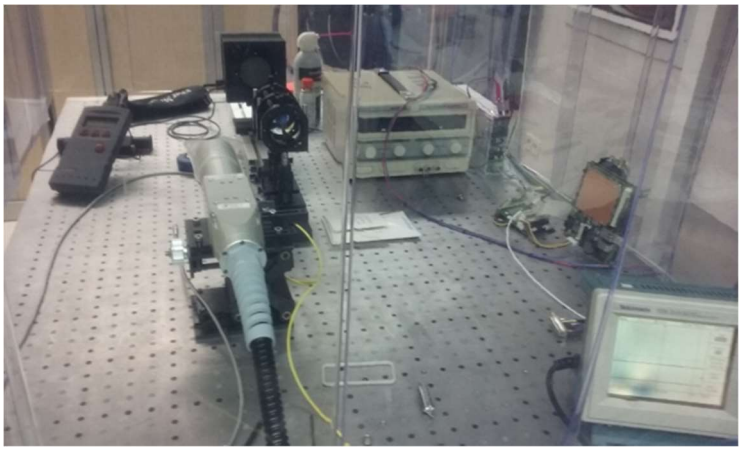

Figure 56: Printhead in the proof-of-concept workbench, to perform optical and electrical measurements

The technical requirements of the optical system differ from the f-LDA system mainly in the laser power density that the optical fibers need to support. I have developed two different printheads with two different fiber bundles to conduct a comparative performance analysis. Figure 57 shows the system designed with 400 µm fiber core diameter with LDs (975nm, 240W) from Bright Solutions that demonstrated a more robust behavior than the 200 µm system with LDs (975nm, 250W) from Dilas-Coherent (Figure 58).

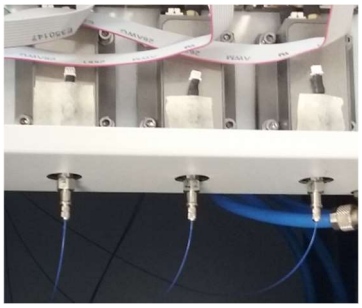

Figure 57: Array of 400µm fiber-coupled laser diodes

Figure 58: 200µm fiber-coupled laser diodes

Figure 59 shows the block diagram of the HP f-LDA laser system with some detail related to the components required for this high-power system (power supplies, drivers, cooling, optical adapters, imaging head).

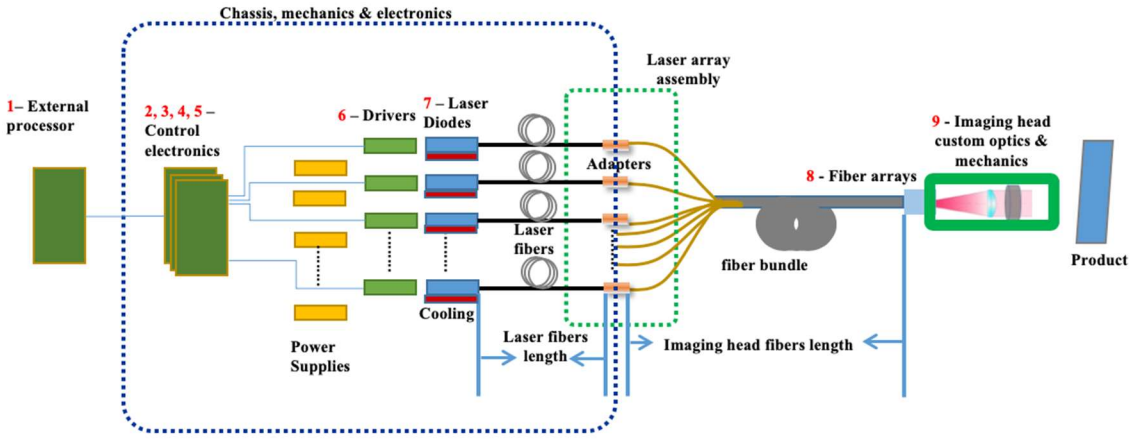

Figure 59: Block diagram of the HP f-LDA laser system

The goal for this laser system is to print high-definition 2D codes (QR, Data Matrix, etc.) compliant with grade A according to ISO/IEC 15415 criteria [20], with precision in the order of microns, for unique serialized coding. We have tested our HP-fLDA system in a real production line by printing up to 100 unique 2D codes per second, achieving grade A at the maximum speed of the production line, which is 10 m/s. The laser system will allow a maximum aspect ratio AR=2 if the laser works at 100% Duty Cycle, but to ensure compliance with the standard in printing 2D codes, we must not exceed AR>1.2 per module. Figure 60 shows graphically this requirement. I propose 400 µm as a reference for the ideal grid with the same value for pitch and dot size.

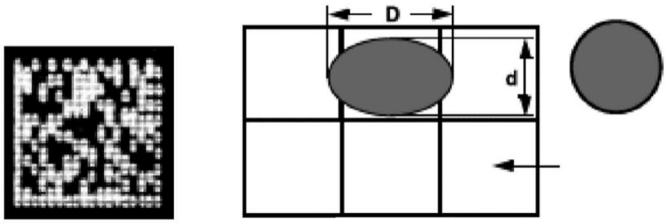

Figure 60: Elongation is measured as a deviation from the perfect circle. The ISO/IEC 15415 standard allows 20% difference between D and d (extracted from [20]*).*

To print 2D codes with a single dot per module, our High-Power f-LDA system manages to print on our test bench of 2D codes up to 16 m/s within the AR<1.2, using materials with Fluence threshold (F_{th}) values around 1 J/cm^2. At higher speeds, dots become too elliptical. Figure 61 shows some examples of ellipticity measurements of dots marked at different speeds

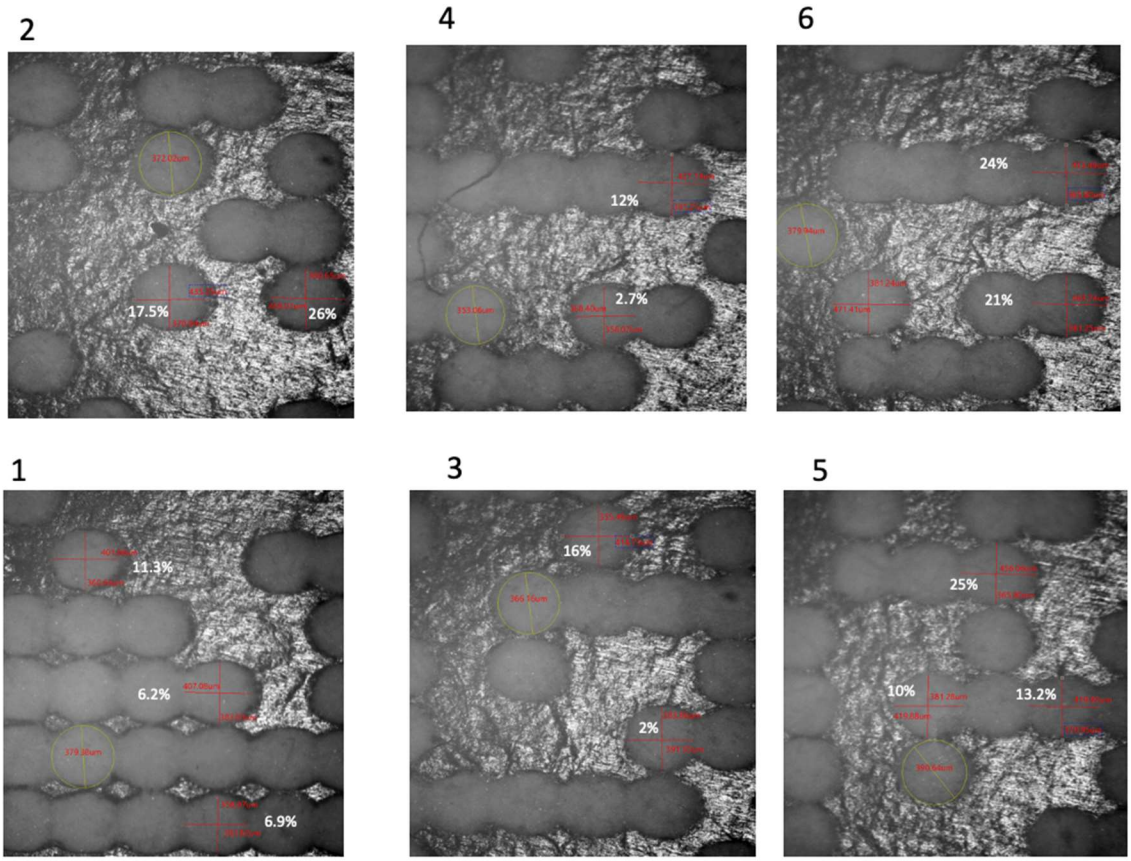

Figure 61: Examples of ellipticity measurements of dots marked at different speeds

We could achieve a higher printing speed for 2D codes with a single dot per module (with AR<1.2) if we use easily ablatable materials ($F_{th} \approx 0.5$ J/cm^2). We can also print 4 dots per module instead of one. Then, with AR=1.4 per dot, we get AR=1.2 per cell (Figure 62) thus complying with the norm. Therefore, we could reach more than 20 m/s according to Equation 25. With this HP f-LDA system, we can mark codes that do not have the AR < 1.2 limitations and therefore we can increase the speed.

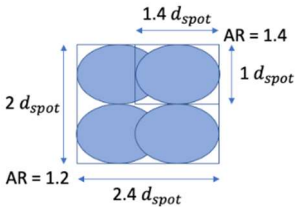

Figure 62: Illustration of how we can get AR=1.2 per cell by printing 4 dots per cell with AR=1.4 per dot.

For a given speed, the variations in the pulse time and the laser power affect the ellipticity and the measurement of the dots and, consequently, the quality of the 2D codes. Figure 64 shows an example where the dots are elliptical and the optical density is low. Complementarily, Figure 63 shows dots with small ellipticity (printed with shorter pulse width) and high optical density (due to higher laser power used). In terms of printed image quality, the second is better and justifies the use of high-power laser diodes.

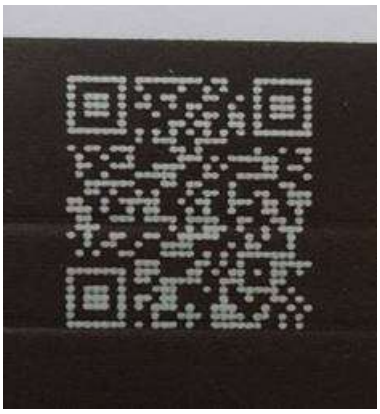

Figure 64: Sample printed with a long pulse width (60 μs) and low laser power (60W).

Figure 63: The same sample printed with a short pulse width (40 μs) and high laser power (240W).

Tests carried out on different colors samples show that color and its tonality are also key parameters. Examples in Figure 65 have been printed with the same parameters in three different areas to test how the result changes depending on the tonality.

Figure 65: Tests performed at 300m/min on samples with different tonalities

At 16 m/s the control system must activate LDs at 40KHz, to keep the horizontal pitch equal to the vertical one (400 μm). Currently, there are not any commercial production lines with speeds above 10 m/s but when they appear, our system will be able to increase the frequency maintaining the pitch. Systems implemented with this configuration are suitable for very high-speed coding.

Again, the achieved speed is very competitive in the market. Printing only codes is often done using black and white images (bpp = 1). In this case, if we want to print at the maximum height of the print head (35 dots of 400 μm) at 16 m/s, Eq. 45 predicts a bandwidth for the required controller of BW > 1.4 Mbps, the pulse period will be

25 µs (Eq. *50*) and the maximum latency (Eq. 51) with AR=1.2, will be 2.5 µs. Therefore, the computing requirement (Eq. 53) will decrease to

$$CT = \frac{m\, I_w I_h V_{line}}{P_w} = \frac{300 \cdot 35 \cdot 35 \cdot 16}{14 \cdot 10^{-3}} = 0{,}42 \text{ GOPS} \qquad (53)$$

The main differences concerning the previous design are a lower number of channels, shorter latencies, and more variable data changes between images. The typical application of the HP f-LDA system is to print up to 100 unique 2D or DM codes per second while the previously presented f-LDA system should print up to 10 images per second (with few digits changing between consecutive images).

In the new platform, the x86 CPU still executes the soft real-time tasks, like image pre-processing and communications with the external world. The hard real-time tasks are implemented in a DSP combined with several FPGAs. In this architecture, the number of laser diodes, diode drivers, and FPGAs is lower. The main FPGA board collects the position feedback information to calculate the position in real-time. The DSP calculates the coordinates of the points in real-time based on the image to be printed and the speed and position information coming from the encoder and the photocell for the figure to print and transfers position-dependent data to the main FPGA. This one distributed them to the FPGAs attached to the LD drivers. This provides precise control of the switching of the LDs, which is a critical point in this system.

Laser Diode drivers have to meet a requirement of rise/fall time (10 - 90%) < 1 µs, typically. 500 ns. Controlling and monitoring data are done on a mix of analog and digital signals with very different requirements in terms of reliability, noise immunity, time bandwidth, and jitter. For a single channel, an effective approach is to have an interface with a mix of analog and digital signals but, in a multichannel system, if the interface wiring is simply replicated for the number of channels, this could lead to troubles in terms of reliability, maintenance, signal integrity, and cost Figure 66 shows the functional block diagram of a single channel.

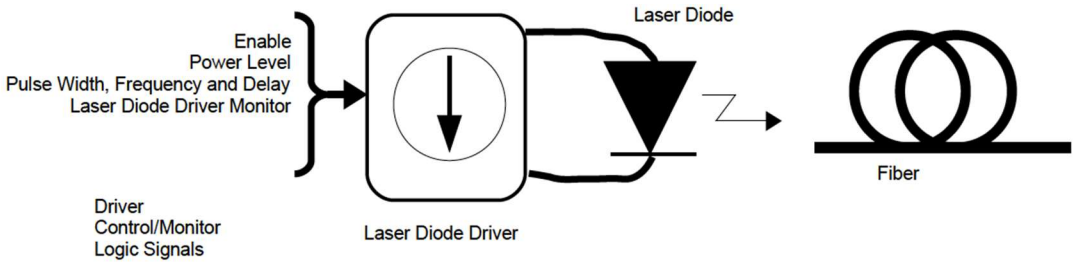

Figure 66: Functional block diagram of a single channel diode driver

All laser diode drivers are equipped with logic to generating laser pulses according to control parameters. Laser diode drivers safely receive from the control system: stop/start emission commands, power level setpoint, pulse width, repetition rate, and delay for each channel. They send to the control system: status monitor signals of laser diode and driver for every channel. Figure 67 shows the current drivers for three diode channels used for the implementation of the HP f-LDA system.

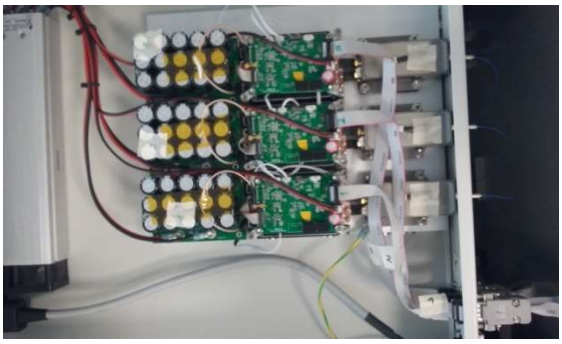

Figure 67: HP f-LDA laser diode current drivers

After power-up, the control system settings are stored in a non-volatile RAM and can be changed during operation. To turn on the laser diodes, the control system applies an Enable signal. Laser pulse emission occurs on-demand, at the output of the requested channels only when a PulseIN trigger is applied. The control system monitors the status of the system and lasing signals. Figure 68 shows the laser control platform whose main components and related characteristics are listed in Table 12.

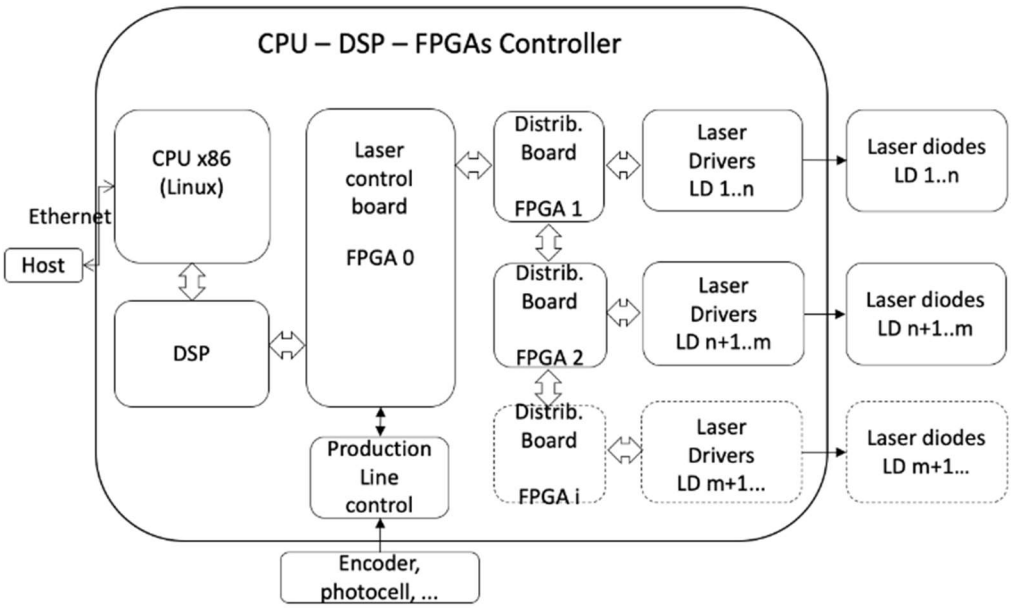

Figure 68: Architecture of the HP f-LDA platform with DSP+FPGA for hard-RT management

Table 12: Main Components of the HP f-LDA Embedded Board Architecture

	Processor	Clock frequency	Communication I/F	Storage capacity
CPU x86	Intel Atom Single Core	1.46 GHz	1 Gb Ethernet / PCIe Gen 2	1 GB DDR3 / 512 MB Flash
DSP	Texas Instruments TMS320DM6 DSP	720 MHz	PCIe Gen2 / EMIFA	512MB DDR2
FPGA 0	Intel Altera Cyclone IV	< 150 MHz	EMIFA / Ad-hoc	270 Kbits
FPGA 1..n	Intel Altera Cyclone IV	< 150 MHz	Ad-hoc	270 Kbits

Figure 69 shows the mechanical enclosure that houses most of the electronic parts. The center of the picture contains the distribution boards (FPGA1, ..., n). The set of vertical PCBs on the top right side contain the x86, the DSP, FPGA0, and the electronics for the encoder, photocell, etc. Yellow boxes (bottom right) are the safety relays (independent of the marking control). LD drivers are into different laser modules, connected to the control via cables (left side).

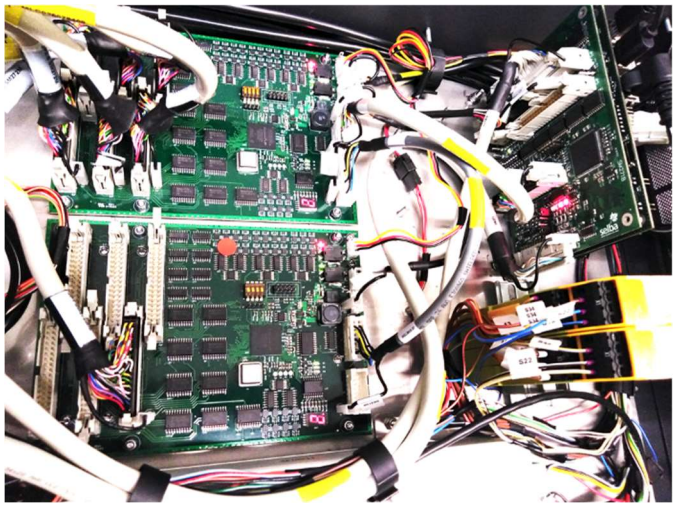

Figure 69: Laser system controller for HP f-LDA.

Figure 70 shows the mapping of the computing elements selected on the architecture developed and its interaction with the user and production line for the HP f-LDA marking system.

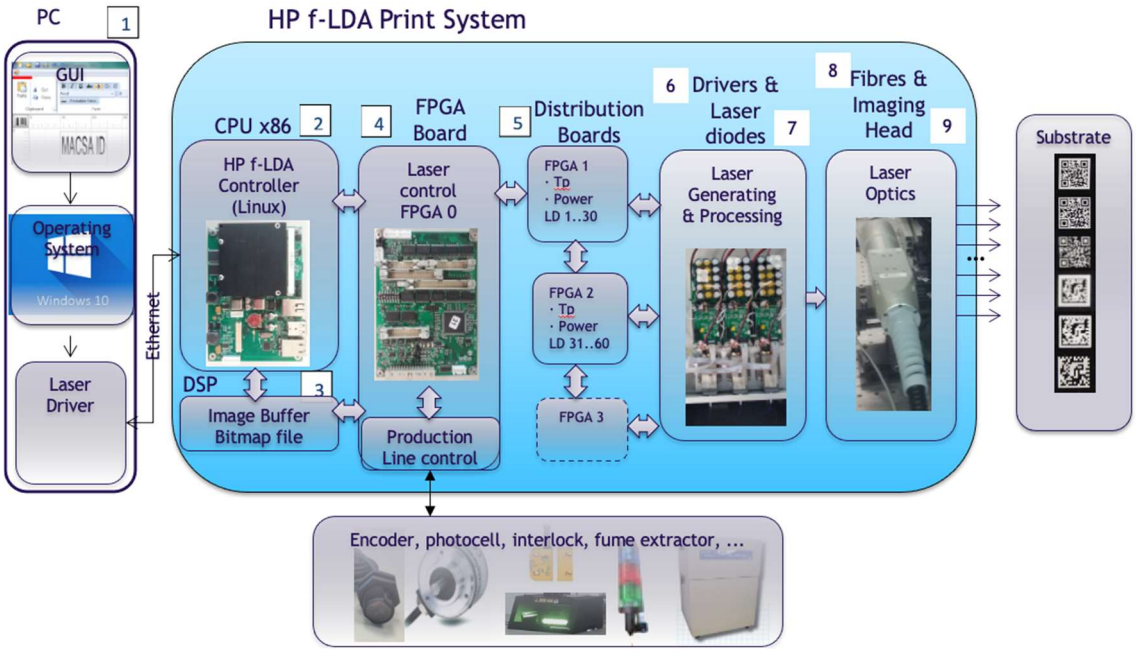

Figure 70: Component mapping showing the data and control flows of the HP f-LDA marking system architecture and its interaction with the user and the production line.

As stated in section 3.3.2, our analysis on the software reference architecture concluded that Macsa's Scanlinux and Marca software will be the basis for our new multibeam systems software platform (see Annex A)

We designed all the hardware systems on modular architectures, meaning that all components can be changed separately (Figure 71).

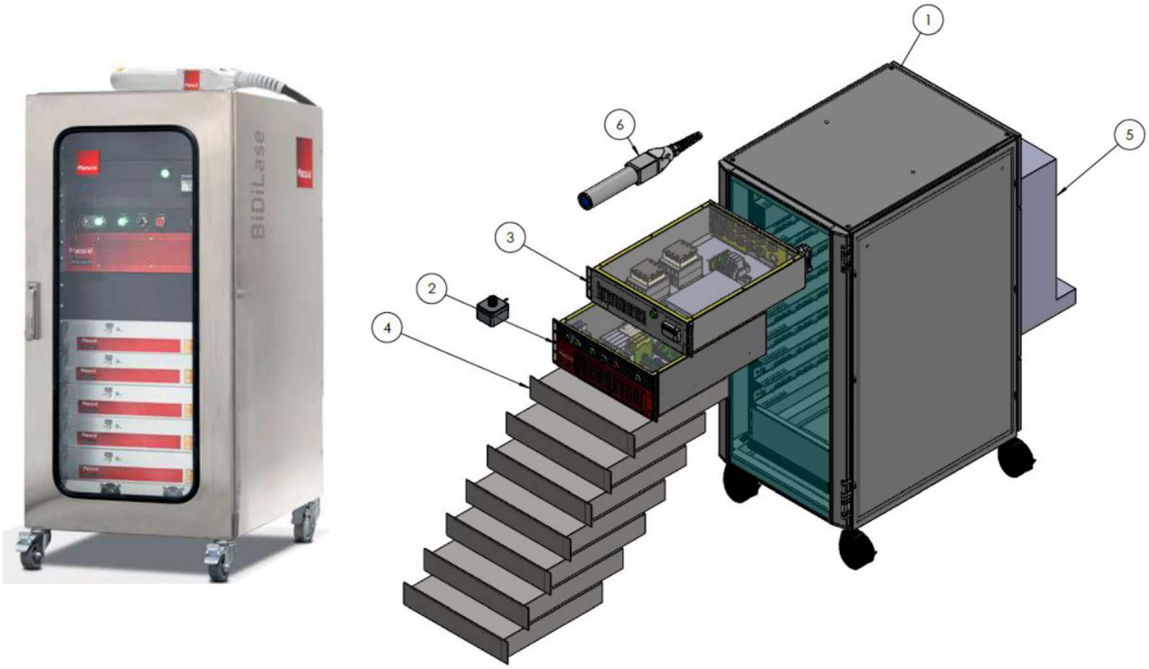

Figure 71: Modular architecture of the HP f-LDA system. All components can be renewed separately

Each of the modules and components has its own lifetime and needs to be overhauled or renewed accordingly. MACSA focuses on reliability analysis at module and component levels. For example, MACSA has a system for up to 14 lanes and each lane has 7 laser modules with multiple laser channels, then for each printing line, there will be 14*7= 98 laser modules in total. If there is any sudden death on any laser diode, its respective laser module needs to be renewed or repaired. Laser diodes have their lifetime, then it is essential to calculate when is expected to renew or change the diodes as equipment maintenance. Additionally, we need to consider other components as fiber cables, laser head, etc.

MACSA identified the components with relevant use-related degradation such as the laser diodes on the optical side and capacitors on the electronic side. These two seem to be the most sensitive components. All others, including fibers and lenses, have negligible or no degradation rate. All through the years, we observed that both laser diodes and capacitors' failure mechanisms seem to show more a regular degradation than a sudden failure, so resulting in some predictable behavior. That allows predicting the expected degradation rate for any given operating regime.

Diode lasers can exhibit both sudden (infant or random failure regimes) and gradual degradation (wear-out regime). [171] In the random failure regime, the AlGaInAs random failure rate is proportional to temperature and drive current, as Eq. (54:

$$FailureRate\ (T_j, I) \propto e^{-E_A/k_B T_j}\ I^m \qquad (54)$$

where T_j is the diode junction temperature, I is the diode drive current, and k_B is the Boltzmann constant. The Arrhenius factor (E_A), exponential current acceleration (m), and the proportionality constant is fitted by measuring device failure rates under various temperature and current accelerations. In the wear-out regime, AlGaInAs-based lasers show negligible degradation except during extremely accelerated high-current and/or high-temperature operation.

Assessing lifetime expectations for semiconductor lasers and, in general, for laser diode modules is a complex activity typically involving several tests for very long times. Usually accelerated lifetime tests are preferred since they allow to estimate very long lifetimes in real operating conditions based on much shorter tests than the expected lifetime. In the case of the high-power fiber-coupled laser diode arrays, after several long preliminary tests, a significant batch of 15 laser modules has been put under test in 2 series of accelerated tests lasting 8700 hours and 1600 hours respectively. All the devices have been tested in accelerated conditions and no failures have been observed over the two tests. The acceleration factor has been estimated from a minimum of 3X to 10X maximum. As a conservative result, we will consider the minimum acceleration factor of 3X (worst case). The lifetime of laser diodes is conventionally defined as the operation time to reach a 20% drop of output power. Average lifetime results for laser diodes are summarized in Table 13.

Table 13: Average lifetime results for laser diodes

Average **degradation rate in accelerated tests** (% / 10k hours)	3.8% to 6.2%
Expected lifetime in accelerated test conditions	32000 to 52000 hours
Average expected degradation rate in normal rated operation (% / 10k hours)	1.3% to 2.1%
Expected lifetime in normal rated operation (worst case)	95000 hours (~11 years)

Aluminum electrolytic capacitors populate two components of the power laser diode drivers' chain: buffer capacitors block and AC/DC power supply. Although the failure rate is generally used in designing an electronic device, the reliability of an aluminum electrolytic capacitor is measured by its life (the expected life, in practical use) rather than failure rate since the failure mode of aluminum electrolytic capacitors is wear-out. An aluminum electrolytic capacitor is determined to have reached its end of life when the capacitance change, tangent "d" and leakage current have exceeded the specified value or when a noticeable external abnormality occurs. The specified lifetime is readily available data on the component datasheet. The factors that most affect the life of aluminum electrolytic capacitors are acceleration according to the ambient temperature (FT), acceleration according to the ripple current (FI), and acceleration according to the applied voltage (FU). The expected life is calculated by multiplying the specified lifetime, FT, FI, and FU. Average lifetime results are summarized in Table 14.

Table 14: Average lifetime results for aluminum electrolytic capacitors

Expected lifetime in normal rated operation (worst case: 75% load, 50°C ambient temperature): AC/DC power supply e-cap	10 years
Expected lifetime in normal rated operation (worst case: 75% ripple current, 50°C ambient temperature): buffer capacitors block	15 years (calculated Lifetime is longer, but manufacturer consider 15 years to be the maximum for estimated life calculation)

5.4. Results and discussion

I have proposed, developed, and tested two laser marking/printing complete solutions for two different application scenarios: (1) fiber-coupled Laser Diode Array (f-LDA) technology for high-speed and high-resolution printing, using thermochromic pigments; and (2) High Power fiber-coupled Laser Diode Array (HP f-LDA) technology for very high-speed coding. Table 15 shows the parameters (upper limits) selected for those platforms.

Table 15: Main parameters achieved for the f-LDA and HP f-LDA implemented platforms.

	f-LDA	HP f-LDA
Resolution (dpi)	203	64
Width (mm)	48	14
Gray levels	256	2
Number of diodes	384	35
Laser wavelength (nm)	980	980
Power per diode (W)	8	250

The laser beams could be used either to expose for example thermochromic ink/labels or to cause ablation on ink-coated material, as shown in Table 16

Table 16: Processes triggered by different power densities in different material surfaces used in this work

Surfaces	Typical Irradiance order	Typical fluence Threshold ranges	Triggered Processes	Laser marking system
Thermochromic ink	W/cm^2	mJ/cm^2	Photochemical transformation	f-LDA
Ink for Food Packaging	kW/cm^2	J/cm^2	Ablation	HP-fLDA

Developed platforms allow achieving the operation parameters shown inTable 17

Table 17: Operating parameters standard values achieved by the platforms

		f-LDA	HP f-LDA
Scribing speed (V_{sc})	m/s	0-2	0-16
Radiant flux per dot (Φ)	W	0-6	0-240
Fluence threshold (F_{th})	J/cm2	0.1-2.2	1-2
Typ. Dot size (d_{spot})	µm	125	400
Max. Beam irradiance (I)	kW/cm2	49	191
Pulse repetition rate (f_p)	kHz	0-16	0-40
Dot pitch (xpitch)	µm	125	400
Pulse width (Δt_p)	µs	-	0-100
Max. Intra pulse Duty Cycle	%	100	100
Max. Burst duration	ms	-	7
Min. Burst period	ms	-	10
Max. Burst Period Duty Cycle	%	-	10

The maximum printing speed by the laser systems is mainly influenced by the scribing speed, number of simultaneous beams, and controller throughput. According to Eq. (*41*), the speed of the production line when using an array of single-column laser

diodes is equal to the scribing speed. Table 17 reflects the parameters determined by Eq. 25.

The control systems have been developed to overcome the computing throughput and latency requirements imposed by the usual applications for marking and printing systems operation. Table 18 shows examples of parameters determined by Eq. 45, 46, and 47.

Table 18: Main top parameters for the developed computing architectures

		Label printing	Coding
Number of pixels (I_h)	Pixel	384	35
Number of pixels (I_w)	Pixel	1152	35
High (P_h)	mm	48	14
Width (P_w)	mm	144	14
Bits per pixel (bpp)	bit	8	1
Speed (V_{line})	m/s	2	16
Position error (ε_{max})	µm	13	40
Operations per pixel (m)	O	300	300
Operations per image (M)	O	1,33·108	3,68·105
Bandwidth (BW)	Mbps	49	1.4
Latency (L_{max})	µs	6,25	2.5
Computing throughput (CT)	GOPS	1,84	0,42

When comparing the obtained results with those found in the literature and industry, the laser marking systems and control methods described in this work can print variable codes (2D codes, barcodes, expiry dates, logos, etc.) with higher throughputs than previously reported in the state of the art (Table 19).

Table 19: Results compared with previous works from the literature

Work	Year	Res. (dpi)	Width (mm)	Gray levels	V_{line} (m/s)
Ravellat [172]	1991	51	2.5	2	0.5
Llado [25]	2000	76	6	2	3.3
Endo [118]	2003	56	1.8	2	8
Jiang [173]	2007	20	10	2	0.6
Chen [79]	2009	51	3.5	2	2.5
Fraser [174]	2018	-	10	-	0.02[1]
My f-LDA	2021	203	48	256	2
My HP f-LDA	2021	64	14	2	16

[1] derived from the reported 2.79 cm2/s assuming a 1 cm marking width

A careful analysis of the Total Cost of Ownership of our laser system vs competitive marking technologies should be conducted for every specific application, considering: production line details (average number of products per minute, the average number of working hours per year, profit per product, profit per hour, labor cost per hour, MTTR, estimated lifetime, etc.); machine end-user price and capital equipment depreciation; operational costs (consumables, maintenance, repairs, downtime, etc.) and

others. In a rough estimate, the end-user price of MACSA equipment for high-performance production lines is in the order of 100s K$, depending on the configuration that is estimated in the same order of the annual savings for high-performance production lines, which provides a reasonable break-even point. For medium and low-performance production lines, MACSA provides alternative marking systems. As proposed by Wudhikarn [125], Overall Equipment Effectiveness (OEE) and Analytic Network Process (ANP) tools can be applied for a complete analysis, which attests that, even with higher acquisition costs, industries will invest in laser marking technology because of the overall economic benefits.

Speed is a function of three main items: laser output power, the efficiency of the laser-matter reaction, and desired optical density. Figure 72 represents the production line speed vs pulse repetition rate printing linear dependency with the developed f-LDA laser system.

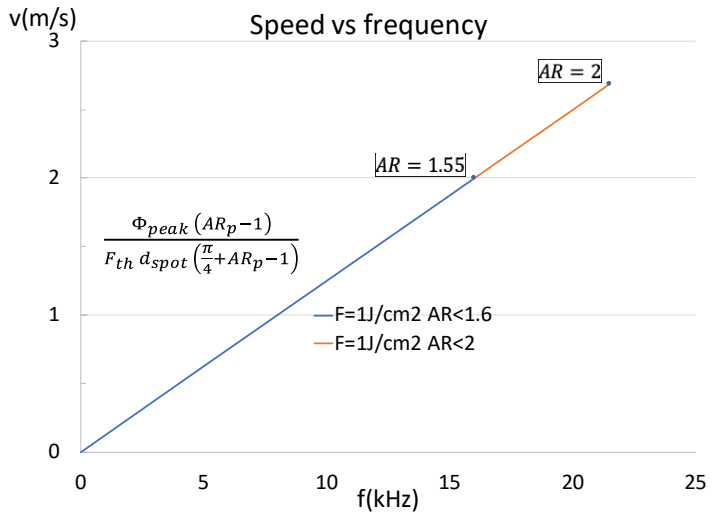

Figure 72: Production line speed vs pulse repetition rate dependency for the f-LDA laser system. Achieved printing speed of up to 2 m/s with AR = 1.55; and 2.7 m/s with AR = 2 (DC = 100%) (Fth = 1 J/cm2)

This system maintains image quality for print speeds from 0 m/s to 2 m/s (blue line) able to manage instantaneous accelerations or decelerations. For a fluence threshold F_{th} = 1 J/cm^2, the laser system can print at speeds up to 2 m/s with AR around 1.5 and, for this fluence threshold, with AR = 2 (DC = 100%), it can print at speeds of up to 2.7 m/s (red line). If the application allows reducing the resolution in the process direction (by increasing the pitch), it is possible to eliminate the AR < 2 restrictions and then speed can increase up to 4.8 m/s, the operating limit in CW for this fluence threshold. In this case, images have very different resolutions in the two axes what has to be taken into account.

I expect that the developed platforms will achieve higher throughputs on inks that reduce the fluence threshold. Moving to different wavelengths, increasing the power, changing resolution, or changing the spot diameter can also lead to higher throughputs. According to Eq. (19), the f-LDA platform will produce enough contrast with 4.6 µs laser

pulses on surfaces with a 0.1 J/cm^2 fluence threshold, thus achieving 27 m/s maximum speeds with a 100% duty cycle. In the case of 1 J/cm^2 fluence threshold, the minimum pulse duration must be 46 µs which allows speeds up to 2.7 m/s with a 100% duty cycle.

Pulse width depends on the intensity of black or gray colors for each dot while the pulse period depends on the production line speed. For example, if we need 56 µs to mark a black dot, and we do not consider the non-linear effects of the laser-matter reaction to simplify the analysis, a production line printing at 203 dpi (125 µm pitch) and a speed of 0.5 m/s requires a period of 250 µs (4 kHz). This means a duty cycle of 22%. To mark the same black dot at 2 m/s, we need a similar ON time in a period of 62.5 µs that requires increasing the duty cycle by approximately 90%. Figure 73 shows some examples of printing with the f-LDA system.

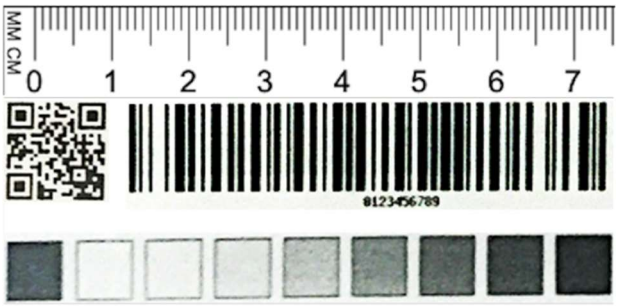

Figure 73: QR grade B and barcode examples of high-resolution (200 dpi) printing at 2m/s for up to 256 gray levels with the f-LDA platform

The High-Power fiber-coupled Laser Diode Arrays (HP f-LDA) platform was used to build a marking system capable to print at 16 m/s above any maximum marking speed reported in the literature. Figure 74 represents the production line speed concerning the pulse repetition rate obtained by the HP f-LDA platform. The speed of 16 m/s corresponds to a Fluence threshold F_{th}= 1 J/cm^2 with a theoretical AR lower than 1.3 (blue line). In practice, dots are less elliptical than the simplified theoretical predictions due to the non-linearities of the laser-matter reaction, non-uniform fluence distribution on the dot area, and the Gaussian distribution of the laser beams. This allows printing at higher speeds.

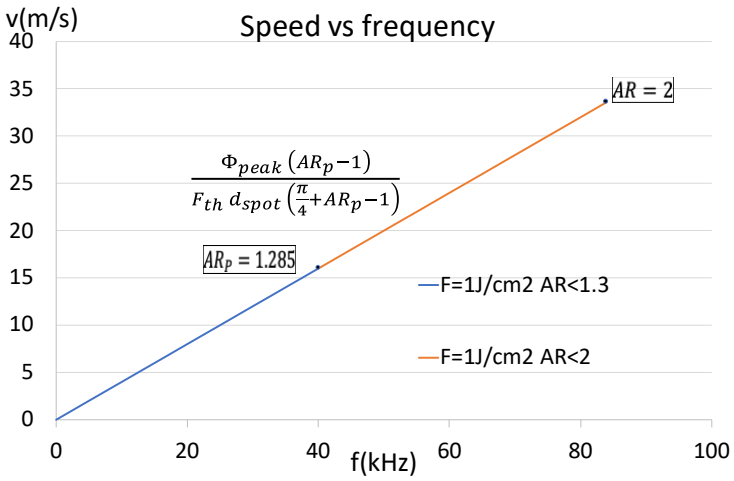

Figure 74: Production line speed vs pulse repetition rate marking with HP f-LDA laser system. For Fth = 1 J/cm2 can print at speeds up to 16 m/s with AR = 1.285; with DC = 100% (AR = 2) could print at speeds up to 33 m/s

Again, the HP f-LDA platform with 12 µs laser pulses produces high contrast on surfaces with a 1 J/cm^2 fluence threshold (as shown in the example of Figure 75).

Figure 75: Example of marking with HP f-LDA laser system for very-high-speed (10 m/s) coding applications

Theoretically, we could achieve 33.6 m/s maximum speeds with 100% duty cycle and AR = 2 (red line) but the industrial product does not support DC = 100% due to safety self-restrictions. Table 20 shows the operating parameters used for the example shown in Figure 75 marking at a maximum speed of 16 m/s.

Table 20: Operating parameters used for the example shown in Figure 75

HP f-LDA		Standard values	Example of Figure 75
Scribing speed (V_{sc})	m/s	0-16	16
Radiant flux per dot (Φ)	W	0-240	240
Fluence threshold (F_{th})	J/cm2	1-2	1-2
Typ. Dot size (d_{spot})	µm	400	400
Max. Beam irradiance (I)	kW/cm2	191	191
Pulse repetition rate (f_p)	kHz	0-40	40
Dot pitch (xpitch)	µm	400	400
Pulse width (Δt_p)	µs	0-100	20
Max. number of dots (ON+OFF) per burst	-	-	101
Number of ON dots per burst (worst case)	-	-	48
Pulse period (Δt)	µs	> 25	25
Max. Intra pulse Duty Cycle	%	100	80
Max. Burst duration	ms	7	2.525
Intra burst pulse-ON time (worst case)	µs	-	960
Intra burst Duty Cycle (worst case)	%	-	38
Min. Burst period	ms	10	10
Max. Burst Period Duty Cycle	%	10	9.6

Figure 76 shows a typical waveform of temporal laser activation signals applied to all individual channels of the HP f-LDA shown to better understand Table 20.

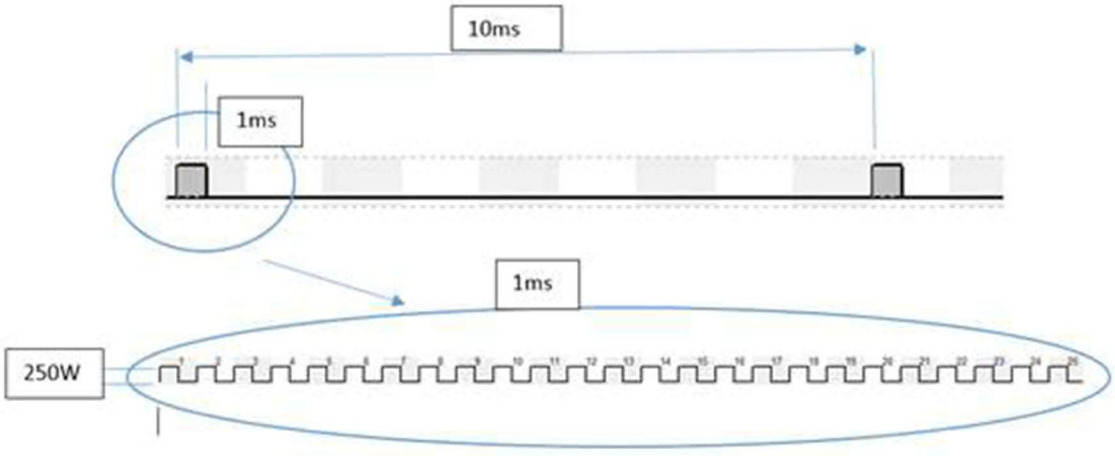

Figure 76: Typical waveform for every individual channel of the HP f-LDA

5.5. Summary of the chapter

I have analyzed existing laser diode arrays technologies and proposed and implemented a complete architecture (optical plus computational) for its industrial use in high-speed printing and high-resolution printing (f-LDA) and very-high-speed coding (HP f-LDA) type of applications intended to be integrated into production lines.

Industrial printing applications demand higher throughput in-line digital laser marking. I have demonstrated that single laser beam sequential processing limits marking speed to a de-facto barrier of 8 m/s. I have shown in this chapter how a laser beam matrix controlled by embedded computing overcomes these marking speed barriers and how to mark and print patterns and images of 50 to 200 dpi resolution, on either black and white or 256-tone grayscale, from 6 to 50 mm substrate widths, and speeds up to 16 m/s. I also claim the higher speeds can be achieved by investing in additional laser beams.

I have proposed, developed, and validated two architectures for fiber-coupled laser diode (f-LDA) multichannel systems for marking and printing applications. The main pitfalls of high peak power multichannel systems and their control have been underlined. The proposed architectures address and solve these issues, assuring easy maintenance, scalability, and a cost-effective solution. I have detailed the optical and electrical components and interconnections, the features required by high-speed and high- types of applications, their computing requirements, and the control architectures of the platforms.

I have presented the development and characterization of marking devices compatible with roll-to-roll processes. The results presented offer detailed descriptions of the device, computational costs, calculation of marking speeds, and marking characterization examples. The conclusions based on the results obtained show that both overall and particular findings are novel and represent an advance in the state-of-the-art.

"Thesis submitted to processes of protection or transfer of technology or knowledge"

This doctoral thesis has been carried out under the framework of an agreement between the UAB and MACSA ID, signed on October 2, 2015.

I request that it be considered as "Thesis submitted to processes of protection or transfer of technology or knowledge"

That is why the following 12 pages, corresponding to chapter 6, are encrypted in a separate file. The summary of the encrypted pages is on the next page of this document, to fulfill the requirement that it should allow the reader to get an idea of the research work carried out.

6.5. Summary of the chapter

MMA and SLM technologies enable high-resolution implementations of laser marking and printing systems. We have analyzed and proposed using these technologies for high-resolution applications as anticounterfeiting with high-resolution coding (SLMs) and high-resolution printing (MMAs). For these applications, besides the resolution, the speed of production lines is also determinant. In this chapter, we review the limiting factors of the laser marking speed for both technologies and analyze how future systems could overcome them.

We have shown in this chapter how technologies based on 2D laser imaging controlled by embedded computing achieves the required resolution at the required speed and how, can produce patterns on either black and white or with a 256-tone grayscale, and images of more than 300 dpi resolution, up to 100 mm width, at speeds over 2 m/s can be printed.

An architecture proposal for the MMA-based systems has been presented. The proposed architectures address high-resolution implementations, assuring scalability. We have presented the optical and electrical descriptions, the features required to assure the high-resolution printing applications, the computing requirements, and the control architectures proposals of the systems.

For the SLM-based systems, we have presented the main results we have achieved up today, which is a proof of concept with a DPSS pulsed laser with a wavelength of 1064 nm, an SLM, and a set of lenses. The control system for the proof of concept was developed for the main function of computation of an iterative Fourier-transform algorithm to be applied on the SLM and create multi-beam output from one single laser beam. The beamlets are independently controlled by software, dynamically. For serialization, the unique code marking rate is defined by the SLM pattern display time (required time to change from one pattern to another). For lot marking, marking rate is defined by the laser pulse repetition rate.

With the MMAs technology, we have achieved the best combination in high resolution with the wider print width, but the lowest speed. With the SLM technology, we have achieved the best combination in high resolution with high speed, but a small print width.

7. Conclusions and Next Challenges

The motivation of this thesis is an Industrial Ph.D. to develop marking and printing methods and control systems that will allow applications for which there is currently no solution, becoming a limiting factor to the market. All through this document, readers have noticed the clear industrial orientation of my thesis while trying to provide both a theoretical framework for the analysis for building laser marking and printing systems and the criteria to evaluate them trying to reach optimal solutions for quality, performance, cost trade-off.

With this aim, I have analyzed the key factors of laser marking that limit the speed of production lines. After an analysis of the state-of-the-art technologies, I have obtained simplified analytical models that facilitate studying the impact of the design parameters for the different parts, especially optical and computational to reach maximum line speeds in the complete systems. The same analysis is used to identify the limits of current technologies and predict the ones that will potentially be part of future systems. The main focus is dealing with multiple beam systems whose implementation depends on the energy requirements and therefore on the quality-speed-width-resolution trade-off. Once multiple beam systems will be widely adopted, I predict that the performance bottleneck will move to the computing throughput of the embedded controller.

7.1. Conclusions

In this thesis, I report on the technology I have developed as a research and R&D manager, to achieve the requirements of very high-speed coding, high-speed printing, high-resolution printing, high-resolution high-speed coding, and inkless printing applications. I detail the laser marking or printing system components (surfaces to be marked, laser sources, multiple beam systems, and control), and I show the parameters and values, which will ensure that the laser system meets the application requirements.

As far as we know, there is not any other published laser marking system that is capable of marking variable information for production lines with speeds like those used by rotary converting printing presses.

The printing platforms must be adapted to the material fluence threshold (F_{th}), and when possible, they should use a coating sensitive to the laser wavelength. The laser system should be designed to provide a high enough beam irradiance (I) so that the marking time (t_{mark}) required to exceed F_{th} is lower than the time imposed by the maximum speed of the production line. A sequential process with a single laser beam, covering the entire marking area, is not feasible for highspeed marking applications. Even though deflection systems for all kinds of applications can be fast enough, multiple laser beams must be used to reach the speeds imposed by high-performance production lines.

This thesis' research reached the development of several laser marking and printing systems, in which I have experienced three different laser-matter interaction physical processes for marking or printing, three different strategies for generating and controlling multiple beams, and five different platforms for multi-beam parallel laser processing.

The three different laser-matter interaction physical processes that I propose for marking or printing are:

1- **Laser inkless eco-printing on paper and cardboard.** I have presented a novel method to print in paper and cardboard without ink. The proposed method aims to reach the carbonization stage in two phases to minimize the generation of debris: (1) preheating below the temperature threshold in which visible changes are manifested. (2) a short wavelength laser heats to produce visual marks while triggering polymerization of some of the volatilized compounds. The reduction of residue and the cost to treat them is incomparable to any other known method in the literature. Moreover, the printing quality both in contrast and resolution meets the typical requirements of the industrial and office environments. This method will allow a significant reduction of consumables in the packaging world. Although there is no visible debris, more research is needed to analyze with more detail the nature of the materials involved in the process and the quantification of the generated by-products using mass spectrometry and gas chromatography.
2- **Thermally driven color change induced by laser absorption in thermochromic print media**. Multiple implementations of the different components of the print media have been developed by various manufacturers like Ricoh or Datalase.
3- **Laser ablation.** High contrast marks are generated using high power density laser irradiation in the marking and etching of various materials using heating, melting, or material removal mechanisms.

My proposal for generating and controlling multiples beams involves three different methods:

1- **Multibeam laser systems with different wavelengths**. A first laser beam heats a wide area of the surface to be printed, which increases temperature sharply. Before the surface is cooled down, the second laser of narrower beamwidth irradiates the required geometry, to increase the temperature above the carbonization threshold.
2- **Laser Diode Arrays-based systems** use a multi-laser array to create images. Objects pass beneath the array and change color in the areas exposed to the laser beam. By selectively pulsing the lasers on and off, the array can choose which areas change color and which areas remain unchanged. The combination of colored areas and blank space form a monochrome image.
3- **Projection-based systems (MMAs and SLMs)**. With the advances of MMA (DMD) and SLM technologies, multiple independent laser beams projected onto surfaces to be marked or printed can be available. This allows for designing laser projection-based systems for marking (using SLMs) or printing (using DMDs). However, the low level of fluence per beamlet that these systems can deliver is a major roadblock

to the success of such systems. I have shown how to use each technology for the appropriate function, with the most suitable architecture to implement a high-resolution laser marking or printing system.

I present five different implementations developed for multi-beam parallel laser processing according to the methods and the laser-matter interaction physical processes presented in this thesis

1- **Different wavelength multibeam laser systems, using carbonization method to print**. The system is implemented using two independent laser sources. A CO_2 laser of 9.3 μm is used as a preheating laser, while an ultraviolet or visible laser acts as the marking laser. The target application is to print paper and cardboard without ink. The best combination achieved up today is printing without ink a high-density image with an area equivalent to A7, with a resolution of 600 dpi, in less than 10 seconds with an optical density and quality equivalent to the best printing systems with ink.
2- **Fiber-Coupled Laser Diode Arrays (f-LDA) systems, printing using thermochromic pigments**. An f-LDA printing system is composed of an array of laser diodes (LDs), some fiber-optics to conduct the laser power from the LDs to a printhead, and a marking control system to generate the signals which are applied to the LDs to produce the marking according to an N x M dot matrix. The target application is high-speed printing. The best results are printing images with a print width of 50 mm, a resolution of 200 dpi at speeds of up to 2 m/s.
3- **High Power fiber-coupled Laser Diode Arrays (HP f-LDA) systems, marking by laser ablation**. The main differences concerning the previous design are the lower number of channels, the higher power of the diodes, the shorter latencies required, and more variable-data changes between images. The typical application of the HP f-LDA system is very high-speed coding. The system can print codes of 14 mm width, a resolution of 63.5 dpi, at speeds of up to 16 m/s, with a grade A quality.
4- **MMAs projection systems, printing using thermochromic pigments**. A single laser beam illuminates an MMA, which orientates each micromirror independently, then the laser beamlets can print 2D images. Additionally, a continuous laser beam preheats the surface to be printed. The system can image very small dots pitch, enabling high-resolution printing of big areas by a color change on thermochromic ink. The achieved top performance for the developed platform is 0.27 m/s, achieving grade B codes, printing images of one-inch width, and 300 dpi resolution.
5- **SLMs projection systems, marking by laser ablation**. The system is composed of a pulsed laser source and an SLM which modulates the phase and polarization of an incident beam. from the laser source, allowing the engraving by ablation of the image generated on the desired surface. The target application is high-speed high resolution marking of very small areas for special coding by ablation across virtually any surface material. The system can achieve to print images with a resolution higher than 1200 dpi, unique codes up to 10 codes/s, and batch codes up to 100 codes/s.

These five implementations developed in this thesis cover applications for printing variable data images with resolutions ranging from 50 dpi up to more than 300

dpi, image widths ranging from 570 μm up to 100 mm, for up to 256 gray levels, at production line speeds of up to 16 m/s, being the highest printing speed published so far.

Computing and communication should not limit the system. The control systems have been developed to overcome the computing throughput and latency requirements imposed by the applications for marking and printing systems operation.

From the computing requirements study conducted, we can infer that communication bandwidth above 100 Gbps (like currently available in last Ethernet standards) would allow printing or marking with a resolution, print width, grayscale, and line speeds higher than the requirements of the new challenges scenarios. Note that the height of the marking area still has an inverse relation with the maximum line speed in the bandwidth equation, but the margin is high enough to consider that it would become an important constraint in future systems

Regarding latency, assuming some correction operations executed in current digital systems with typical clock frequencies in the order of GHz, we get a high margin in the speed limit.

A common problem in high-speed marking and printing is having to adapt the laser marking system to changes in the printing image. The control system separates constant repetitive information, variable information plus real-time variables (counters, time data, etc.). By separating these information sources, the control system reduces the processing and communication time between the printing of one image and the next one (with common elements to the first one), reduce the latency, and increase the throughput by a separate parallel process that handles the minimum variable information needed between printing sequential images thus achieving better performance in real-time. This parallel processing prevents bandwidth limitations and computing redundant information among images.

The different values of the resolution, width, gray levels, and velocity of the different applications force to use of different hardware for image forming (e.g., laser diode arrays, MMAs), and also different control architectures. Below I describe the features common to all of them.

As a digital printing system, the control architectures implemented in this thesis incorporates a Digital Front End (DFE) which accepts a print file and converts it into a format that the print engine can use to transfer the content onto the substrate. The DFE is the raster image processor (RIP), interprets the incoming file to generate the corresponding bitmap and applies sets of algorithms to create the screened file ready to be used by the print engine. The DFE supports complex functionalities to manage grayscale, print speeds, variable data, process automation, two-way communication with other workflow processes, and enable sensors to participate in the process. The DFE can compute the next image in parallel to marking the current one.

Although many microprocessors could reach the computing requirements of the architectures developed in this thesis, a slight increase in the number of operations per pixel on the input image would create a bottleneck on the controller. Given the latency requirements and the safety-critical requirements, we decided to divide computation between hard real-time computing and soft real-time computing.

The soft real-time part of the system includes HMI control, marking image and data processing, and communications. It is implemented in an x86 CPU running embedded Linux. The CPU communicates with the external world to receive the marking workloads using Gigabit Ethernet.

FPGAs are the best option to have predictable behavior in the hard real-time part of the system (e.g., image forming, laser marking on-the-fly, triggering, speed monitoring). The hard-real-time controllers provide the appropriate pulse repetition rate (f_p) and pulse width (Δt_p) for every beamlet with low latency and jitter, even dealing with variable data for every label. I have proposed several architectures using FPGA cording to the different applications: (1) Single SoC-FPGA (with embedded ARM) processors for f-LDA solution; (2) DSP + multiple FPGAs for the HP f-LDA; (3) DSP + SoC-FPGA + small FPGA for DLP solution. All of them reach the proposed real-time constraints for latency and throughput of these complex control systems that include digital printing.

7.2. Next Challenges

Following the Demand-Pull model, I have proposed technological changes to boost the company's economic activity; in particular, the inventions associated with this thesis will be commercialized through a novel product range of industrial equipment.

Our main target market is the fast-moving consumer goods (FMCG), also known as the consumer-packaged-goods (CPG) industry. FMCG industry is increasingly using digital technologies to address the challenges it faces. Bellow, I show some examples of target applications for the lines of research that continue this thesis

Codified Packages. The high-performance production lines of the FMCG industries, as beverages or packaged foods, require products coding at rates around 1000 products per minute, with linear speeds between 120 and 180 m/min, with prospects of being able to code with rates up to 1500 products per minute, and speeds above 200 m/min. The low ranges of these speeds can be covered with laser marking using galvanometers, but with markings very limited to a few lines of characters, without the possibility of printing barcodes or 2D codes with sufficient quality.

Intelligent Packaging. To make the packages unique to make them identifiable throughout the entire value chain is key for digital technologies made possible by the Industry 4.0 revolution. The converting industry processing machines (such as printing presses) work at speeds up to 600 m/min, being able to produce in one of the multiple

lanes of a single production line more than 6000 products per minute. Until now, there was no solution on the market capable of printing codes of sufficient quality at these production rates.

Late-stage customization of products and packaging. Moving the printing of variable data to the point of pack or fill enables a broad range of marketing and other consumer-oriented messages to be applied to a product or pack. The labeling machines for the FMCG industry work with production rates of around 1000 products per minute with projections exceeding 1500 labels per minute. It is a great advance for the packaging industry to have printers capable of printing variable product information on labels of lengths between 100 and 400 mm, with label heights between 30 and 150 mm, printing with resolutions around 200 dpi, at current speeds of 120 m/min, with the prospect of doubling the speed in the near future.

Digitally Printed Packaging. Digitally printing onto plastics and flexible substrates, or folding cartons, printing directly onto objects of nearly all shapes and sizes, enables relevant personalization, reduced process costs by eliminating the need for labels, rich graphics, hard-to-produce greyscales, and small text that's customized at the latest stages of production. There is great interest in the industry, especially in FMCG, to be able to digitally print with resolutions of more than 300 dpi products at rates of 150 products per minute and shortly 200 products per minute with production line speeds between 30 and 60 meters per minute, customizing the printing of each product. There is currently no such solution on the market.

Smart packaging with printed electronics that sense, store, compute and communicate information using a thin flexible label that can contain sensors, power, circuits, communication, and displays, can improve processes and outcomes by authenticating products, monitoring quality and environmental conditions, tracking supply chain conditions, providing information for analytics, enhancing customer experiences. Research in this field has a growing interest in large FMCG industries. The know-how acquired during the completion of this doctorate helps us to start this path.

Our Demand-Pull model is combined with our Science-Push model. Below I explain some research lines open after this thesis and aimed at solving the previous challenges.

Inkless printing

The printing devices described in this thesis obtained good results in a controlled testing environment. However, for commercial applications, further challenges need to be solved. Although there is no visible debris in our lab tests, more research is needed to analyze with more detail the nature of the materials involved in the process and the quantification of the generated by-products using mass spectrometry and gas chromatography.

It is desired that the printing system can deal with a variety of circumstances as different paper types and paper conditions. Moreover, the permanency of the print should be of high quality, even for the variety of circumstances encountered in practice. Permanency refers both to the print lasting over a long duration of time and resistance to being removed by abrasion.

The results obtained so far reach combinations of speed, print width, and resolution lower than industrial requirements. As stated in this thesis, these results can be improved by increasing the power and quality of the laser beam. Currently, there are no laser sources with the required combination of wavelength, power, and beam quality.

LDA based multibeam marking and printing

I predict that industries will demand in a near future a gradual increase in production line speed. In this context, multiple beam systems will become the most relevant technology in future laser marking systems. Laser Diode Arrays can solve the problem of the scanning bottleneck to increase the production line speeds to the next level while addressing the demand for bigger marking areas The performed analysis suggests that higher speeds and wider print width can be achieved by investing in additional laser beams.

The use of this technology will open new challenges. Specifically, by improving the energy efficiency of the semiconductor laser arrays to reduce heat dissipation, increase laser power density, and reduce the size of laser diodes, we could achieve more compact print heads working on higher speed production lines.

The most important entry barrier for dissemination of this technology among potential clients is the high initial investment so that only very high-performance production lines can adapt the solution. Research is required aimed at reducing the costs of components, especially laser diodes.

I explained in this thesis the importance of the characteristics of the surface to be printed, such as the fluence threshold and the linearity of the response in optical density of the print for the received irradiance. Research into thermochromic pigments will improve print quality and speed.

MMA-based printing

The future goal for this technology is printing grade A 2D codes at 1 m/s process speed and 300 x 300 dpi resolution. At the time we developed this printing method, the DMD technology is unable to handle high irradiances and power loads because of limited cooling capability and its not optimized coating.

The next ways to achieve the objectives of this research could be to improve the coating increasing fluence sensitivity and reducing background Optical Density, the optimization of the process, wavelength, beam footprint, spot size, power uniformity,

addressability. A more detailed sensitivity study would be needed to validate the model. New tests could also be done with the new DMD chips that are appearing with improved efficiency and thermal behavior.

SLM-based marking

A target market for the devices resulting from this research is direct marking in small products with high peak power pulsed lasers. The direct laser marking on the product itself must not imply the loss of primary properties and functionalities (e.g., composition, mechanical properties), since the laser may exert a different effect on the different components and lead to microcracking, selective melting, etc., the use of ultrashort laser pulses (picosecond and femtosecond) can minimize the thermal impact on the material.

Different pulsed laser sources are available: femtosecond, picosecond, nanosecond, and microsecond laser sources with different emission wavelengths (ultraviolet, visible, infrared). Specific characterization concerning morphological changes and material integrity needs to be considered.

The cases which require high writing resolution (about 20µm laser spot diameter) could involve high-performance laser sources in terms of available laser power per beamlet which could make the solution quite expensive. The risk of too high performance imposed on the laser source by the beam delivery system needs to be investigated.

Enough contrast of the generated marks is the key parameter to obtain since it will impact the code readability, based on the wide range of materials to be processed. High contrast marks are the new challenge to be achieved.

The dynamic beam shaping system based on the SLM requires a significant (2-3 fold) increase of pattern switching frequency, restructuration of the data management by embedded hardware and software evolutions, and upgrade towards hardware generated synchronization signals (rather than some current software signals).

Real-time computing

If the beam deflection barrier is surpassed by using multiple beams, the next probable bottleneck to continue increasing print width, resolution, grayscale, and line speeds will be the controller computing concerning throughput, latency, and jitter that can introduce constraints to the communication and computation requirements.

On the other hand, the combination of high-end requirements in resolution, print width, grayscale, and line speeds of the new challenges scenarios increase considerably the requirements for the computing platform throughput, which will require parallelization strategies, and heterogeneous computing platforms, since clock frequency cannot be increased unlimitedly.

I'm currently working on several research projects in which I plan to address some of the aspects presented as future goals:

- EUROSTARS project UDILAS: "Unique Device Identification of medical devices through advanced LASER marking technology"
- CDTI CIEN Enterprise Research Consortium: "Applied research for the development of high-level hygienic products using surface laser technologies"
- CDTI PID: "Research and development of an ecological inkless printing system"

Bibliography

[1] N. Mukoyama, H. Otoma, J. Sakurai, N. Ueki, and H. Nakayama, "VCSEL array-based light exposure system for laser printing," in *Vertical-Cavity Surface-Emitting Lasers XII*, 2008, vol. 6908, p. 69080H.

[2] M.-F. Chen, Y.-P. Chen, W.-T. Hsiao, S.-Y. Wu, C.-W. Hu, and Z.-P. Gu, "A scribing laser marking system using DSP controller," *Opt. Lasers Eng.*, vol. 46, no. 5, pp. 410–418, May 2008.

[3] L. Lazov, H. Deneva, and P. Narica, "Laser Marking Methods," *Environ. Technol. Resour. Rezekne, Latv. Proc. 10th Int. Sci. Pract. Conf. Vol. I, 108-115*, vol. 1, pp. 108–115, Jun. 2015.

[4] A. HAN and D. GUBENCU, "Analysis of the laser marking technologies," *Nonconv. Technol. Rev. – no.4/ 2008*, vol. 4, no. 10, pp. 17–22, 2008.

[5] J. Hecht, "A short history of laser development," *Opt. Eng.*, vol. 49, no. 49, pp. 99–122, Sep. 2010.

[6] R. E. Russo, "Laser Ablation," *Appl. Spectrosc. Vol. 49, Issue 9, pp. 14A-28A*, vol. 49, no. 9, pp. 14A-28A, Sep. 1995.

[7] D. Schuöcker, "Light Amplification by Stimulated Emission of Radiation (LASER)," in *High Power Lasers in Production Engineering*, vol. 15, 1999, pp. 27–37.

[8] R. Sans-Ravellat and J. M. Ibanez-Baron, "Marking procedure through laser beams by images projection," ES2192485, 2003.

[9] Nakahanada, "Image forming method and image forming apparatus," 2004.

[10] H. YAMAMOTO, "Image forming apparatus , image processing method , and program JP5454368B2," 2010.

[11] S. T. S. Holmstrom, U. Baran, and H. Urey, "MEMS Laser Scanners: A Review," *J. Microelectromechanical Syst.*, vol. 23, no. 2, pp. 259–275, Apr. 2014.

[12] Y. Song, R. M. Panas, and J. B. Hopkins, "A review of micromirror arrays," 2018.

[13] D. Castells-Rufas, F. Bravo-Montero, B. Quezada-Benalcazar, J. Carrabina, and M. Codina, "Automatic real-time tilt correction of DMD-based displays for augmented reality applications," in *Emerging Digital Micromirror Device Based Systems and Applications X*, 2018, vol. 10546, p. 22.

[14] K. Kim, K. Yoon, J. Suh, and J. Lee, "Laser Scanner Stage On-The-Fly Method for ultrafast and wide Area Fabrication," *Phys. Procedia*, vol. 12, pp. 452–458, 2011.

[15] D. Castells-Rufas, O. Vila-Closas, and J. Carrabina, "Design of a multi-soft-core

based Laser Marking controller," in *2012 International Conference on Reconfigurable Computing and FPGAs, ReConFig 2012*, 2012.

[16] D. Castells i Rufas, "Scalable parallel architectures on reconfigurable platforms." Universitat Autònoma de Barcelona, Feb-2016.

[17] H. J. Eichler, J. Eichler, and O. Lux, "Material Processing," in *Springer Series in Optical Sciences*, vol. 220, 2018, pp. 409–421.

[18] L. Sobotova and M. Badida, "Laser marking as environment technology," *Open Eng.*, vol. 7, no. 1, pp. 303–316, Feb. 2017.

[19] J. Cridland, A. Jarvis, M. Walker, and C. Wyres, "Inkless printing apparatus," 2013.

[20] GS, "GS1 DataMatrix Guideline Overview and technical introduction to the use of GS1 DataMatrix," 2018.

[21] V.-F. Duma, "Laser scanners with oscillatory elements: Design and optimization of 1D and 2D scanning functions," *Appl. Math. Model.*, vol. 67, pp. 456–476, Mar. 2019.

[22] S. Xiang, S. Chen, X. Wu, D. Xiao, and X. Zheng, "Study on fast linear scanning for a new laser scanner," *Opt. Laser Technol.*, vol. 42, no. 1, pp. 42–46, Feb. 2009.

[23] C. Wei, C. Sihai, L. Dong, and J. Guohua, "A compact two-dimensional laser scanner based on piezoelectric actuators," 2015.

[24] G. R. B. E. Römer and P. Bechtold, "Electro-optic and Acousto-optic Laser Beam Scanners," *Phys. Procedia*, vol. 56, pp. 29–39, 2014.

[25] J. Llado-Abella, R. Sans-Ravellat, and J. M. Ibanez-Baron, "System and process for marking or perforating," US6130402A, 2000.

[26] P. Gecys, G. Raciukaitis, A. Wehrmann, K. Zimmer, A. Braun, and S. Ragnow, "Scribing of Thin-Film Solar Cells with Picosecond and Femtosecond Lasers," *JLMN-Journal of Laser Micro/Nanoengineering*, vol. 7, no. 1, 2012.

[27] A. Jarvis, M. Walker, A. O'Rourke, and R. Cook, "Novel ink formulation," 2014.

[28] F. Bravo-Montero, D. Castells-rufas, S. A. Vogler, J. Carrabina, and D. Castells-rufas, "Laser Inkless Eco-Printing on Paper and Cardboard," in *2020 IEEE International Conference on Industrial Technology (ICIT)*, 2020, vol. 2020-Feb, pp. 59–64.

[29] M. PLANCK, "On an Improvement of Wien's Equation for the Spectrum," *Old Quantum Theory*, pp. 79–81, 1967.

[30] A. Einstein, "On the Quantum Theory of Radiation," *Old Quantum Theory*, vol. 18, no. 18, pp. 167–183, 1967.

[31] A. L. Schawlow and C. H. Townes, “Infrared and optical masers,” *Phys. Rev.*, vol. 112, no. 6, pp. 1940–1949, 1958.

[32] G. Gould, “The LASER, light amplification by stimulated emission of radiation,” in *The Ann Arbor conference on optical pumping, the University of Michigan*, 1959, p. 92.

[33] M. Rose and H. Hogan, “A History of the Laser: 1960-2019,” 2019.

[34] T. H. Maiman, “Stimulated Optical Radiation in Ruby,” *Nature*, vol. 187, no. 4736, pp. 493–494, 1960.

[35] B. Gefvert, C. Holton, A. Nogee, and J. Hecht, “Laser markets navigate turbulent times | Laser Focus World,” 2020. [Online]. Available: https://www.laserfocusworld.com/lasers-sources/article/14073907/laser-markets-navigate-turbulent-times. [Accessed: 06-Jun-2021].

[36] B. Lee *et al.*, “Semiconductor & Electronics Forecast Update, 1Q21, Presentation Materials,” 2021. [Online]. Available: https://www.gartner.com/en/documents/4001333. [Accessed: 06-Jun-2021].

[37] H. J. Eichler, J. Eichler, and O. Lux, “Material Processing,” in *Springer Series in Optical Sciences*, vol. 220, 2018, pp. 409–421.

[38] M. Hemmerich, M. Darvish, J. Conroy, L. Knollmeyer, and J. Way, “Galvanometer scanning technology and 9 . 3µm CO2 lasers for on-the-fly converting applications,” in *Lasers in Manufacturing Conference*, 2017.

[39] I. Fomenkov, S. Hsu, and R. van Es, “Extreme UV Keeps Pace with Moore’s Law,” *Photonics Spectra*, 2018.

[40] B. Schmidt and M. Schaefer, “Advanced industrial laser systems and applications,” in *SPIE LASE, 2018, San Francisco, California, United States Downloaded*, 2018, vol. 1052502, no. February 2018, p. 203.

[41] R. Zafar, “TSMC Shares Major EUV Chipmaking Lead and Plans For 2nm Production Plant,” *https://wccftech.com/*, 2021. [Online]. Available: https://wccftech.com/tsmc-shares-major-euv-chipmaking-lead-and-plans-for-2nm-production-plant/. [Accessed: 12-Jun-2021].

[42] B. Gu, “Review - 40 years of laser-marking - industrial applications,” in *SPIE*, 2006, vol. 6106, p. 610601.

[43] COHERENT INC., “Lasers: Understanding the Basics | lasers | Photonics Handbook | Photonics Marketplace,” 2021. [Online]. Available: https://www.photonics.com/Articles/Lasers_Understanding_the_Basics/a25161/p4. [Accessed: 12-Jun-2021].

[44] V1adis1av, “File:Stimulated Emission.svg - Wikimedia Commons,” 2008. [Online]. Available:

https://commons.wikimedia.org/w/index.php?curid=3983414. [Accessed: 14-Jun-2021].

[45] A. E. Siegman, *Lasers*. 1986.

[46] W. M. Steen, “Laser Material Processing,” *Laser Mater. Process.*, 1991.

[47] Tatoute, “File:Laser.svg - Wikimedia Commons,” 2006. [Online]. Available: https://commons.wikimedia.org/w/index.php?curid=577575. [Accessed: 14-Jun-2021].

[48] DrBob, “File:Modelock-1.png - Wikimedia Commons,” 2003. [Online]. Available: https://commons.wikimedia.org/w/index.php?curid=12622465. [Accessed: 15-Jun-2021].

[49] DrBob, “File:Hermite-gaussian.png - Wikimedia Commons,” 2004. [Online]. Available: https://commons.wikimedia.org/w/index.php?curid=18064771. [Accessed: 15-Jun-2021].

[50] D. Naidoo, I. A. Litvin, and A. Forbes, “Brightness enhancement in a solid-state laser by mode transformation: publisher’s note,” *Optica*, vol. 5, no. 9, p. 1135, 2018.

[51] R. Paschotta, “RP Photonics Encyclopedia - lasers, principle of operation, properties of laser light, applications, resonator, cavity, laser beam, stimulated emission,” 2021. [Online]. Available: https://www.rp-photonics.com/lasers.html. [Accessed: 13-Jun-2021].

[52] Danh, “File:Commercial laser lines.svg - Wikimedia Commons,” 2009. [Online]. Available: https://commons.wikimedia.org/w/index.php?curid=8187485. [Accessed: 15-Jun-2021].

[53] W. Dongyun and Y. Xinpiao, “An Embedded Laser Marking Controller Based on ARM and FPGA Processors,” *Sci. World J. Vol. 2014, Artic. ID 716046, 7 pages*, vol. 2014, pp. 702–705, 2014.

[54] D. Wang, Q. Yu, and X. Ye, “Correction of the field distortion in embedded laser marking system,” *Opt. Laser Technol.*, vol. 57, pp. 52–56, Apr. 2014.

[55] I. K. Silverbrook, S. R. Walmsley, T. Plunkett, M. J. Pulver, J. Robert, and M. J. Webb, “Printer controller for supplying data to a printhead module having one or more redundant nozzle rows,” US7252353, 2004.

[56] X. Ye, Y. Li, Y. Du, and Z. Cai, “Design of data transmission system for speed measurement radar between ARM and FPGA based on embedded Linux,” *2016 IEEE Int. Conf. Signal Image Process. ICSIP 2016*, pp. 343–346, 2017.

[57] M. Montón, “Checkpointing for Virtual Platforms and SystemC-TLM-2.0,” 2010.

[58] J. Montero and A. Sabé, “Arquitectura de Software embebida,” 2015.

[59] Jacob Beningo, “Real-Time Operating System (RTOS) Best Practices Guide.” pp. 1–14, 2017.

[60] M. Mundt, “Seven fatal mistakes to avoid when choosing an embedded OS,” pp. 1–9, 2016.

[61] Altera, “Cyclone V Hard Processor System User Guide.” 2014.

[62] B. Rogers, “The Coming Data Avalanche,” 2016.

[63] P. P. Chu, *Embedded SoPC Design with Nios II Processor and VHDL Examples*. New Jersey: Wiley, 2011.

[64] Altera, “Embedded Design Handbook.” 2016.

[65] Rory Dear, “‘ C ’ lands on FPGAs to make embedded multicore computing a reality,” pp. 1–5, 2016.

[66] D. Castells-Rufas, “Scalable Parallel Architectures on Reconfigurable Platforms,” Universitat Autònoma de Barcelona, 2016.

[67] J. Joven Murillo, “HW-SW Components for Parallel Embedded Computing on NoC-based MPSoCs,” 2009.

[68] E. Fernández Alonso, “Offloading techniques to improve performance on MPI applications in NoC-based MPSoCs,” 2014.

[69] K. Asanovic *et al.*, “A view of the parallel computing landscape,” *Commun. ACM*, 2009.

[70] “Digital printing - Wikipedia.” [Online]. Available: https://en.wikipedia.org/wiki/Digital_printing. [Accessed: 09-Jul-2021].

[71] “Laser printing - Wikipedia.” [Online]. Available: https://en.wikipedia.org/wiki/Laser_printing. [Accessed: 10-Jul-2021].

[72] G. Hennig *et al.*, “Lasersonic® LIFT Process for Large Area Digital Printing,” *J. Laser Micro Nanoeng.*, vol. 7, no. 3, pp. 299–305, Nov. 2012.

[73] “Batch coding machine - Wikipedia.” [Online]. Available: https://en.wikipedia.org/wiki/Batch_coding_machine. [Accessed: 10-Jul-2021].

[74] “Inkjet printing - Wikipedia.” [Online]. Available: https://en.wikipedia.org/wiki/Inkjet_printing#Other_uses. [Accessed: 09-Jul-2021].

[75] M. C. Patel, A. J. Patel, R. C. Patel, and P. G. Student, “A Review on Laser Marking Process for Different Materials,” *IJSRD-International J. Sci. Res. Dev.*, 2017.

[76] J. Qi, K. L. Wang, and Y. M. Zhu, “A study on the laser marking process of stainless steel,” *J. Mater. Process. Technol.*, vol. 139, no. 1–3, pp. 273–276, Aug. 2003.

[77] Y. M. Noor, S. C. Tam, L. E. N. Lim, and S. Jana, “A review of the Nd: YAG laser marking of plastic and ceramic IC packages,” *J. Mater. Process. Tech.*, vol. 42, no. 1, pp. 95–133, Apr. 1994.

[78] P. Deprez, C.-F. Melian, F. Breaban, and J.-F. Coutouly, “Glass Marking with CO 2 Laser: Experimental Study of the Interaction Laser-Material,” *J. Surf. Eng. Mater. Adv. Technol.*, vol. 2, pp. 32–39, 2012.

[79] M.-F. F. Chen, W.-T. T. Hsiao, W.-L. L. Huang, C.-W. W. Hu, and Y.-P. P. Chen, “Laser coding on the eggshell using pulsed-laser marking system,” *J. Mater. Process. Technol.*, vol. 209, no. 2, pp. 737–744, Jan. 2009.

[80] I. S. Nasution and T. Rath, “Optimal laser marking of 2D data matrix codes on Cavendish bananas,” *Res. Agric. Eng.*, vol. 63, no. 4, pp. 172–179, 2017.

[81] Y. Angelova, L. Lazov, S. Mezinska, S. Mežinska, and L. Lazov, “Innovative Laser Technology in Textile Industry: Marking and Engraving,” *Environ. Technol. Resour. Proc. Int. Sci. Pract. Conf.*, vol. 3, p. 15, 2017.

[82] J. Li *et al.*, “Experimental investigation and mathematical modeling of laser marking two-dimensional barcodes on surfaces of aluminum alloy,” *J. Manuf. Process.*, vol. 21, pp. 141–152, Jan. 2016.

[83] L. M. Cabalín and J. J. Laserna, “Experimental determination of laser induced breakdown thresholds of metals under nanosecond Q-switched laser operation,” *Spectrochim. Acta Part B At. Spectrosc.*, vol. 53, no. 5, pp. 723–730, May 1998.

[84] J.-F. F. Bisson *et al.*, “Laser Damage Threshold of Ceramic YAG,” *Japanese J. Appl. Physics, Part 2 Lett.*, vol. 42, no. 8 B, p. L1025, 2003.

[85] G. Raciukaitis and M. Gedvilas, “Processing of polymers by uv picosecond lasers,” in *International Congress on Applications of Lasers & Electro-Optics*, 2005, vol. 2005, no. 1, p. M403.

[86] E. . Kreutz, H. Frerichs, J. Stricker, and D. . Wesner, “Processing of polymer surfaces by laser radiation,” *Nucl. Instruments Methods Phys. Res. Sect. B Beam Interact. with Mater. Atoms*, vol. 105, no. 1–4, pp. 245–249, Nov. 1995.

[87] L. V. Zhigilei, P. B. S. Kodali, and B. J. Garrison, “On the threshold behavior in laser ablation of organic solids,” *Chem. Phys. Lett.*, vol. 276, no. 3–4, pp. 269–273, Sep. 1997.

[88] C. Li, P. Du, H. Tian, and P. Erk, “Novel thermochromic copolymers with two luminescent colors,” *Chem. Lett.*, vol. 32, no. 7, pp. 570–571, 2003.

[89] P. P. Pronko, S. K. Dutta, J. Squier, J. V. Rudd, D. Du, and G. Mourou, “Machining

of sub-micron holes using a femtosecond laser at 800 nm," *Opt. Commun.*, vol. 114, no. 1–2, pp. 106–110, 1995.

[90] C. S. Lee, N. Koumvakalis, and M. Bass, "Spot-size dependence of laser-induced damage to diamond-turned Cu mirrors," *Appl. Phys. Lett.*, vol. 41, no. 7, pp. 625–627, 1982.

[91] L. Lévesque, "Law of cooling, heat conduction and Stefan-Boltzmann radiation laws fitted to experimental data for bones irradiated by CO2 laser," *Biomed. Opt. Express*, vol. 5, no. 3, p. 701, 2014.

[92] M. M. Alhashem, "Optimization of Paper Discoloration via Pyrolysis Using Lasers for Inkless Monochrome Printing," King Abdullah University of Science and Technology, 2017.

[93] P. Bamfield and M. Hutchings, *Chromic Phenomena Technological Applications of Colour Chemistry*. 2018.

[94] J. Chen, Y. Wang, J. Xie, C. Meng, G. Wu, and Q. Zu, "Concept of heat-induced inkless eco-printing," *Carbohydr. Polym.*, vol. 89, pp. 849–853, 2012.

[95] J. Chen, J. Xie, L. Pan, X. Wang, L. Xu, and Y. Lu, "The microstructure of paper after heat-induced inkless eco-printing and its features," *J. Wood Chem. Technol.*, vol. 34, no. 3, pp. 202–210, Jul. 2014.

[96] Y. Nakamura and A. Aoki, "Irradiated ignition of solid materials in reduced pressure atmosphere with various oxygen concentrations - for fire safety in space habitats," *Adv. Sp. Res.*, vol. 41, no. 5, pp. 777–782, 2008.

[97] M. Karlovits and D. Gregor-Svetec, "Durability of cellulose and synthetic papers exposed to various methods of accelerated ageing," *Acta Polytech. Hungarica*, vol. 9, no. 6, pp. 81–100, 2012.

[98] J. S. Tumuluru *et al.*, "A review on biomass torrefaction process and product properties for energy applications," *Ind. Biotechnol.*, vol. 7, no. October, pp. 384–401, 2011.

[99] E. Biagini, F. Barontini, and L. Tognotti, "Devolatilization of biomass fuels and biomass components studied by TG/FTIR technique," *Ind. Eng. Chem. Res.*, vol. 45, no. 13, pp. 4486–4493, 2006.

[100] L. L. . Pan, J. J. . Chen, C. C. . Wan, H. H. . Ren, H. . H. Zhai, and J. J. . Zheng, "Investigating the environmental impact of pyrolysis volatiles of printing paper under a nitrogen atmosphere," *Cellul. Chem. Technol.*, vol. 49, no. 9–10, pp. 863–871, 2015.

[101] A. Jarvis, M. Walker, C. Wyres, and T. Phillips, "Laser imaging," US8663902, 2015.

[102] N. Yao and X. Zhao, "Laser high temp carbonized paper printing method," 2007.

[103] M. M. Alhashem, A. Bayonis, Y. Yuan, and C. Bennett, “Inkless printer,” 2014.

[104] V. Chandrasekar, M. J. Boerkamp, and S. Lemkaddem, “Printing apparatus with improved permanency of the print,” 2018.

[105] J. W. Restrepo, J. M. Fernández-Pradas, M. A. Gómez, P. Serra, and J. L. Morenza, “Influence of preheating and hematite content of clay brick pavers on the characteristics of lines marked with a Nd:YAG laser,” *Appl. Surf. Sci.*, vol. 253, no. 4, pp. 2272–2277, Dec. 2006.

[106] J. Chen, U. Xu, J. Xie, Y. Wang, L. Pan, and Q. Zu, “The effect of laser inkless eco-printing on the carbonizedmi crostructure of paper,” *Cellul. Chem. Technol.*, vol. 50, no. 1, pp. 101–108, 2016.

[107] S. Preuss, A. Demchuk, and M. Stuke, “Sub-picosecond UV laser ablation of metals,” *Appl. Phys. A Mater. Sci. Process.*, vol. 61, no. 1, pp. 33–37, Jul. 1995.

[108] Anthony Jarvis, “Ink for laser imaging,” US9663675, 2017.

[109] M. Gagean and J. M. MERMET, “Comparison of ultraviolet laser ablation and spark ablation of metals and alloys for analysis by axially viewed inductively coupled plasma atomic emission spectrometry,” *J. Anal. At. Spectrom.*, vol. 12, no. 2, pp. 189–193, Jan. 1997.

[110] J. Diaci, D. Bračun, A. Gorkič, and J. Možina, “Rapid and flexible laser marking and engraving of tilted and curved surfaces,” *Opt. Lasers Eng.*, vol. 49, no. 2, pp. 195–199, Feb. 2011.

[111] B. Dusser *et al.*, “Controlled nanostructrures formation by ultra fast laser pulses for color marking,” *Opt. Express*, vol. 18, no. 3, p. 2913, 2010.

[112] N. Goffin, L. C. R. Jones, J. R. Tyrer, and E. Woolley, “Just how (in)efficient is my laser system? Identifying opportunities for theoretical and auxiliary energy optimization,” *J. Laser Appl.*, vol. 33, no. 1, p. 012030, Feb. 2021.

[113] K. Yamazawa, T. Niino, S. Hayano, and T. Nakagawa, “High Speed UV Laser Beam Scanning by Polygon Mirror,” in *1997 International Solid Freeform Fabrication Symposium*, 1997.

[114] A. Li, W. Sun, W. Yi, and Q. Zuo, “Investigation of beam steering performances in rotation Risley-prism scanner,” vol. 24, no. 12, pp. 12840–12850, 2016.

[115] D. A. Scrymgeour *et al.*, “Large-angle electro-optic laser scanner on LiTaO_3 fabricated by in situ monitoring of ferroelectric-domain micropatterning,” *Appl. Opt.*, vol. 40, no. 34, p. 6236, Dec. 2001.

[116] X. T. Nguyen, V. L. Dinh, H.-J. Lee, and H. Kim, “A High-Definition LIDAR System Based on Two-Mirror Deflection Scanners,” *IEEE Sens. J.*, vol. 18, no. 2, pp. 559–568, Jan. 2018.

[117] S. Hosaka, E. Seya, T. Harada, and A. Takanashi, “High speed laser beam scanning using an acousto-optical deflector (AOD),” *Jpn. J. Appl. Phys.*, vol. 26, no. 7R, pp. 1026–1030, 1987.

[118] K. Endo, H. Nishida, and T. Kusano, “Photosensitive material and laser marking method,” US6876377, 2005.

[119] L. Hartwig *et al.*, “Material processing with a 3kW single mode fibre laser,” *J. Laser Micro Nanoeng.*, vol. 5, no. 2, pp. 128–133, 2010.

[120] J.-H. Park, H.-S. Lee, J.-H. Lee, S.-N. Yun, Y.-B. Ham, and D.-W. Yun, “Design of a Piezoelectric-Driven Tilt Mirror for a Fast Laser Scanner,” *Jpn. J. Appl. Phys.*, vol. 51, p. 09MD14, Sep. 2012.

[121] H. Exner *et al.*, “High speed laser micro processing using high brilliance continuous wave laser radiation,” *J. Laser Micro Nanoeng.*, vol. 7, no. 1, pp. 115–121, 2012.

[122] A. Wetzig *et al.*, “Fast laser cutting of thin metal,” *Procedia Manuf.*, vol. 29, pp. 369–374, 2019.

[123] N. J. Bruton, “Profiling user coding in the packaging,” *Opt. Photonics News*, 1997.

[124] L. Bassi, “Industry 4.0: hope, hype or revolution?,” *IEEE RTSI 2017 Res. Technol. Soc. Ind. 3rd Int. Forum*, 2017.

[125] R. Wudhikarn, “A Framework for Integrating Overall Equipment Effectiveness with Analytic Network Process Method,” *Int. J. Innov. Manag. Technol.*, vol. 4, no. 3, 2013.

[126] S. A. Vogler, F. Bravo-Montero, C. Gannau, and J. Almirall, “Procedure and system for marking paper, cardboard and textile,” EP3771572, 2021.

[127] S. A. Vogler, F. Bravo-Montero, C. Gannau, and J. Almirall, “Method and system for marking paper, cardboard and/or fabric,” WO2021/023898, 2021.

[128] J. Camps Claramunt, F. Bravo Montero, S. A. Vogler, and V. Boira Plans, “Aparato LASER,” ES2324275, 2009.

[129] J. Camps Claramunt, F. Bravo-Montero, S. A. Vogler, and V. Boira Plans, “LASER apparatus,” EP2214271, 2010.

[130] J. Camps Claramunt, F. Bravo Montero, S. A. Vogler, and V. Boira Plans, “Chamber for laser apparatus with extruded base frame,” US8388194, 2013.

[131] S. A. Vogler and F. Bravo-Montero, “Dispositivo y procedimiento para marcar mediante LASER un objeto en movimiento,” ES2380480, 2012.

[132] S. A. Vogler and F. Bravo-Montero, “Dispositivo y procedimiento para marcar mediante LASER un objeto en movimiento,” ES2401499, 2013.

[133] S. A. Vogler and F. Bravo-Montero, “Device and process for marking a moving object by LASER,” EP2380693, 2011.

[134] S. A. Vogler and F. Bravo-Montero, “Device and process for marking a moving object by LASER,” US8466944, 2013.

[135] S. A. Vogler, V. Boira-Plans, F. Bravo-Montero, and J. Camps-Claramunt, “Procedimiento de control de un sistema matricial de marcaje LASER,” ES2644261, 2017.

[136] S. A. Vogler, V. Boira-Plans, F. Bravo-Montero, and J. Camps-Claramunt, “Procedure for controlling a laser marking matrix system,” EP3251783, 2017.

[137] S. A. Vogler, V. Boira-Plans, F. Bravo-Montero, and J. Camps-Claramunt, “Control procedure for a laser marking matrix system,” US10265967, 2019.

[138] S. A. Vogler, V. Boira-Plans, F. Bravo-Montero, and J. Camps-Claramunt, “Control procedure for a laser marking matrix system,” JP6518719, 2019.

[139] F. Bravo-Montero, S. Vogler, and J. Camps Claramunt, “Procedimiento de fabricación de equipos para marcaje de productos por LASER bajo demanda, y equipo para marcaje de productos por láser obtenido con dicho procedimiento,” ES2603751, 2017.

[140] F. Bravo-Montero, S. A. Vogler, and J. Camps Claramunt, “On-demand LASER marking device manufacturing method and LASER marking device obtained by said method,” EP3136521, 2017.

[141] F. Bravo Montero, S. A. Vogler, and J. Camps Claramunt, “On-demand LASER marking device manufacturing method and LASER marking device obtained by said method,” US10220470, 2017.

[142] Bravo-Montero F, S. A. Vogler, and J. Camps Claramunt, “On-demand LASER marking device manufacturing method and LASER marking device obtained by said method,” JP2017042820, 2017.

[143] F. Bravo Montero, S. A. Vogler, and J. Camps Claramunt, “Equipo para marcaje de productos por LASER,” ES2576962, 2015.

[144] S. A. Vogler, J. Camps Claramunt, F. Bravo Montero, and F. Bravo-Montero, “Device for LASER marking of products,” EP3043428, 2016.

[145] S. A. Vogler, J. Camps Claramunt, and F. Bravo-Montero, “Device for the LASER marking of products,” US20160236300, 2016.

[146] R. Sans-Ravellat, J. M. Ibanez-Baron, and J. Beringues-Algue, “Laser marking apparatus with diode laser matrix,” US6201210, 2001.

[147] T. Phillips and J. Cridland, “Improvements in or relating to laser marking,” GB2575832A, 2020.

[148] T. Kuntze, U. Klotzbach, and E. Beyer, “Excimer lasers turning flexible: variable marking with micromirror devices,” *Phot. Process. Microelectron. Photonics III*, vol. 5339, p. 518, 2004.

[149] K. Kataoka, Y. Shibayama, and K. Doi, “Multiple Beam Scanning Optics for Laser Printer: Application of Optical Fiber Array Method,” *Opt. Rev.*, vol. 8, no. 4, pp. 218–226, Jul. 2001.

[150] O. P. Kowalski, “The Development of Laser Diode Arrays for Printing Applications,” in *Semiconductor Laser Diode Technology and Applications*, IntechOpen, 2012.

[151] T. Phillips, J. Cridland, L. GOMEZ, and A. AL-WAIDH, “Improvements in or relating to laser marking,” WO2020021260A1, 2020.

[152] T. Phillips and J. Cridland, “Improvements in or relating to laser marking,” GB2579653A, 2020.

[153] K. UETAKE, Y. HOTTA, I. SAWAMURA, T. ISHIMI, and Y. YOKOTA, “Recording method and recording apparatus,” EP3412465A1, 2018.

[154] H. J. Eichler, E. Jürgen, and O. Lux, *Lasers. Basic, Advances and Applications*, vol. 220. Cham: Springer International Publishing, 2018.

[155] “Late-Stage Package Printing is Poised for a Makeover.” [Online]. Available: https://digitalprinting.blogs.xerox.com/2016/11/07/late-stage-inline-laser-package-printing-poised-for-a-makeover/. [Accessed: 14-Aug-2021].

[156] X. Blogs, D. Printing, and H. Spot, “Late-Stage Transformation with New Digital Laser Packaging Print Technology,” pp. 1–5, 2016.

[157] Datalase, “What is Inline Digital Printing ?” 2016.

[158] A. N. Jarvis and M. R. Walker, “Laser marking,” US20100015558, 2010.

[159] “Laser ablation - Wikipedia.” [Online]. Available: https://en.wikipedia.org/wiki/Laser_ablation. [Accessed: 24-Aug-2021].

[160] E. Kannatey, *Principles of Laser Materials Processing*. 2009.

[161] “BiDiLase - Ultra-high-speed laser coding - Macsa ID.” [Online]. Available: https://www.macsa.com/en/hardware/traceability-coding/high-speed-laser-printer/bidilase/. [Accessed: 28-Aug-2021].

[162] B. Y. R. E. Russo, L. Berkeley, and R. E. Russo, “Laser Ablation,” *Appl. Spectrosc. Vol. 49, Issue 9, pp. 14A-28A*, vol. 49, no. 9, pp. 14A-28A, Sep. 1995.

[163] I. Quintana, J. Etxarri, C. Sanz, and A. Aranzabe, “Laser Micro–Milling and Drilling Using Microsecond Pulses. Applications for Mould and Aeronautical Industry,” *Proc. 3rd Int. Conf. Manuf. Eng.*, no. October, pp. 1–3, 2008.

[164] J. Li, “Advanced laser beam shaping using spatial light modulators for material surface processing,” no. January, 2018.

[165] L. Li, “Advances and characteristics of high-power diode laser materials processing,” *Opt. Lasers Eng.*, vol. 34, no. 4–6, pp. 231–253, 2000.

[166] “Variable data printing - Wikipedia.” [Online]. Available: https://en.wikipedia.org/wiki/Variable_data_printing. [Accessed: 09-Jul-2021].

[167] T. West, “The Evolution of Industrial Machine Architectures.” 2017.

[168] U. Eklund and J. Bosch, “Architecture for embedded open software ecosystems,” *J. Syst. Softw.*, vol. 92, no. 1, pp. 128–142, 2014.

[169] Y. T. T. Liao and J. S. T’ien, “A numerical simulation of transient ignition and ignition limit of a composite solid by a localised radiant source,” *Combust. Theory Model.*, vol. 17, no. 6, pp. 1096–1124, 2013.

[170] J. Kolar, M. Strlic, S. Pentzien, and W. Kautek, “Near-UV, visible and IR pulsed laser light interaction with cellulose,” *Appl. Phys. A Mater. Sci. Process.*, vol. 71, no. 1, pp. 87–90, 2000.

[171] “Reliable laser-diode technology impacts the industrial-laser marketplace | Laser Focus World.” [Online]. Available: https://www.laserfocusworld.com/lasers-sources/article/16554534/reliable-laserdiode-technology-impacts-the-industriallaser-marketplace. [Accessed: 22-Sep-2021].

[172] Ramon S. Ravellat, “System for marking moving objects by laser beams,” US5021631, 1991.

[173] Y. Jiang, “Study of laser flying marking system,” *Opt. Eng.*, vol. 46, no. 9, p. 094302, 2007.

[174] A. Fraser, J. Maltais, and X. P. Godmaire, “Analysis of Laser Marking Performance on Various Non-ferrous Metals,” *Miner. Met. Mater. Ser.*, vol. Part F4, pp. 937–941, 2018.

[175] Y. Yang, Y. Yang, T. Yu, and Y. Zheng, “Software design of SD card reader and image processor based on FPGA,” *Proc. 2011 Int. Conf. Mechatron. Sci. Electr. Eng. Comput. MEC 2011*, pp. 1864–1867, 2011.

[176] Z. Kuang, “Parallel diffractive multi-beam ultrafast laser micro-processing,” 2010.

[177] J. Goodman, *Introduction to Fourier Optics*. 1996.

[178] J. Liang, S. Y. Wu, F. K. Fatemi, and M. F. Becker, “Suppression of the zero-order diffracted beam from a pixelated spatial light modulator by phase compression,” *Appl. Opt.*, vol. 51, no. 16, pp. 3294–3304, 2012.

Annexes

Annex A: ScanLinux and Marca Software

ScanLinux is the LINUX-based software that runs in the internal CPU to manage the diode array laser marking system. It monitors the position of the surface to be printed related to the laser beams position and controls the laser beams activation. ScanLinux can calculate corrections during the marking process, and monitors inputs/outputs of the electronics board. It offers all the necessary operations to display and change the marking parameters.

Marca is the software for high-resolution applications, running in Windows located on an external PC. It communicates. through the Ethernet TCP/IP connection with the ScanLinux contained in the laser system. It has a powerful WYSIWYG design editor providing zoom, unlimited layering, barcode and 2D barcode marking, font editor, character-filling features, etc. Marca can handle BMP, JPG, GIG, TIF, PCX, and other graphic files and DXF vector files with multiple import options. It enables the modification of objects and characters. It has ODBC database features and messages activated by hourly, daily, or monthly changes. It has networking capabilities for several laser systems via TCP/IP over Ethernet and access registration for all the users. It also allows creating reports of the markings saved in the CPU laser memory, synchronizing PC and laser clocks, adjusting power, frequency, resolution, and speed. Marca software can be used to edit any message using any of the available fonts and create any type of drawing or design (Figure 87).

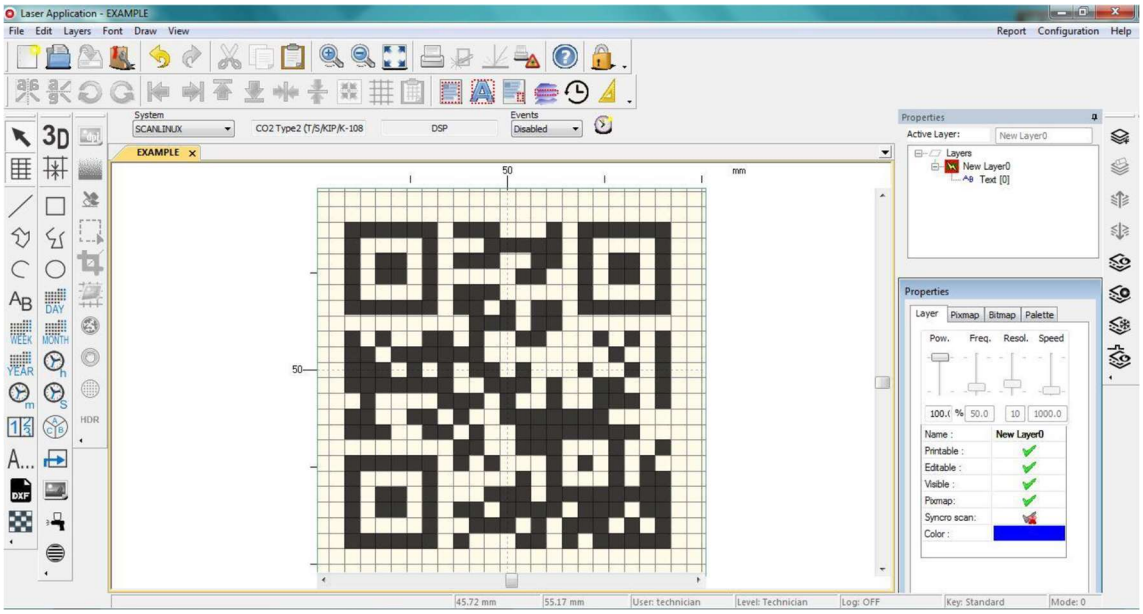

Figure 87: Example of creation of new messages in Marca

In Macsa we have created in Marca software for diode array systems (Figure 88) that can only print pixmaps in dynamic mode. The size, especially the height, of the pixmaps should be chosen to fit the number of available channels. The 'used channels' are channels that will be supervised during marking for any error state.

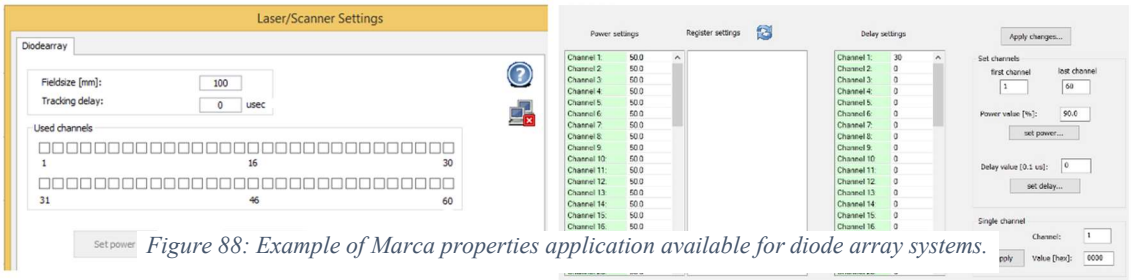

Figure 88: Example of Marca properties application available for diode array systems.

The software has powerful capabilities to establish a complex and comprehensive laser marking environment, including the generic and diode-array system configuration parameters and system variables (Figure 89).

All these system parameters and variables can be established in a file in the laser

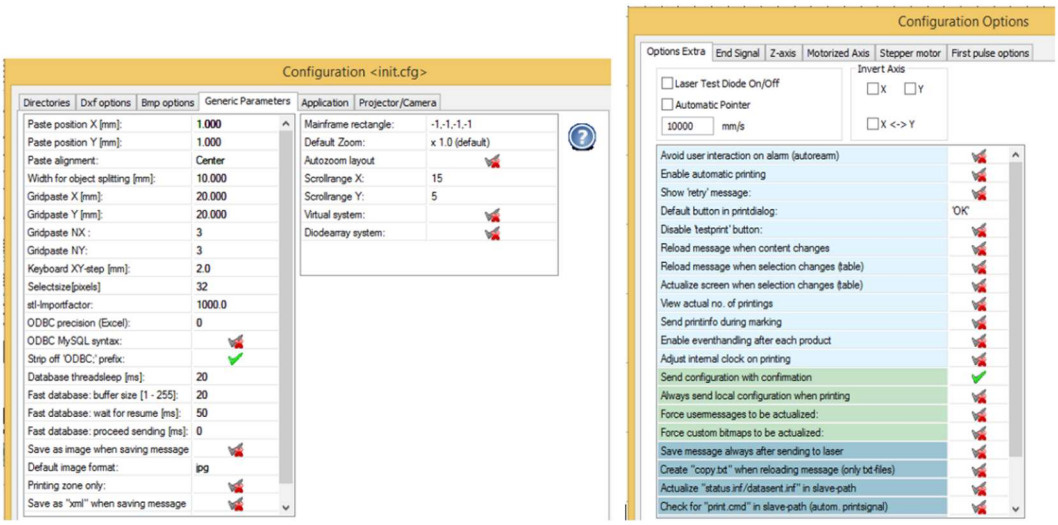

Figure 89: Examples of generic parameters and diode array system configuration parameters.

CPU ./bin directory, ScanLinux analyses the file and assigns some special variables (Figure 90).

```
Laserconfig: 5.7.8.7 03/20 23/03/2020
Dynamicmode: 1
Autoshift: YES
Autodistance: 100.000
N-prints: 0
Sortobjects: 1
Direction: RIGHT
Encoder: EXTERNAL
Position: POS2
Encoder_type: 0
Activation: 4
Type: PHOTOCELL1
Stopsignal: 0
Velocity: 10.000
Encoder_steps: 3000
Photocell_dist: 20.000
Encoder_mm: 152.333
Offset: 0.000
```

Figure 90: Example of file in the ./bin directory with some generic and diode array system configuration parameters.

As a manufacturer, Macsa views software as a strategic element and a business differentiator. Software is key to our laser marking systems and is critical to the success of our products. We have developed an embedded software architecture based on an open software ecosystem. Our reference architecture is Macsa's development that we call Scanlinux - Marca, which has been evolving over the last 20 years. Scanlinux - Marca is continually validated through deployment in multiple industrial settings. I have evaluated it based on several quality attributes [168] to see how it could serve as the basis for our new multibeam systems platform, with the conclusion that, while it does not fit perfectly, it does have the fundamental mechanisms necessary for our new laser marking systems platform. Table 23 shows the decision table I have considered to make Scanlinux - Marca the reference architecture for the new multibeam systems.

Table 23: Reference architecture decisions and how the Scanlinux - Marca architecture relates to them

Decision	Scanlinux - Marca	Comment
Deployment of New Applications	Yes	Being based on an open embedded ecosystem is a fundamental principle in Scanlinux - Marca
Ways-of-Working	Yes	The functions of the Scanlinux - Marca platform are developed by Macsa and adapted to each application.
H/W Abstraction	Yes	Scanlinux - Marca provides an abstraction to a standardized set of hardware from several Macsa suppliers
H/W Access	Yes	The certification of what the marking application can access in terms of hardware and information from other applications is controlled by Macsa, which means that is sufficient for laser-safety-critical features.
Modes of Usage	Yes	The laser system provides several modes of usage.
Platform Evolution	Yes	There is a process for evolving applications features into the platform.
Application Updates During Run-time		Updates are possible while the laser system is on, but needs to stop printing
Deployment of Critical Applications	Yes	Different applications are executed on different hardware with physical separation
Data Integrity	Yes	The laser system is developed as a safety-critical device

Decision	Scanlinux - Marca	Comment
Dependability Mechanisms	Yes	The laser system is developed as a safety-critical device
H/W Configuration Awareness	Yes	The integrated laser system components are standardized by Macsa and do vary between individual laser systems
Common Data Model	Yes	Macsa defines each application data model
Data Dictionary	Yes	Macsa defines each application data model
Layering	Yes	The platform can be verified independent of the applications running on top of it

Table 24 shows the different scenarios in which the new platform must work for the new multibeam systems and how Scanlinux- Marca adapts to these scenarios.

Table 24: Scenarios in which the new platform should work

Scenario	Scanlinux - Marca
The architecture should allow development, integration, and validation of applications independently	Yes
Applications must be possible to deploy independently of each other	Yes
The platform must be stable over time to provide a return on development investments	Yes
The platform must provide backward compatibility	Yes
The platform must support variability in the hardware configuration of sensors and actuators	Yes
Consistent User Interface	Yes
The platform must support necessary dependability requirements	Yes

The embedded software architecture that we use is a Linux microkernel that allocates memory and CPU to different threads of execution. Changing tasks and communications between tasks are fast. Some examples of software components we use are network protocol stacks (UDP, TCP / IP), storage management (FAT), etc. The tools for embedded software design that we use are the GNU software development tools and the development tools for PC-based systems. We debug using the simple shell provided by the embedded operating system; as well as external debugging using the output of a serial port to trace the operation and also an in-circuit debugger (ICD), which we connect via JTAG. The debugging of the microprocessor-centric part is different from the debugging of the processing done by the DSP and the debugging of the processing done by the FPGAs. To analyze and optimize the performance of the marking process the system can dump a trace of all the operations it performs at a very low level. This trace is sent to an external computer through the JTAG UART device that works over the USB cable of the board.

In the previous section, I have stated the computing requirements calculations for the laser marking and printing applications. These are average values of the set of necessary processes, and I can anticipate that they are already in the range of the

computing throughput of desktop systems; an increase of any of the considered parameters would require a high-performance computing system.

I can establish common functionalities to all the applications that we have seen in the different methods of marking and printing with multiple laser beams explained in the previous sections.

The controller receives the image information from the host, and for each printing, it creates a new image combining the fixed part with the variable part. This requires the controller to have some rendering software, which is based on Linux and specific type fonts to render the variable part in the controller. The final raster is stored in a memory. The system uses a double-buffering strategy to increase the throughput. While some CPU is building the next image to mark, another one is controlling the laser marking process of the previous one. The alternation of buffers is triggered by a photo-sensor. A hard-real-time process coordinates the printing of each pixel considering the movement of the surface. The maximum positioning error of the print is around the radius of one pixel (few tens of microns). Considering that the speed in some applications is above 10 m/s, the maximum allowed latency is few units of microseconds. The maximum positioning error between rasters in a print must be on the order of a few microns, so the maximum jitter allowed is on the order of nanoseconds. The system can be scaled to higher resolutions (up to 300dpi) or higher widths (up to 100mm) by fragmenting the raster image in several memories and creating multiple isolated processes responsible for marking a subset of the image. The hard-real-time marking process controls the modulation of the laser drivers so that laser diodes deliver more or less energy (from μJ up to hundreds of mJ) per pulse. The degree of ablation or the color change induced in the material is proportional to the amount of energy received, but the relation is not always linear. So, the marking process must decide the modulation depending on the desired color for each pixel (up to 256 grayscale levels). The marking processes are synchronized with the movement information reported by the encoder, which supplies position data in real-time (in the order of μs) to adapt the printing to the surface to be marked.

Annex B: Dissertation's Copyright

All the ideas, statements, figures, tables, IPs, and information presented in this dissertation belong to their respective authors, including myself. All of them have been rigorously referenced. If there were no references for specific information it is because such knowledge is considered to be either well-known industry-related facts or the results of my original research and findings.

Annex C: Implementation's Copyright & Disclaimer

The implementation of the methods and systems shown in this thesis are protected by industrial and intellectual property rights and are not eligible for distribution. All rights are reserved.

****

****

Annex D: Curriculum Vitae

Francesc Bravo-Montero was born in El Rubio, Spain, in 1963. He graduated in Industrial Engineering (1984) from Universitat Politècnica de Catalunya (UPC), M.Sc. in Microelectronics (1991) from Universitat Autonoma de Barcelona (UAB), in Electronics Engineering (1997) from Universitat de Barcelona (UB), and Postgraduate in Product Development Engineering (2008) from UPC. Currently, he's pursuing an Industrial Ph.D.at UAB.

Since 1984 he has been developing his professional career as Project Engineer, Process Engineer, Service Director, Project Manager; in companies as IS2 (Siemens group), INDO, SOLAIC. He currently works as an Engineering Manager at Macsa (Spain). His core expertise is project management and technical departments' management. His experience includes activities in electronics, optics, mechanics, laser, communications, AIDC, IT; and innovation and R&D management.

His research interests include photonics and embedded systems.

Francesc participation in R&D projects has led to developments that have subsequently resulted in new products in the Macsa portfolio. He has been participating in different national and European research programs, with high success rates and mostly in collaboration with universities, technology centers, and companies. Some examples of previous collaborative projects with a key role from Francesc include:

- LA-DP. Laser Array - Digital Printing. EUREKA E! 10351
- SWITCH. Nuevos dispositivos basados en la tecnología de materiales ópticos electro-activos para aplicaciones multisectoriales. CDTI CIEN 2016
- GREEN. Green pulsed fiber laser. Desarrollo de un láser verde de fibra pulsado para aplicaciones industriales. CDTI IDI-20120435
- MSLA. Nueva generación de equipos láser con sistema de sincronización micrométrica para aplicaciones de alta definición. CDTI IDI-20101051
- BCO2. Desarrollo del primer codificador láser de bajo coste. CDTI IDI-20080901
- I+DFL. Desarrollo de un generador de láser de fibra de tecnologías propia. CDTI IDI-20070557
- I+D LAS. Sistema de marcaje por láser de estado sólido bombeado por diodos. CDTI IDI-20060381.